Sediment traps

for reducing maintenance dredging costs in the Port of Rotterdam

Auke H. Tempel

Port of Rotterdam

Technical University of Delft

A thesis submitted for the degree of

Master of Science

June 21, 2019

Acknowledgements

This thesis is the end of an era as it is the last contribution to my MSc degree in Hydraulic Engineering at Delft University of Technology. This phase of my life is of much importance to me, as I have had the possibility to develop myself on an intellectual and social level. It has been a lot of fun to do this work, and it now feels like the right time to move on. Port of Rotterdam made it possible for me to get a taste of the now coming phase of my life by funding and providing a workspace for the graduation research. A very special gratitude goes out to Port of Rotterdam and the colleagues I was able to work with. A first glimpse of the office life at the Port of Rotterdam has resulted in many exciting stories and a great perspective of the joys ahead.

I would like to thank Lamber Hulsen for taking the time to give me in-depth feedback on all the steps I have chosen. Lamber, your intensive support was very helpful. I was supervised by Prof. dr. ir. Mark van Koningsveld, Prof. dr. ir. Julie Pietrzak, dr. ir. Alex Kirichek, dr.ir. Claire Chassagne and of course Lamber. Alex and Mark, thank you for getting me back on track by intervening when it seemed necessary. Julie and Claire, I have enjoyed your views on the problem and you helped me to look at the problem from a different perspective. I have also enjoyed the countless discussions during each of the meetings we had with the committee. To me, this is a sign that the subject drew your attention.

I received valuable support from Deltares. I would like to thank Thijs van Kessel for his modelling advice and Alex for his knowledge on the behaviour of the difficult to comprehend sediment in the port of Rotterdam.

Finally, I am grateful to my parents, who have always been ready for me during the difficult or stressful times of conducting the master thesis.

Abstract

Regular maintainance dredging is a large expense to the Port of Rotterdam, therefore the installation of sediment traps is considered. By increasing the bathymetry locally, an increase of local accumulation is expected and a decrease deeper in the harbour basin. This thesis describes the functioning of sediment traps in a stratified tidally energetic estuary, where sediment is supplied by the river and sea.

A numerical 2DV representation is set up for the Botlek Harbour with the hydrostatic Delft3D software. A calculated salinity time-series by Operationeel Stromingsmodel Rotterdam (OSR) is combined with a measured water level time series for the same time period to describe the hydrodynamic boundary conditions. Simulations are done with a variable and constant Suspended Particulate Matter (SPM) time-series boundary conditions, that were generated based on the measurements of De Nijs (2012).

Flow expansion caused by the sediment trap reduces the flow velocity, but increases the turbulent kinetic energy locally. A reduction of bed shear stress is observed in the trap, except near the edges where an increase is observed. Density currents caused by salinity differences govern the vertical flow velocity distributions, while tidal filling causes the net exchange. The depth of the trap plays a significant role in the internal flow characteristics. The sediment trap changes the properties of the internal flow, which may change the hydraulic state of the flow, i.e. from supercritical to subcritical, resulting in large instabilities and even an internal hydraulic jump. Shallow sediment traps result in less frequent internal hydraulic jump and weaker jumps compared to deeper sediment traps.

To investigate the dominant mechanism for the trapping of sediment in the sediment trap, a distinction is made between an erosion and a fluid mud scenario. The erosion scenario shows the largest agreement with the survey data, i.e. maintenance dredging data and Echosounder multibeam surveys, but contribute only marginally to the trapping of sediment. The

fluid mud scenario yields the largest contribution to the trapping of sediment. The decreased amounts of accumulated sediment in the basin for substantial to lots of fluid mud behaviour may vary between 10 % and 14 %, depending on how this fluid mud behaviour is modelled.

Various shapes have been tested on erosion and fluid mud scenarios. Both for erosion and fluid mud a more extreme choice of parameters might yield also more extreme results, this is however not considered realistic. The creation of an overdepth has shown to result in a marginal improvement in the capturing of sediment in an environment where erosion is important. A regular sediment trap decreases accumulation in the harbour basins by 2%. A trap twice as shallow increases this amount to 4%, but deepening the trap further may even enhance accumulation in the basins. A shorter or longer trap did not improve the situation. Installation of a sill did however result in a decrease of 6 % compared to the situation without trap. It is concluded that this effect can be largely contributed to the internal flow properties and the presence of internal hydraulic jumps.

The presence of an overdepth results in a significant improvement in the capturing of fluid mud flow. For the trapping of fluid mud flow, an overdepth results in 6% less sediment in the harbour basins no matter the depth or shape of the trap. The length of the trap did influence the accumulation in the basins. A trap twice as short shows an increase of 4 % of accumulation in the basins compared to a regular trap. A trap twice as long or installation of a sill results in similar accumulation in the harbour basins as a regular trap.

For fluid mud flows, any type of overdepth decreases accumulation of sediment considerably. The amount of overdepth or the shape does not influence this. The length of the trap should be sufficient. A trap that is too short results in an increase of accumulation in the basins. For environments where erosion is important, only shallow sediment traps have proven to reduce accumulation in the basins. Traps that are too deep actually increase accumulation in the basins. A sill has proven to be the best measure for both mechanisms. If overdepth is desirable for navigation a shallow sediment trap is advised. This leads to a reduction of accumulation in the harbour basins for both erosion and fluid mud scenarios.

Contents

List of Figures

List of Tables

Acronyms

ETM Estuarine Turbidity Maximum.

MKO Minimalisering Kosten Onderhoudsbaggerwerk.

NGD Nautical Guaranteed Depth.

OSR Operationeel Stromingsmodel Rotterdam.

PRISMA Programme Innovative Sediment MAnagement.

RANS Reynolds-Averaged Navier-Stokes equations.

ROFI Region Of Freshwater Influence.

SPM Suspended Particulate Matter.

WID Water Injection Dredging.

Chapter 1

Introduction

Located in the Rhine-Meuse estuary, the port of Rotterdam is the largest port in Europe and the 10th worldwide (World Shipping Council, 2013). The port is of major socio-economic importance as it is the engine of the economy of Rotterdam and hinterland. The port handles more than 30000 sea-going vessels each year of which the largest, with draughts up to 24 m, are docked in the Maasvlakte 2 (Port of Rotterdam, 2019). The exact depth is guaranteed in the so-called port Atlas, where each area is defined by certain Nautical Guaranteed Depths (NGDs). To safeguard navigation, regular maintainance dredging is needed, which is a large expense for Port of Rotterdam. Dutch government agency Rijkswaterstaat is responsible for the guaranteed depth of the main waterways such as the New Waterway and New Meuse, while Port of Rotterdam is responsible for the channel and harbour basins, as can be seen in Figure 1.1. The ongoing growth of the size of ships causes the NGD to keep increasing. This causes a significant increase in accretion, thus requiring more frequent maintenance dredging. Silt is the main type of sediment that consolidates in the harbour basins. Its cohesive character and low settling velocities make it a very unpredictable type of sediment to cope with. In the main waterways more sandy material can also be found. Port of Rotterdam has had to cope with the problem of harbour siltation for many years and has expertise in the removal of sand and silt from the Rotterdam harbour area. For the years 1982 to 2013 the quantities of maintenance dredging varied between three and seven million cubic meters per year. After the completion of Maasvlakte 2, the quantities almost doubled to values between eight and twelve million cubic meters per year (Appendix A 'Dredging in the port of Rotterdam', Figure A.1). This increase may have many reasons such as the adapted flow pattern of Maasvlakte 2 found by De Bruijn (2018) and the before-mentioned increased overall NGD in harbour basins.

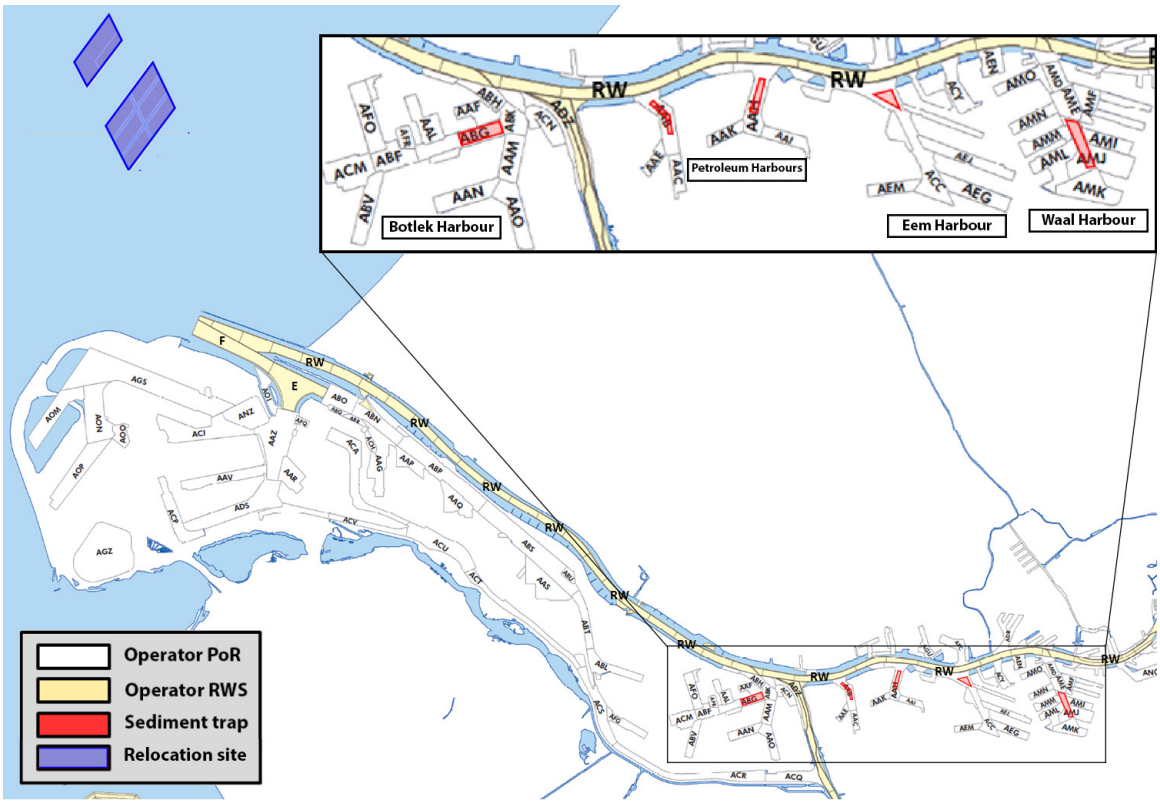

Figure 1.1: The maintenance responsibility of each of the dredging areas is given in white for the Port of Rotterdam and yellow for Rijkswaterstaat (De Bruijn, 2018). The locations of the sediment traps are given in a red colour. The location of the relocation site in the North Sea are shown with a blue colour (Port of Rotterdam, 2019).

In 1987, a joint research project with Rijkswaterstaat and the municipality of Rotterdam (now: Port of Rotterdam) called Minimalisering Kosten Onderhoudsbaggerwerk (MKO) was initiated to combine knowledge and experience in the battle against harbour siltation in the port of Rotterdam. Authors Van Vechgel, Veltman, Dollée, & De Haan (1987) proposed many mitigation measures, of which some were tested, such as a siltscreen from air bubbles, a fixed flat siltscreen from polyester and a moveable siltscreen. The idea was that these screens would repulse dense sediment flows. Each of these measures was however rejected as none of them were favourable or profitable compared to maintenance dredging.

A proposed mitigation measure that was in effect executed, was the installation of a sediment trap. The deepening of local bathymetry is expected to result in an increase of local sedimentation rates and a decrease of sedimentation rates elsewhere. One of the benefits is that the dredging area is located closer to the dropping point, i.e. the relocation site in the North Sea or the Slufter for contaminated material. This results in cheaper dredging per cubic meter. Another benefit is that the dredging activities are mostly concentrated in a single location. Locations that are difficult to

dredge, e.g. quay walls for the mooring of ships, can be avoided. Hoppers are filled faster and larger vessels may be deployed. The sediment is able to consolidate, which allows the dredging of material with a larger density. On top of these benefits, the extra depth at the location of the sediment trap causes an extra safety margin for peak sedimentation periods. A downside of the sediment traps is that the presence of sediment traps is said to attract net extra sediment, causing an increase in the total quantity of material that needs to be dredged. The MKO report states that theoretically the sediment trap should increase local sedimentation, yet it is hard to quantify based on calculations and measurements. In the MKO report the initial results of the implementation of the Botlek sediment trap are discussed. The first conclusion is that the border between the water and the silt layer within the trap consists of a strong density gradient, but after a few centimeters this gradient stagnates and a quite constant density can be observed towards the consolidated bed. It is concluded that the density of the material to be dredged therefore barely increases for larger sediment trap depths. The trap should however be filled as much as possible, i.e. the fluid mud layer should be as thick as possible, during maintenance dredging to prevent dilution of the dredgeable material. Conclusions about the quantitative contribution to maintenance dredging quantities remain absent.

El Hamdi (2012) investigated various mitigation measures for the Botlek harbour. Some of the mitigation measures questioned are that of a current deflecting wall, the sediment trap and the silt screen. No solutions were proposed ready to implement, but El Hamdi suggests that more research should be done for sediment traps and current deflecting walls as these are believed to result in an improvement in flow patterns and a reduction in sedimentation rates. Current deflecting walls are however not advisable, as they hinder navigation. The research done by De Bruijn (2018) suggests that the increasing trend in maintenance dredging quantities is not necessarily due to an increase of maintenance dredging quantities in general, but a relocation of these quantities from Rijkswaterstaat operating locations towards Port of Rotterdam operating locations. His proposed mitigation measure is the installation of sediment traps, but the quantification of this measure has not been investigated and further research must be conducted on this subject.

Because of the increasing costs of maintenance dredging Port of Rotterdam has brought a project to life, called the Programme Innovative Sediment MAnagement (PRISMA). The goal of PRISMA is to prevent sedimentation, predict amounts of sedimentation and optimizing the maintenance dredging strategy to tackle the harbour siltation problem. It consists of three time-spans to reduce the maintenance

dredging costs. The short-term solutions focus on more efficient dredging by making use of Water Injection Dredging (WID), creating favourable bed slopes inside port basins, making use of ebb currents and the sediment traps this research is committed to. The mid-term solutions focus on the reduction of sediment return flow by releasing sediment in a smart way, optimizing the release locations, optimizing the tidal window for the release of sediment and using sediment in an alternative re-use, e.g. for reconstruction or clay for dikes. The long-term solutions are focused on modification of an intervention protocol by revising the criteria for NGDs, sailing through fluid mud and developing (continuous) measuring equipment such as Rheotune and Graviprobe.

A research project that did quantify the sediment trap measure with a Delft3D modelling study is Van Kessel (2005), which investigated a 2m and 3m sediment trap in the Caland-Beerkanaal in the Rotterdam Waterway. The location is located close to the North Sea and therefore siltated with silt, but also marine sand enters the trap. The design of the trap can be seen as a uniform deepening of local bathymetry. The model includes average tide and salinity profiles with a constant boundary sediment concentration. Advection due to tides, density driven flows due to salinity and sediment are included in the model. Sediment is mainly driven by the interplay of tides and the stratified structure. Including a trap of 2m depth shows a significant improvement compared to the same situation without a trap. Including a sediment trap results in an increase of sedimentation within the trap location of 7 to 12 %. A net increase of 1 to 2 % over the domain is also observed. A deeper trap of 3m shows little improvement compared to the 2m trap. Therefore, Van Kessel concludes that deepening a trap even more is not very effective.

The mechanisms that determine the trapping of sediment traps are rather unknown. MKO states that the capturing of sediment is due to the reduced flow velocity, but clear mechanisms remain absent. Some experiments with sediment traps have been executed in the freshwater Markermeer by Witteveen en Bos (2005) and Vijverberg (2008). Some physical experiments were done by research of Witteveen en Bos (2005) and filling rates that were observed were much higher than theoretical calculations due to sedimentation of suspended material only. The report suggests that three possible mechanisms cause this. In the sediment trap the deepened part reduces the flow velocity as a result of which more suspended material settles. This is the main known function of the sediment trap. Apparently other mechanisms need to be investigated as well. In the deepened part, the wave effect decreases, so that the resuspension of material decreases. Possibly a density flow (mud flow) is present

at the bottom, whereby the deeper part is filled relatively quickly. These are however hypotheses and need to be researched further. Vijverberg (2008) investigated the sediment trap behaviour in this freshwater environment Markermeer with physical and numerical model tests. Vijverberg distinguishes two sediment fractions: coarse and fine material. Conclusions were that the filling of sediment traps due to fine material is entirely due to advection and settling. For the coarse material, 80 % of the filling of the sediment traps is due to advection and settling, the remaining 20 % is due to sediment induced density currents. The mechanisms of erosion and deposition are however absent in this study. Sediment does not exchange with the bottom, but remains in a dense suspension in the lowest layer of the water column. One of the recommendations of the report is to study erosion and deposition further, together with consolidation, flocculation and larger time scales.

Port of Rotterdam currently has five sediment traps installed, namely in the Botlek Harbour, 1st Petroleum Harbour, 2nd Petroleum Harbour, Eem Harbour and Waal Harbour as can be seen in Figure 1.1. Little is known of the use and effectiveness of these traps. They are not emptied regularly, used for temporal storage and they are not surveyed enough to obtain reliable analyses about the data and the functioning of the traps. Of these five sediment traps the Botlek trap is the most interesting, as large quantities of material are maintenance dredged compared to the other locations (Appendix A 'Dredging in the port of Rotterdam', Figure A.1). On top of that, its dimension are large compared to the other traps.

Research done by De Nijs (2012) is dedicated to describe the mechanisms that drive sedimentation in the Botlek harbour basin. Density currents due to salinity variations are said to be the main cause for transport of Suspended Particulate Matter (SPM) into the harbour. The buoyant fresh riverwater discharge drives a flow seaward at the surface, while the tide advects a dense near-bed seawater flow landward. The oscillating character of this saltwater mass is a phenomenon described by De Nijs as the salt wedge. For the port of Rotterdam, this salt wedge oscillates between the harbour mouth and the Botlek harbour. The interface between landward limit of the salt wedge and fresh water often experiences larger contents of SPM compared to other along-channel locations. The stratification suppresses turbulence which greatly enhances the trapping of SPM (Geyer, 1993). This up- and downward moving location of maximum SPM concentration is often referred to as the Estuarine Turbidity Maximum (ETM) (Grabemann et al., 1997). Basins located near the ETM may experience large siltation rates. The occurrence of the salt wedge and ETM have been confirmed with measurements carried out by De Nijs in the Botlek harbour.

Most sediment and hydrodynamic related problems the Port of Rotterdam encounters are currently solved with operational Operationeel Stromingsmodel Rotterdam (OSR) with SIMONA hydrodynamic models with a fine and course grid. The coarse OSR SIMONA hydromodel is the basis for the Delft3D-WAQ sediment model, which assumes one way coupling between sediment and hydrodynamics. Sediment therefore does not influence the flow, but can merely be seen as a tracer. Sediment does not update the bottom grid. The advantages of these assumptions are that long periods can be modelled for the entire port area. The model describes hydrodynamics quite well. On top of tackling sediment and hydrodynamic problems in the port of Rotterdam, OSR is used to predict discharges and salinity values. Stationary measurements are input in the system such as water levels at certain points in the harbour. The model has shown to have many applications, but even the fine grid may possibly be too large for the detailed processes going on in a small bathymetry change, e.g. the case of a sediment trap.

1.1 Aim of the study

The main objective of the research is to quantify the benefits of the implementation of sediment traps. Sediment traps should theoretically contribute to the maintenance dredging strategies, this is however hard to quantify. The driving mechanisms for harbour siltation should be understood in combination with the mechanisms that enhance the trapping of SPM in the sediment trap. To actually quantify the theory, the application of numerical models is considered. It is questioned whether the currently available one way SIMONA flow and Delft3D-WAQ models are able to represent the hydrodynamics, SPM transport and SPM entrapment around sediment traps in a sufficient matter. The shortcomings of these models have been investigated and emphasized before continuing to do simulations regarding sediment traps with these models. A Delft3D-FLOW online SED model would help to understand the degree of influence these online processes have, and therefore if they can be neglected. A survey of the currently installed Botlek sediment trap in combination with the available maintenance dredging quantities closely monitored by Port of Rotterdam yields reliable data to calibrate the model. The Delft3D-FLOW online SED model includes sediment-hydrodynamic coupling and can be used to test various shapes and sizes for the sediment traps to optimize sediment trapping. This is followed by a substantiated choice of locations of the sediment traps. Ideally, an operational monitoring and

maintenance plan would be made for the entire port of Rotterdam by implementing the most successful shape and locations in the SIMONA flow and Delft3D-WAQ models. These objectives introduce the following main research objective:

Determine if the sediment trap is an effective mitigation measure to significantly reduce maintenance dredging costs.

The general goal of the study is to gain knowledge about the application of sediment traps as a mitigation measure. Ideally, a sophisticated plan about the implementation of sediment traps is obtained in the port of Rotterdam. An excellent understanding of the mechanisms that drive the flow and transport of SPM is paramount, which should be represented by numerical models. The processes that influence the functioning and efficiency of sediment traps should be known. Based on this research objective the following research questions are proposed:

1. What are the dominant processes that drive harbour siltation?
2. What is the most relevant mechanism that determines the trapping of sediment in sediment traps?
3. To investigate the balance between mechanisms that govern the trapping of sediment in the sediment trap, are we able to set up a numerical model?
4. How much do the mechanisms contribute to the trapping of sediment in the sediment trap?
5. What shape and volumes result in an ideal design for sediment traps?

1.2 Research methodology

The current available three-dimensional hydrostatic SIMONA flow and Delft3D-WAQ models represent the hydrodynamics in the port of Rotterdam quite well. But because it does not use a two-way coupling, the influence of sediment on the hydrodynamics is absent. Sediment is however hypothesized to have an important influence on the hydrodynamics on the sediment traps scale. Therefore, a 2DV two-way coupling numerical Delft3D-FLOW online SED model is set up to include the effect of sediment on the hydrodynamics. The 2DV model serves a number of goals:

- To improve the knowledge of the dominant mechanisms that enhance the entrapment of SPM within the sediment trap.
- To analyze various designs of sediment traps.
- To improve knowledge about the shortcomings of the one-way coupling SIMONA-flow and Delft3D-WAQ models.
- To draw conclusions about an operational use and maintenance plan for a sediment trap.

At the start of the thesis the Botlek Harbour sediment trap is used as a model test for the numerical 2DV model. The trap is emptied, and not used for temporal storage of sediment to be able to follow the natural accretion of sediment. During the test period, the frequency of bathymetry surveys are increased to obtain an accurate measurement for the numerical model.

1.3 Outline of thesis

The first research question is addressed in Chapter 2 'Understanding the system', where the theoretical background of important mechanisms and processes that determine harbour siltation are elaborately explained. Three main processes are assessed as these are important to provide a solid foundation for successive modelling decisions.

Chapter 3 'Sediment trap dynamics' is dedicated to answer the second research question and explains the dominant processes that happen around the sediment trap for both hydrodynamics and sediment. Most research describe that sediment traps should function, but they never discuss the dynamics. Relations between hydrodynamics, sediment and bathymetry give a thorough understanding about the theoretical benefits of a sediment trap.

To answer the third research question, Chapter 4 'Setup of hydrostatic Delft3D-FLOW online SED model' describes the application of current model practises and sets up a numerical Delft3D-FLOW online SED model. This setup of the model is used to answer the remaining research questions.

Chapter 5 'Analysis of trapping mechanisms' is dedicated to answering the fourth research question. The chapter treats the hypothesized mechanisms of Chapter 3 'Sediment trap dynamics' in the numerical model, setup in Chapter 4 'Setup of hydrostatic Delft3D-FLOW online SED model'.

The fifth and final research question is treated in Chapter 6 'Optimization of the sediment trap design'. Mechanisms described in Chapter 5 'Analysis of trapping mechanisms' are analyzed for various sediment trap shapes to yield substantiated conclusions about sediment trap designs.

Chapter 7 'Conclusions' answers all the research questions posed in this chapter. Findings of Chapters 2 to 6 are treated in a discussion, conclusions and recommendations for further research.

Chapter 2

Understanding the system

This chapter provides literature based knowledge to understand the physics that drive sedimentation in the harbour basins of an estuarine system and is appointed to the first research question: 'What are the dominant processes that drive harbour siltation?'. First, general information is given about the mechanisms that drive hydrodynamics and govern the transport of Suspended Particulate Matter (SPM) in estuarine systems. The main mechanisms that govern the import of sediment in harbour basins are explained. Finally, some characteristics of the Botlek harbour basin are given. Larger scale dynamics, such as that of the North Sea, the coastal zone or the inland character of the estuarine system are left out of the research, as they are not within the scope of this research. For more information about the SPM concentrations in the dutch coastal zone, Suijlen & Duin (2002) describe it accurately. The three-dimensional current structure is described by Van der Giessen et al. (1990). Otto et al. (1990) discuss the physical oceanography of the North Sea.

2.1 Estuarine systems

Semi-enclosed bodies of water where inland fresh river water and saline seawater meet are referred to as estuaries. The body has a free connection with the open sea, where seawater is diluted with freshwater (Pritchard, 1967). The interaction between these water fluxes govern the exchange of water and concentration substances, i.e. salinity and SPM. Estuaries are mostly situated at convenient locations for ports as they are easily accessible. Keeping estuaries at artificial depths requires understanding of the system and the consequences of certain measures.

Fresh river run-off contributes an important input of buoyancy within an estuarine system. The Region Of Freshwater Influence (ROFI) system experiences constantly

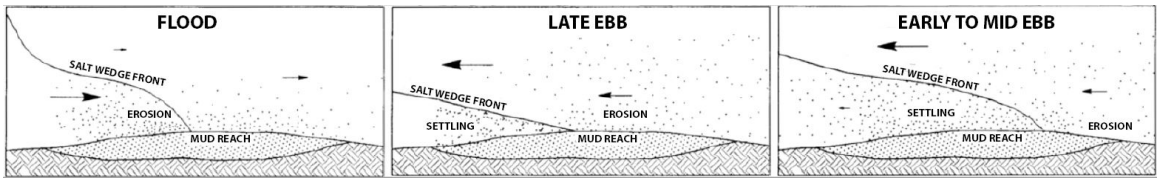

Figure 2.1: The formation of the ETM according to Geyer (1993). For very little salt water intrusion the Estuarine Turbidity Maximum (ETM) is located closer to the North Sea in the New Waterway, while for much salt water intrusion this location may penetrate inland and even reach the Waal Harbour (De Nijs, 2012).

alternating behaviour due to variations in spring-neap cycles and semi-diurnal variation of stirring and mixing of the density field due to variable river discharge, wind velocity, waves and tidal currents (Simpson et al., 1993). Understanding the mechanisms within the ROFI is of paramount importance to predict the behaviour of sediment and substances within the system. ROFIs are known to have strong density gradients in the cross-shore direction, but also density variations over the vertical are generally present. Together with wind, wave and tidal forcing stratification is established (de Boer et al., 2009). These forcings govern the water motion. Various forcings vary over time such as the differences in tidal strength between spring and neap tides, differences in freshwater discharge between freshets and droughts and the occurrence of surges. Because of the many influencing factors including their fluctuations the system can have a strong stochastic character. The horizontal and vertical density variations combined with gravity govern buoyant forces, namely the baroclinic pressure gradient and stratification. These buoyancy forces have a distinctive influence on the vertical variation of the turbulent forces and transport of SPM. Stratification gives rise to baroclinic density currents. Due to the horizontal and vertical density variations combined with gravity, an along-channel baroclinic pressure gradient governs a dense saltwater flow within the estuary near the bottom. The barotropic tidal forcing advects the saline structure back and forth. This phenomenon is referred to as the salt wedge (De Nijs, 2012) and its penetration in the harbour area can vary depending on various factors, such as the fresh-water discharge, storms at sea and tidal strength due to spring-neap cycles (Jay & Smith, 1990). The degree of stratification can vary from highly mixed conditions to strongly stratified conditions. In a strong stratification vertical fluctuations are dampened by the density gradient. This limits the turbulent mixing length. Stratification therefore induces the dampening of turbulence, resulting in less turbulent kinetic energy near the pycnocline. This results in a reduction of upward turbulent forces, causing the SPM to settle through the pycnocline. SPM cumulates in the tip of the salt wedge, where it is able to settle during small flow velocities such as slack water tide. During larger flow velocities

the tip of the salt wedge picks up sediment while eroding the channel bed as can be seen in Figure 2.1. The accumulation of the SPM in this saltwater tip is called the Estuarine Turbidity Maximum (ETM). The ETM is weakened in concentration due to the exchange with harbour basins. On top of the turbulence damping at a pycnocline, concentrated substances such as SPM and salinity in the fluid increase the fluid density according to the Equations of State (Chapter 3 'Sediment trap dynamics'). The increase in density due to these substances increases the density gradient, which in turn increases the turbulence dampening. This effect can be seen as a positive feedback mechanism.

2.2 Driving mechanisms harbour siltation

Sediment rich river water is exchanged with harbour basins, where a mild climate is present. On top of the above mentioned ETM, also water exchange mechanisms are considered important. Various flow exchange mechanisms can carry the sediment into the harbour basins. Exchange of water and SPM can be induced by three main mechanisms described by Langendoen (1994). These are the horizontal exchange by variation in flow velocities between the river and basin, the exchange governed by tidal flow and the exchange by a density difference between the water in the basin and the river water. Other mechanisms, such as exchange by wind set-up and shipping, are of minor importance to the exchange between rivers and basins according to Langendoen.

2.2.1 Horizontal exchange

At harbours that are located along a river, difference in current velocities of the river and the harbour basin may create a mixing layer. The mixing layer transfers mass and momentum between the basin and river. An exchange flow occurs across the interface between the flow outside the harbour basin and shear-induced circulation inside the basin. Turbulent eddies are able to develop in the upstream corner and are able to grow further downstream. The separating streamline is slightly directed in the harbour as seen in Figure 2.2, following from the conservation of mass for a larger river velocity than basin velocity (Vanlede & Dujardin, 2014). The location of the stagnation point is determined by the amount of river and basin water that is entrained. More entrainment results in a stagnation point deeper in the basin and wider mixing layers. Geometry plays a large role here. A circulation flow is caused by

the entrainment of water in the mixing layer. Secondary eddies are able to develop. The net exchange of water is always zero due to this mechanism.

For the transport of sediment the mixing layer and eddies are important phenomena. Entrainment processes exchange water between the basin and river, but the eddies are mainly responsible for the siltation of the basin. Sediment is able to settle in the center of the eddy because velocities are small there, also known as the teacup effect. Exchange of matter can be decreased by disabling the formation of the vortexes.

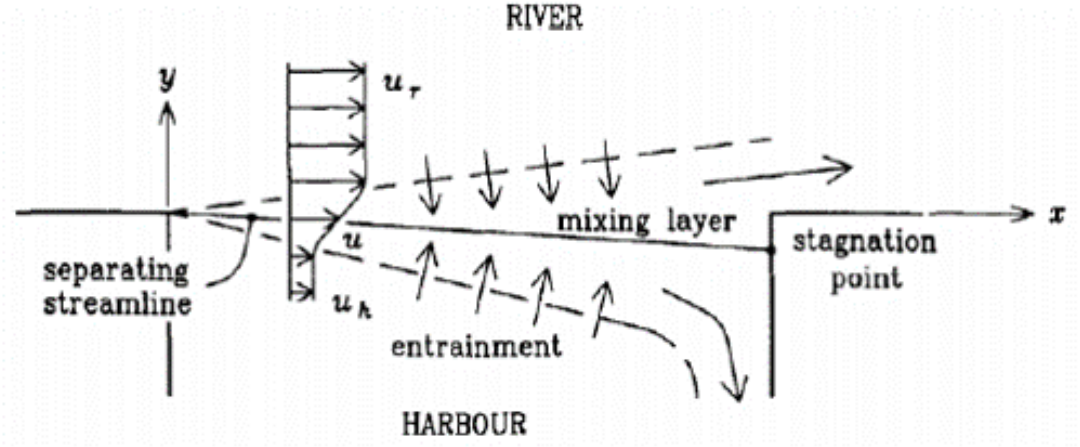

Figure 2.2: Flow velocity differences between the river and basin govern the exchange of water and SPM.

2.2.2 Tidal filling

Tidal filling is a mechanism that drives the exchange of water within the tidal basin. The tide causes a water level variation at the entrance of the basin. This water level variation causes an exchange of water between the basin and the harbour entrance. Sediment-rich water flows during rising tide into the basin. The sediment has time to settle during slack water periods and sediment-poor water flows out during ebb flow. No net amount of water is exchanged over a tidal period. A net import of sediment is however present. The mechanism plays a role in tidal rivers and along open coasts. If the x-axis is aligned with the channel-axis, the tidal propagation can be approximated with a set of one-dimensional equations. These are the balance equations for mass and momentum in x-direction (Bosboom & Stive, 2015). The full mass and momentum balance can be found in Appendix C 'Hydrodynamics by Delft3D-FLOW'. The mass balance, also known as the continuity equation, balances the volume change due to water level change and the volume change due to in- and outgoing transport indicated by terms [1] and [2] in Equation 2.1 respectively. The

momentum balance gives a balance between the momentum change, in- and outflow of momentum, pressure gradient and bottom friction indicated by terms [1] to [4] in Equation 2.2 respectively.

$$\underbrace{B\frac{\delta\zeta}{\delta t}}_{1} + \underbrace{\frac{\delta Q}{\delta x}}_{2} = 0 \tag{2.1}$$

$$\underbrace{\frac{\delta Q}{\delta t}}_{1} + \underbrace{\frac{\delta}{\delta x}\left(\frac{Q^2}{A}\right)}_{2} + \underbrace{gA\frac{\delta\zeta}{\delta x}}_{3} + \underbrace{\frac{g}{C^2}\frac{Q\,|Q|}{AR}}_{4} = 0 \tag{2.2}$$

In these equations the following parameters correspond with the basin: B is the width, ζ is the water level, Q is the discharge, A is the cross-section, g is the gravitational acceleration, C is the Chézy coefficient and R is the hydraulic radius. The discharge through the entrance can be estimated with Equation 2.3, which describes the discharge as the product of the storage area of the harbour basin A_h and the varying water level.

$$Q = A_h\frac{\delta\zeta}{\delta t} \tag{2.3}$$

2.2.3 Density driven currents

That siltation of harbour basins depends on the combination of tidal filling and emptying and density currents was first quantified by Eysink (1989). The salinity in the estuary is larger in the basin during flood and near-bed sediment-rich density currents flow into the basin. During ebb the opposite happens. The salinity in the estuary is smaller than in the basin and near-bed sediment-poor density currents flow out of the basin. Near-bed density currents transport large quantities of sediment against the direction of the gradient. Depending on the degree of stratification, sharp gradients or well mixed situations can occur. Stratification can be broken down by bed generated turbulence, local turbulence, and internal wave instabilities (De Nijs, 2012). For highly stratified situations, entrainment is the dominant sedimentation process. The peak salinity values are slightly delayed compared to peak water levels, depending on harbour geometry. The harbour basin acts as a buffer for water and salinity, where tidal forcing and salinity profiles result in stratified flows, comparable to the lock-exchange flows. The density variation over the horizontal drives a baroclinic flow, see Equation 2.4. For the entire Reynolds-Averaged Navier-Stokes equations (RANS), see Appendix C 'Hydrodynamics by Delft3D-FLOW'.

$$\frac{\delta u}{\delta t} = \frac{g}{\rho_0}\int_z^\zeta \frac{\delta\rho}{\delta x}\delta z \tag{2.4}$$

The direction of the flow velocities may vary over the vertical. This results in near-bed inflow after high water has taken place. For highly stratified situations, the dense saltwater current drives a near-bed density current, possibly opposing tidal currents. The near-bed inflow is sediment-rich, siltating the harbour basin. When the salt wedge in the river retreats further toward the harbour mouth, the salinity in the basin is larger than in the adjacent river body, driving a density driven flow out of the basin. The stratification of this flow depends again on the degree of mixing of the flow. Highly stratified situations result in a near bed outflow, containing little to no sediment. For salinity induced density currents, the effect can be visualized by looking at Figure 2.3.

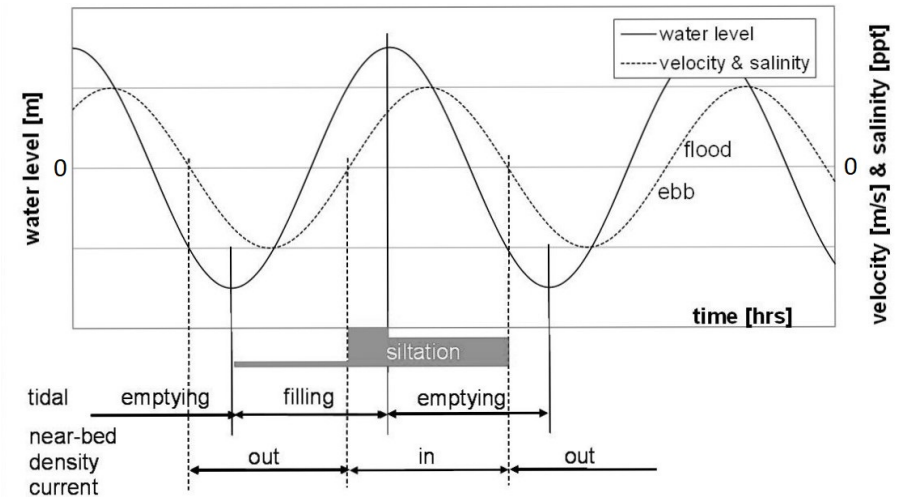

Figure 2.3: The figure shows a phase difference between water level and salinity profile. This causes an exchange process over a tidal period.

2.3 Port of Rotterdam area

2.3.1 Sediment in the port of Rotterdam

The interaction between hydrodynamics and sediment is complex, especially for very fine cohesive silt-like sediment as we are dealing with in the harbour area. The 'mud' dredged from harbour basins consists mostly of silt particles with a particle size of $< 63\ \mu m$, but may also contain various clay types, sand and organic matter (Van Vechgel et al., 1987). Generally, sand is transported as a bed load, while the smaller and more cohesive silt is transported as a suspended load. The energy needed to mobilize sediment from the bed is much larger than the energy needed to mix sediment over the water column (van Prooijen et al., 2017). No equilibrium conditions exist for the starved bed and sediment is supply limited. The sediment in the Rotterdam

port area can originate from the river Rhine-Meuse or from the North Sea. Marine sediment is brought in suspension by the bed shear stress induced by ocean waves, kept in suspension by turbulence and transported with the flow. Locations close to the harbour entrance such as Maasvlakte or Europoort are mostly siltated with marine sediment (Verlaan & Spanhoff, 2000). Locations more landward experience a combination of fluvial and marine sediment or almost exclusively fluvial sediment. Fluvial sediment is suspended by bed shear stress induced by the river current, kept in suspension by turbulence and transported by the water motion. The Botlek harbour experiences little to no influence of marine sediment and is mainly siltated with fluvial sediment (De Nijs, 2012).

Seasonal SPM variations are caused by seasonal variations in weather conditions, in particular wind, waves and river discharge conditions. Vertical transport is determined by a balance that persists between the downward settling velocity and the upward turbulent motion. Horizontal transport of sediment is determined by advection by the flow. The motion of sediment particles can be described using the advection-diffusion relation for sediment concentrations (provided in Chapter 3 'Sediment trap dynamics'). The fall or settling velocity of fines is a subject that has been researched very much and that describes how difficult the subject is. The fall velocity determines the distribution of the SPM concentration over the vertical water column, where the near-bed sediment interacts with the bed. This interaction is governed by the hydrodynamic forcing, settling velocities of the fines and the state of the bed, i.e. the (non-)cohesive character and degree of consolidation (van Prooijen et al., 2017). The mostly used formulation for this exchange is Partheniades-Krone boundary model, with formulations for erosion of well-consolidated, homogenous beds by Partheniades (1962) and deposition by Krone (1962) (provided in Chapter 3 'Sediment trap dynamics'). The settling velocity of silt particles is not easy to determine as it is a function of turbulence, degree of flocculation (depending on SPM concentration, saline concentration, depth and composition), water temperature and strength of the flocs (Van Vechgel et al., 1987). For low concentrations, Stokes' Law can be used to determine the settling velocity of a single spherical grain (Lamb, 1932) (Appendix B 'Additional formulations hydrodynamics and sediment transport'). Large concentrations may cause hindered settling. The settling velocity of a single sediment grain is reduced due to the presence of other sediment particles. This effect mostly occurs for high SPM concentrations (J. C. Winterwerp & van Kessel, 2003). One method to describe the hindered settling of velocities is the Mehta's approach (Li

& Mehta, 1998) (Appendix B 'Additional formulations hydrodynamics and sediment transport').

Flocculation is the combined effect that cohesive sediment particles aggregate to form larger particles, called flocs, or the breakup of these flocs into fine-grained sediment. The larger flocculated particles are heavier and experience a larger settling velocity. The increase in size also increases the resistance on the flocs, causing them to slow down and may cause deflocculation again. Flocculation is largely dependent on salinity difference in the water and organic content, and is a subject that is still intensively researched. In an estuarine environment, flocculation is caused by aggregation due to the overtaking of particles with a low settling velocity by particles with a large settling velocity or collisions between particles carried by eddies due to turbulent motions. Turbulent shear, on the other hand, may cause deflocculation. A network develops when the floc concentration is so high that it reached unity. As long as the concentration, therefore density, remain below a certain gelling concentration, effective viscosities are so high that the flow behaviour remains laminar. The settling velocity becomes zero. When this state is reached, generally is referred to the fluid mud layer (J. C. Winterwerp, 2002). The presence of fluid mud drives a density driven flow due to the gravity force and can cause high transport rates (Kessel & Kranenburg, 1996). When accelerating, shear and resulting instabilities at the pycnocline, i.e. the interface between the fluid-mud layer and the water column, cause entrainment of water into the fluid mud and mud particles into the water column. This causes dilution of fluid mud below the gelling concentration. The mud is now in a highly concentrated suspension and can flow turbulently.

2.3.2 The Botlek harbour

A number that can be used to predict what kind of estuary the Rotterdam port and surrounding area is, is by making use of the Estuary-Richardson Number as given in Equation 2.5. The number balances ϵq_f as a measure for the amount of work that is needed to mix the fluid with the amount of turbulent mixing created by the tide u_T^3 (Pietrzak, 2017). q_f represents the freshwater discharge, u_T the root mean square value of the tidal velocity near the river mouth, ϵ represent the relative density between the salt and freshwater and g the gravitational acceleration. Typical values of the Estuary-Richardson Number are $Ri_E < 0.08$ for well-mixed estuaries and $Ri_E > 0.8$ for strongly stratified estuaries that experience a salt wedge. The freshwater discharge through the Rotterdam Waterway is regulated to about 1500 m^3/s and tidal currents in the harbour mouth may exceed 1 m/s. A density difference of 25

kg/m3 between the salt and fresh water then results in a partially mixed to stratified environment (De Nijs, 2012).

$$Ri_E = g\frac{\epsilon q_f}{u_T^3} \tag{2.5}$$

The Botlek harbour can be described as a partially mixed to stratified environment. It has a meso-tidal character, is located 20km from the North Sea and has larger siltation rates than other inland harbours as can be seen in Figure A.1 in Appendix A 'Dredging in the port of Rotterdam'. Van Vechgel et al. (1987) pose that the large quantities of maintenance dredged material may be appointed to the occurrence of fluid mud.

For the years 2015-2017, an overview of dredged material of the Botlek harbour is shown in Figure 2.4. These years no deepening of the harbour has taken place or any other measures that would affect natural sedimentation. For the events that took place or tabled values of each dredge area, referred is to Appendix A 'Dredging in the port of Rotterdam'.

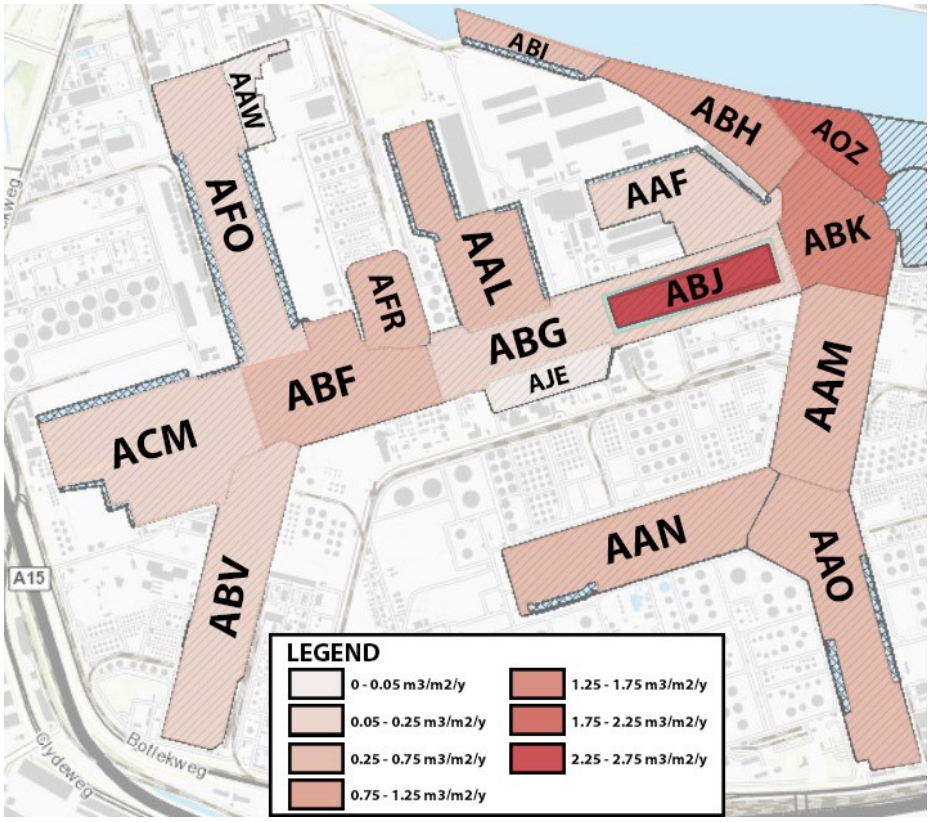

Figure 2.4: Overview of dredged material in cubic meters in hopper per surface area for the years 2015 - 2017 in Botlek port area.

Chapter 3

Sediment trap dynamics

This chapter provides theoretical background about the hydrodynamics, SPM transport and sediment entrapment around sediment traps. The chapter answers the second research question: 'What is the most relevant mechanism that determines the trapping of sediment in sediment traps?' The sediment trap, also known as the siltation trap, has as function to trap the sediment at a favourable location. Accumulation of sediment at this location is expected to increase, while accumulation at less favourable locations such as near quay walls is expected to decrease (Van Vechgel et al., 1987). The application of sediment traps in harbour basins should lead to economical benefits for maintenance dredging. Many reports such as MKO (1987), Witteveen en Bos (2005), El Hamdi (2012), lecture slides of coarse 'Sediment Dynamics' (van Prooijen et al., 2017) and De Bruijn (2018) tend to mention sediment traps as a mitigation solution, yet do not elaborate on physics. Therefore, physics are elaborated in this chapter and a first estimation is done about the importance of each of the trapping mechanisms. A closer look is taken at the description of the hydrodynamics and sediment transport processes in navigation channels by van Rijn (2005). The hydrodynamics of these channels are thought to resemble the hydrodynamics of the sediment trap well. Van Rijn also mentions this resemblance. Also a look is taken at the hydrodynamics that occur with the flow expansion over a sill as researched by Blom & Booij (1995). The fresh and saltwater exchange that occurs in estuarine environments greatly affects the flow structure. Bidirectional stratified flow is present in harbour basins, varying over each tidal cycle. Therefore theory about the internal and composite Froude number is provided, which tells us something about the hydraulic state of the flow. After the hydrodynamics have been elaborated, attention is paid to sediment transport processes and their relation with the hydrodynamics.

3.1 Hydrodynamics

While looking at the hydrodynamics of a sediment trap, the focus lies on the processes that occur in a 2DV sediment trap. The exchange of water between the river and harbour basin is governed by the tidal prism, density driven currents by salinity and horizontal exchange as explained in Chapter 2 'Understanding the system'. And Chapter 4 'Setup of hydrostatic Delft3D-FLOW online SED model'.

3.1.1 Flow expansion

3.1.1.1 Local flow velocity

The sediment trap expands the flow by having an increased depth. Transporting a similar discharge over a larger cross-sectional area results in smaller flow velocities. The 2D flow is bound by the bed and the free surface. The flow profile adapts and lower average flow velocities are present. This can be represented by the continuity equation shown in Equation 3.1, where u_i is the flow velocity and h_i is the water-depth of location 0, 1. The amount of mass that flows over the basin area without a sediment trap, indicated by subscript 0, equals the amount of mass that flows over the area with a sediment trap, indicated with subscript 1. (van Rijn, 2005) shows this in Figure 3.1 for perpendicular flow over a navigation channel, but this shows a large analogy with the 2D flow over a sediment trap. In the figure a decrease of flow velocity towards the bottom can be observed. The flow approached with a logarithmic flow distribution for turbulent steady open channel flow. In the expansion a re-circulation zone with a reattachment point is observed due to a flow separation. According to Van Rijn flow separation occurs for slopes steeper than 1:5. For sediment traps less steep slopes are present so the actual separation is not expected to occur. A deceleration on the other hand does occur. The difference is that the flow is all directed in the same direction and a re-circulation zone as in Figure 3.1 does not exist. Van Rijn describes the velocity profile inside the trap as a linear combination of a logarithmic profile and a perturbation profile F as can be seen in Equations 3.2 and 3.3 respectively. Here, A_1 and A_2 are coefficients depending on the distance from the start of the flow deceleration and t is a coefficient depending on the flow. Flow profiles are based on the surface flow component u_s. The first dominant effect of the sediment trap on the hydrodynamics can be observed:

The flow expansion caused by the sediment trap theoretically reduces the flow velocity locally.

$$u_0 h_0 = u_1 h_1 \tag{3.1}$$

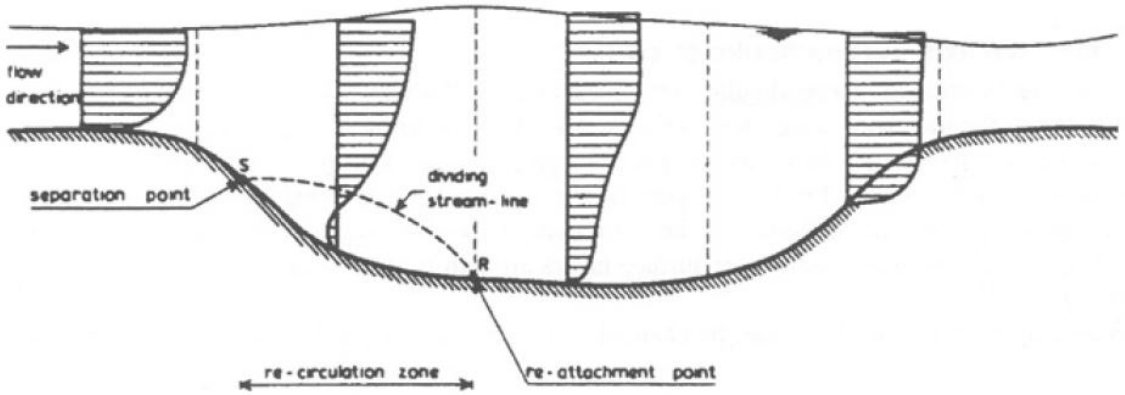

Figure 3.1: Flow characteristics after a navigation channel from van Rijn (2005). A decrease in depth averaged flow velocity can be observed.

$$u(z) = A_1 \ln\left(\frac{z}{z_0}\right) u_s + \left(1 - A_2 \ln\left(\frac{z}{z_0}\right)\right) u_s F \tag{3.2}$$

$$F = 2\left((z - z_0)(h - z_0)\right)^t - \left((z - z_0)(h - z_0)\right)^{2t} \tag{3.3}$$

3.1.1.2 Local turbulent kinetic energy

Flow separation and flow deceleration result in an increased amount of turbulence as can be seen with the analogy with the backward facing step. It is important to include turbulence as it induces an effective drag on top of the regular friction and it induces turbulent mixing, which causes suspended matter a.o. to be transported in space. Turbulent shear stress can be expressed by decomposition and averaging over the turbulent time scale of the non-linear terms in the momentum equations. The diffusive character of turbulence and formulations of a.o. the k-ϵ model can be found in Appendix C.1.1 'Hydrodynamics governing flow'. The increased depth at the start of the trap widens the flow profile and decelerates the flow. Flow deceleration and even separation results in an energy transfer to turbulence as can be demonstrated with a backward facing step. This effect is called the Carnot energy-loss in basic hydraulic engineering. Although the expansion elapses more gradually than with a sudden drop at a backward facing step, the analogy is strong. If actual flow

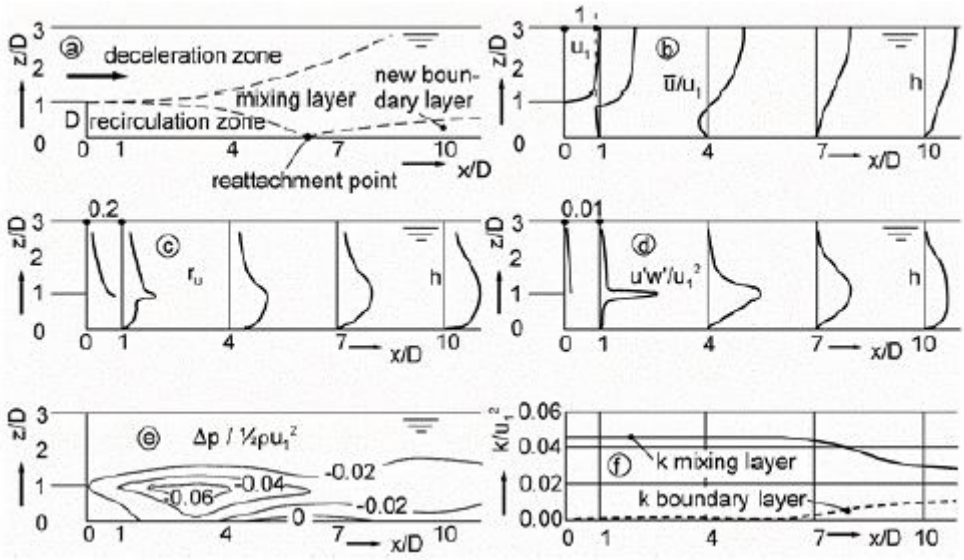

Figure 3.2: Flow characteristics after a backward facing step from an experiment done by Nakagawa & Nezu (1987). Figure a shows the characteristic areas in the flow situation. Figure b, c and d show the vertical distributions of the mean velocity $\overline{u}/u_t$, relative turbulence intensity r_u and relative turbulent shear stress $\frac{u'w'}{u_t^2}$ respectively, where u_t is the maximum time averaged velocity on top of the sill. Figure e shows the dimensionless deviations of the hydrostatic pressure combined with the velocity pressure on top of the sill and Figure f shows the transition of the turbulence in the mixing layer to the new boundary layer after the reattachment point (Versteeg & Malalasekera, 2007).

separation takes place in case of a sediment trap is questionable. Figure 3.2 shows measurements done by Nakagawa & Nezu (1987). The deceleration after widening of the flow profile results in an increase of turbulent mixing. Here, the backward facing step is a sudden expansion which results in flow separation. In the mixing layer a strong increase in turbulence can be observed with relative turbulence values of r_u = 0.35 - 0.4, expressed as $r_u = \frac{\sqrt{\overline{u'^2}}}{\overline{u}}$. After the mixing layer hits the reattachment point, a new boundary layer is build up and the flow develops to a uniform flow again. The reattachment point lies 5-7 times the height downstream of the step and experiences the most severe attack on the bottom due to the turbulence. Blom & Booij (1995) repeated the experiments for a sill with a sloping expansion instead of a sudden expansion. This experiment was carried out such that flow separation did not occur, hence no recirculation zone and a complete free mixing layer, and lower values of $r_u = 0.3$ were found. This is still an increase in relative turbulence compared to the situation before the flow expansion, where $r_u \approx 0.2$ (Schiereck, 2003). The second dominant effect of the sediment trap on the hydrodynamics can be observed:

The flow expansion caused by the sediment trap theoretically increases the turbulent kinetic energy locally.

3.1.2 Stratified flows

Locations where salt water and fresh water interact, e.g. ROFIs, stratification may occur. This stratification may typically result in two-layered, bidirectional flow defined by a strong halocline. Stratified flows that encounter a sudden contraction or expansion result in an analogous problem as the external flow of water over a barrier or drop (Long, 1954). In the latter case a control condition is expressed in terms of the squared Froude number $F^2 = u^2/gy$. The dimensionless Froude number expresses the ratio of the current velocity over the velocity of the gravity waves (Baines, 1995). The partitioning between kinetic and potential energy of the flow is described by the number. It describes the hydraulic state of the flow whether it is physically possible for disturbances to propagate upstream, called subcritical for $F^2 < 1$. If all disturbances are swept downstream, the flow is supercritical for $F^2 > 1$. The flow is considered critical for $F^2 = 1$. Here, u is the depth-averaged flow velocity, g is the gravitational acceleration and y is the fluid depth. Hydraulic jumps occur when the hydraulic state of the flow switches from supercritical to subcritical.

3.1.2.1 Hydraulic state of the internal flow

With stratified flows the determination of the hydraulic state of the flow is not as straightforward. For the determination of the Froude number of the internal flow over obstacles, many different perspectives are debated in the literature. A distinction is made between literature on two-layered flow by Armi (1986), for which the internal Froude number between the two layers of the flow is determined, and a continuously stratified flow based on literature of Winters & Armi (2012). The two-layered flow is considered first as it is easy to understand and elegantly formulated. Definitions for the continuously stratified flow are reminiscent to the two-layered flow theory. The flow is decoupled in an active flow layer, a stagnant water layer and a dynamically uncoupled layer.

Two-layered flow With two-layered stratified flows the domain of interest is the intersection between the two layers of the fluids, further referred to as internal flow. For two-layer flow a few assumptions are made: The stratification should be stable, the hydrostatic pressure assumption is valid, the density in a layer is constant and there is no mass transfer between layers (Pietrzak, 2017). The behaviour at this intersection is different from the homogeneous case for one fluid layer. Small density differences

between the fluid layers are approached with a reduced gravity. The internal waves in a two-layer fluid travel more slowly than with surface gravity waves. The pressure difference is determined by the reduced gravity g' rather than gravity g as can be seen in Equation 3.4. The amplitude of the displacement of a similar disturbing force is however larger by a factor $\frac{\rho_2}{\rho 2 - \rho 1}$ (Pietrzak, 2017). Long (1954) describes the hydraulic state of the internal flow based on the internal Froude number as given in Equation 3.6 based on the reduced gravity g'.

$$g' = \frac{\rho_2 - \rho_1}{\rho_1} g \tag{3.4}$$

Long describes the three ranges of motion for two-layers flow over a sill. The first is typically for absolutely subcritical flow. If the velocities of the layers are sufficiently small, also small internal Froude numbers describe the flow. For flow over a sill, the interface between the layers of fluids is little disturbed. If the velocities are sufficiently high the interface swells symmetrically over the obstacle. If the velocities are sufficiently high and internal Froude number as well, the interface swells symmetrically over the obstacle. This is typical for absolute supercritical flow. There may also be a transition point. At intermediate speeds a hydraulic jump occurs in the lee of the barrier and the lower layer increases in depth upstream. This is typical for supercritical flow changing into subcritical flow.

Where the backwater curve for an external free surface is determined by the external momentum and continuity equations, the internal backwater curve can be derived by the external continuity equations and the internal continuity and momentum equation (Pietrzak, 2017). The formulation of the internal backwater curve can be seen in Equation 3.5. In the equation, the slope of the interface $\frac{\delta h_2}{\delta x}$ is determined. Shear stresses are given with τ_i with subscript 0 at the surface, subscript 1 for the upper layer and subscript 2 for the lower layer. The formulation for reduced gravity is given in Equation 3.4. The discharge per layer is given by q_i and the height of each layer by h_i. When the denominator approaches zero, the slope of the interface reaches infinity according to the equation. In reality, this condition is called internally critical flow and an internal hydraulic jump occurs. If we look at 2DV flow with a constant width, i.e. to replace specific discharge q with flow velocity u, internally critical flow occurs for $\frac{u_1^2}{g' h_1} + \frac{u_2^2}{g' h_2} = 1$. The flow is critical when the denominator is zero, subcritical when the denominator is negative and supercritical if the denominator is positive. A small denominator indicates large vertical accelerations and non-hydrostatic pressure forces start to affect the flow.

$$\frac{\delta h_2}{\delta x} = \frac{\frac{1}{\rho g}\left[\frac{\tau_0-\tau_1}{h_0} - \frac{\tau_1-\tau_2}{h_2}\right] - \left[1 - \frac{q_1^2}{g'h_1^3}\right]\frac{\delta h}{\delta x}}{\frac{q_1^2}{g'h_1^3} + \frac{q_2^2}{g'h_2^3} - 1} \tag{3.5}$$

Based on the internal backwater curve the two superimposed layers of fluids are described with the composite Froude number G^2 described by Armi (1986) as given in Equation 3.7 where, $r = \frac{\rho_1}{\rho_2}$.The composite Froude number goes under the assumptions of a Boussinessq, rigid-lid, two layer flow. The last term in Equation 3.7 can be neglected for small density differences. The composite Froude number is a composition of internal Froude numbers of both layers of fluid as in Equation 3.6. The hydraulic state of the flow is subcritical for $G^2 < 1$, critical for $G^2 = 1$ and supercritical for $G^2 > 1$ as the three regimes described above. For stratified flows the fronts created in this hydraulic state can be a significant source of turbulence and mixing, even with strong stratification.

$$F_i^2 = \frac{u_i^2}{g'y_i} \tag{3.6}$$

$$G^2 = F_1^2 + F_2^2 - (1-r)F_1^2F_2^2 \tag{3.7}$$

Hydraulic jumps appear when the hydraulic state switches from supercritical with $G^2 > 1$ to subcritical with $G^2 < 1$. The flow follows the obstacle until it reaches the point where it is critical. At this point the flow switches from supercritical to subcritical. The rapidly flowing bottom layer is abruptly slowed and increases in height, converting some of the flow's initial kinetic energy into an increase in potential energy. Some energy is irreversibly lost through turbulence. The interface jumps more or less abruptly to the downstream water level. For increasing Froude numbers in the critical flow regime, the jump moves downstream and increases in intensity (Long, 1954). Figure 3.3 shows the energy switch from kinetic to potential energy in an internal hydraulic jump. Winters & Armi (2012) studied the flow of a continuous stratification over a cylinder. The flow changes from supercritical to subcritical and the same amount of energy is maintained by a larger layer depth.

The concept of layered internal hydraulics has been developed and studied. The region of motion of bidirectional flow, which can be typically observed with the exchange within a stratified basin, can be described with the composite internal Froude number G^2. A close look is taken at this Froude number.

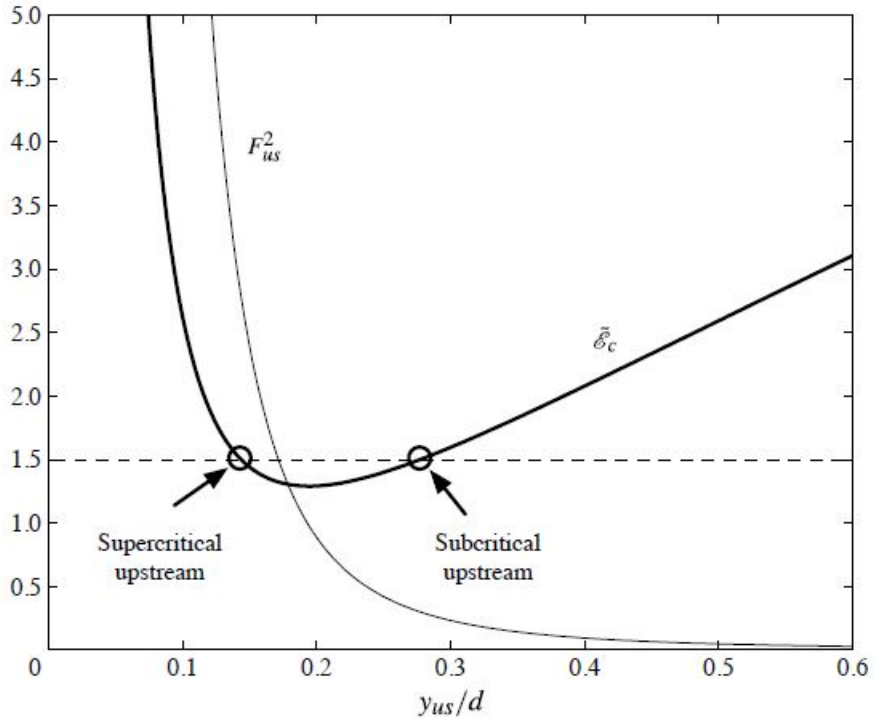

Figure 3.3: Hydraulic jump phenomenon graphically explained by Winters & Armi (2012) for continuous layered flow over a cylinder. Normalized specific energy is expressed as a function of the upstream Froude number F_{us}. y_{us} is the upstream layer depth and d the height of the obstacle.

Continuously stratified flow For continuous density gradient, i.e. with a not so strict definition of densities between layers but a varying density profile, the hydraulic flow structure can be approached by introducing an active layer, a stagnant layer and a dynamically uncoupled layer (Winters & Armi, 2012). The theory recognizes that flow well above and well below the active, accelerated layers is dynamically uncoupled. By using continuity, transport in the accelerated layers is calculated. Asymmetrical flow around an obstacle then allow us to determine the active layer thicknesses, reduced gravity and flow properties. For these layers, an integral approach for the characteristic values of the velocity and density is adopted. Details such as the distribution of the velocity and densities within these layers, mainly the active layer, are therefore sacrificed. Algebraically, this does however yield a simple and straightforward approach to determine the hydraulic state of the flow similar to the two-layered flow. For continuously stratified bidirectional flow, the above two-layered flow may not be sufficient. The theory is quite reminiscent on the other hand. Instead of having two layers, we decouple the top layer, leaving us with an active layer and stagnant layer. The active layer is the bottom layer that is accelerated over an obstacle. The stagnant layer is approached as the layer where flow velocities are ab-

sent. The active layer is averaged over its properties, yielding a flow velocity, density and layer depth. The active layer is indicated with subscript 2. The stagnant layer is defined exactly at the top of this accelerated layer, yielding a reference density. The stagnant layer is indicated with subscript 1. All flow above the stagnant layer does not influence the internal hydraulic state of the flow and is dynamically uncoupled. The internal Froude number is then calculated similarly to the two-layered flow. The internal gravity between the two layers is calculated according to Equation 3.4 and the internal Froude number for the active layers by Equation 3.6. The flow is called subcritical for $F_2^2 < 1$ and supercritical for $F_2^2 > 1$.

It must be noted that the internal Froude number given in Equation 3.6 does not represent the classical Froude number by expressing a ratio of advection to wave speed. $\sqrt{g'y_2}$ is not the propagation speed of the internal gravity wave. It is rather a balance between inertia and buoyancy (Mayer & Fringer, 2017).

A third effect of the sediment trap on the hydrodynamics is thought to be of importance:

The sediment trap changes the properties of the internal flow, which may theoretically change the hydraulic state of the flow resulting in large instabilities and even an internal hydraulic jump.

3.1.2.2 Richardson number

$$\mathrm{Ri} = \frac{\frac{g}{\rho}\frac{\delta\rho}{\delta z}}{|\frac{\delta u}{\delta z}|^2} \tag{3.8}$$

With bidirectional stratified flows the vertical shear created by the interface between the flows may be sufficiently high to disturb the interface between the flow. This can be best explained by the lock-exchange experiment. A bidirectional stratified flow is created by separating two fluids. Non-hydrostatic effects are present at the tip of the propagating front. These are typically neglected in numerical models. Whether the stratification is stable can be approached by using the gradient Richardson number as given in Equation 3.8 (de Nijs et al., 2011). The Richardson number expresses the ratio of the buoyancy term to the flow shear term. For values $\mathrm{Ri} \geq 0.25$ the water column is considered stable as the damping of turbulence balances the generation of turbulence (Miles, 1961), while for values $\mathrm{Ri} < 0.25$ Kelvin-Helmholtz instabilities

may develop and non-hydrostatic effects may be important (Pietrzak, 2017). The dynamics of the Kelvin-Helmholtz instabilities can be described by the Taylor-Goldstein equations. The differential equation describes the dynamics of the internal waves in the presence of a density stratification and shear flow. This is however left out of the scope of the research and recommended for further research.

3.2 Sediment transport processes

This section treats various sediment transport processes that may be relevant for the trapping mechanisms of sediment traps. Some trapping mechanisms are assessed and their importance is hypothesized. Sediment is vertically distributed over the water column and transported with the corresponding flow (Appendix C 'Hydrodynamics by Delft3D-FLOW'). When sediment hits the bed, it settles and is able to erode when a certain shear stress value is exceeded. With cohesive sediments dense suspension layers are able to form. The presence of sediment is able to increase the density of the liquid, resulting in density gradients that govern flow in horizontal direction. Three trapping mechanisms for the sediment trap that are hypothesized to be important are elaborated below: sedimentation of fines, erosion and deposition, and dense suspension flows.

3.2.1 Sedimentation of fines

The settling velocity of fine sediment particles is influenced by many factors. A distinction is made between the Stokes settling for low sediment concentrations, flocculation and hindered settling for high sediment concentrations in Appendix B 'Additional formulations hydrodynamics and sediment transport'. If a look is taken at the balance between the settling velocity and the upward turbulent forces on the silt, for dilute suspensions with a constant settling velocity this results in a Rouse profile (van Prooijen et al., 2017). More information about the Rouse profile is given in Appendix D 'Generation SPM time-series' as it is applied in the generation of a sediment boundary condition time series. The advection-diffusion relation for sediment concentrations is given in Equation 3.9. The rate of change [1] is determined by the advection terms [2] , settling velocity [3], diffusion terms determined by the horizontal background viscosity [4], vertical diffusion terms determined by the $k-\epsilon$ turbulence model [5] and sources and sink terms [6]. If a look is taken at the vertical distribution of sediment in the water column, the exchange over the vertical is mainly determined

by the turbulent diffusion terms, the settling velocity and by sinks and sources, that is in this case the exchange with the bed.

$$\underbrace{\frac{\delta C}{\delta t}}_{1} + \underbrace{\frac{\delta uC}{\delta x} + \frac{\delta vC}{\delta y}}_{2} + \underbrace{\frac{\delta (w - w_s)C}{\delta z}}_{3} - \underbrace{2D_h \left(\frac{\delta^2 C}{\delta x^2} + \frac{\delta^2 C}{\delta y^2} \right)}_{4} - \underbrace{\frac{\delta}{\delta z} \left(D_t \frac{\delta C}{\delta z} \right)}_{5} = \underbrace{S_C}_{6} \tag{3.9}$$

3.2.2 Erosion and deposition

The relation between the vertical mixing and settling velocity determines the vertical distribution of sediment particles over the water column. The actual exchange between the sediment fractions in the lowest layer and the bed follows erosion and deposition formulations, such as the commonly used Partheniades-Krone formulation. Bed shear stress plays a large role in the functioning of sediment traps. If the water movement exerts a large enough shear stress τ_b on the grains, sediment is set in motion. A certain critical threshold value $\tau_{c,e}$ determines if sediment that is attached to the bed is brought in suspension. A commonly used formulation for erosion is that of (Partheniades, 1962), see Equation 3.10. Bed shear stress for uniform flow is a function of the velocity squared $\bar{\bar{u}}^2$, roughness coefficient c_f and density ρ as can be seen in Equation 3.11 for uniform flow. The reduction of the flow velocity within a sediment trap would reduce the bed shear stress induced by the flow on the bed, therefore it reduces the ability of the flow to pick up sediment, i.e. erode. Turbulent fluctuations on the other hand cause fluctuations in the flow velocities, enabling the exceedence of the threshold value more often. The deposition of sediments depends on the turbulence level in the flowing water and the settling velocity. Deposition occurs when the bed shear stress τ_b is smaller than a certain threshold value $\tau_{c,d}$. Equation 3.12 shows the deposition formula from Krone (1962). More advanced formulations for erosion and deposition are also possible. An example is the two-layer system by Van Kessel et al. (2011). Here, we have a fluffy boundary layer and a solid bottom layer. Each of the layers has its own critical shear stress threshold values for erosion and deposition, resulting in a two-layer system. This is formulated in Appendix H 'Two-layer system'.

$$E = M \left(\frac{\tau_b}{\tau_{c,e}} - 1 \right) \text{ for } \tau_b > \tau_{c,e} \tag{3.10}$$

$$\tau_b = c_f \rho \bar{\bar{u}}^2 = \frac{g}{C^2} \rho \bar{\bar{u}}^2 \tag{3.11}$$

$$D = w_s c_b \left(1 - \frac{\tau_b}{\tau_{c,d}}\right) \text{ for } \tau_b < \tau_{c,d} \tag{3.12}$$

3.2.3 Dense suspension flows

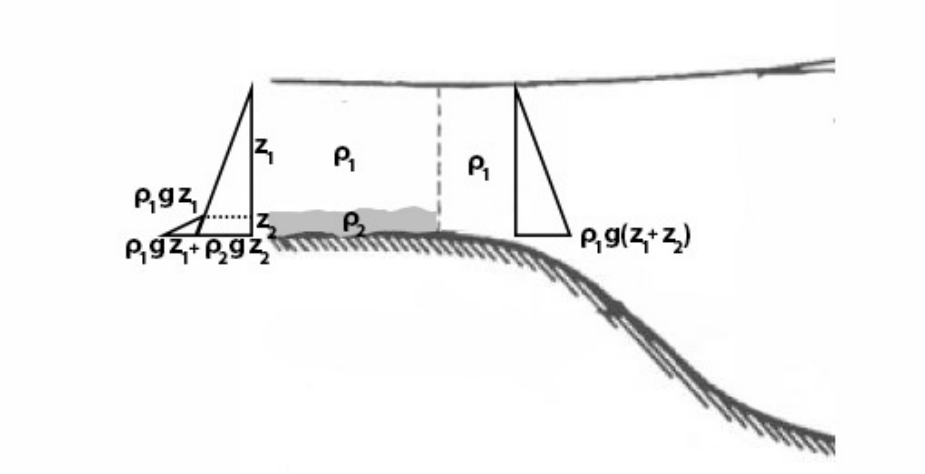

Figure 3.4: A horizontal impulse balance shows the forces driving the dense suspension flow (Kranenburg, 1998).

Sediment concentrations increase towards the lower part of the water column. On top of temperature and salinity also high concentrations of sediment that are typically located near the bed, increase the corresponding density of the water according to the Equations of State. The Equations of State relate various properties of state of the fluid to each other. An elaborate approximation such as the commonly used 1980 UNESCO algorithm, also known as the EOS-80 algorithm, can be found in (Gill, 1982), or a simpler approximation for a single sediment fraction can be used in Equation 3.13 (J. C. Winterwerp & Van Kesteren, 2004). This approximation would suffice for the applications in this report. $\rho(S,T,c)$ is the density of the water as a function of temperature T, salinity S and sediment concentration c, ρ_w is the water density and ρ_s is the solid density of the mud.

$$\rho\left(S,T,c\right) = \rho_w\left(S,T\right) + \left(1 - \frac{\rho_w(S,T)}{\rho_s}\right) c \tag{3.13}$$

The density gradient in combination with gravity governs baroclinic driven flows near the bed in the direction of the basin. The governing terms in the 3D momentum equation are given in Equation 3.14, or more elaborately in Appendix C.1.1 Hydrodynamics governing flow. The high concentrations near the bed and sediment may be able to consolidate and form a fluid-mud layer.

$$\frac{\delta u}{\delta t} = \frac{g}{\rho_0} \int_z^\zeta \frac{\delta \rho}{\delta x} \delta z \tag{3.14}$$

Near the edge of the sediment trap the gradient in density may be large. The area next to a trap may have a large concentration near the bed, while this layer above the trap is absent for the same depth. The density gradient governs flow of the dense suspension layer towards the trap. To give a rough description of the flow velocity of the dense suspension flow, the approach of Kranenburg (1998) is used. The method is adapted to fit the dense suspension flow in the sediment trap. The Bernoulli equation is used for the locations with the dense suspension and just at the start of the trap. The horizontal impuls balance that drives the flow is shown in Figure 3.4. A dense suspension with density ρ_2 flows at the bottom of the water column with water density ρ_1, such that $\rho_2 > \rho_1$. The Bernoulli is constant in the general form along a streamline (Kranenburg, 1998). Analytical derivations are done by Vijverberg (2008) for a situation without friction and by Kranenburg (1998) with friction. Solving the Bernoulli equation including bed friction yields the average flow velocity of the dense suspension layer u_c as seen in Equation 3.15. $\Delta\rho$ is the relative density given by $\Delta\rho = \frac{\rho_2 - \rho_1}{\rho_1}$.

$$\overline{u_c} = \frac{1}{2}\sqrt{\Delta\rho g z_2} \tag{3.15}$$

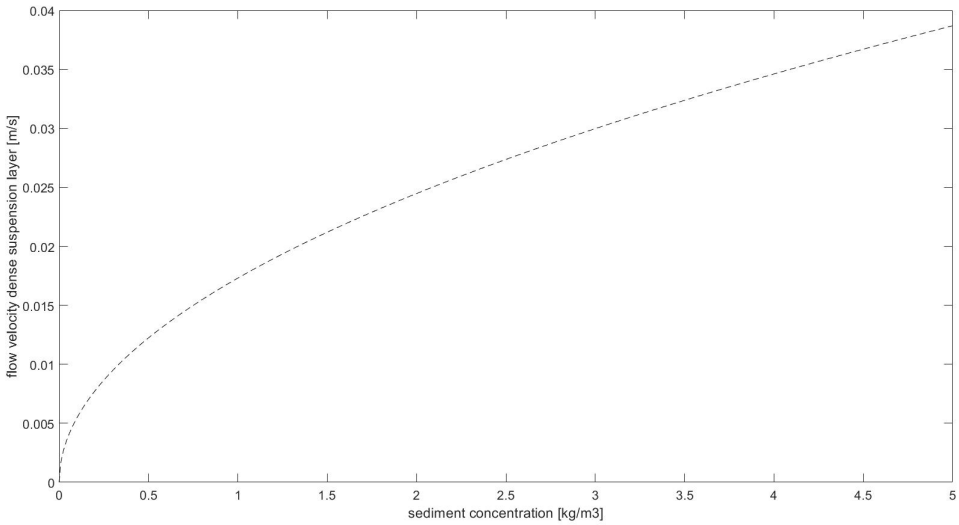

Figure 3.5: The relation between the sediment concentration and the average flow velocities of the dense suspension layer. An increasing sediment concentration increases the dense suspension flow velocity considerably.

If we would combine the Equation of State in Equation 3.13 with the average flow velocity for the dense suspension layer of Equation 3.15, a relation between layer concentration and propagation velocity can be plot. This is done for a suspension layer of 0.20 m as can be seen in Figure 3.5. The flow effect of dense suspension

layers may be small. Measurement from De Nijs (2012) show concentrations of order $1kg/m3$, while for fluid mud layers where the complete damping of turbulence occurs concentrations of tens to a few hundred $kg/m3$ may occur (J. C. Winterwerp & van Kessel, 2003). For concentration values from 10 to 200 $kg/m3$ average flow velocities of the dense suspension layer u_c may vary from 0.05 to 0.25 m/s respectively. The focus here lies however on the impact of the lower concentrated dense suspension flows.

3.3 Hypotheses trapping mechanisms

In this section the sediment transport processes from the previous section are related to the sediment trap. The mechanisms that are treated are the sedimentation of fines, erosion and deposition, and dense suspension flows. Each of the mechanisms are hypothesized on how they would significantly contribute to the trapping of fines in the trap compared to a situation without trap. It is important to make this distinction, as sediment is known to settle in a harbour basin anyway. The function of the sediment trap is to enhance the trapping of fines in a favourable way.

3.3.1 Sedimentation of fines

The vertical distribution of SPM over the water column is a balance between upward turbulent mixing and downward settling velocity. Sediment traps are located in mild conditions, such as the entrance of a harbour basin to prevent sediment from reaching the quay walls or other difficult to dredge areas. Sediment is trapped in the sediment trap by sedimentation of fines if the sediment is able to settle fast enough to reach the bottom before the end of the sediment trap. The settling of sediment can be determined using Stokes' law for spherical objects, but can be influenced by many processes such as hindered settling and flocculation (Appendix B 'Additional formulations hydrodynamics and sediment transport'). Sediment that is moved to milder conditions, i.e. from a turbulent river to a mild harbour basin. This transition results in a reduction of upward turbulent mixing and sediment redistributes over the vertical. This effect occurs regardless of the sediment trap. The sediment trap however may have a trapping enhancing property. The reduction of the local flow velocity may give the fines more time to settle. The effect of the increased settling time due to a local flow velocity reduction would increase the sedimentation of fines. On the other hand, the flow deceleration increases local turbulent kinetic energy. The increased turbulent eddy viscosity energy increases upward forces on the sediment.

Increased turbulent eddy viscosity stirs up the sediment over the water column, redistributing the sediment higher in the water column. The effect of the increased turbulent eddy viscosity due to the flow deceleration decreases the sedimentation of fines. On top of the contradictory effects of the flow deceleration, the actual capturing of fines due to sedimentation is hypothesized to be small. Settling velocities may be of the order mm/s while the flow velocities in the water column above traps may be orders of magnitudes larger, i.e. of the order m/s. The dimensions of a silt trap become prohibitive if large parts of the passing fines should be caught. This decrease in flow velocity is however expected to be very small compared to the occurring flow velocities and would therefore only marginally increase capturing of fines due to an increased settling time. Perhaps the effect of sedimentation of fines may be of importance for a basin with low flow velocities, and a drastic decrease of flow velocities due to the presence of a sediment trap. Generally, this is not the case. Both the mechanism of sedimentation of fines is hypothesized to be small, as the improvement of this mechanism due to the installation of a sediment trap. The effect of a sediment trap on the sedimentation of fines is therefore hypothesized:

The sedimentation of fines due to the presence of a sediment trap is hypothesized to not significantly improve compared to a situation without sediment trap.

3.3.2 Erosion and deposition

The flow deceleration may play a more dominant role for the determining of bed shear stresses. Lower flow velocities result in lower bed shear stresses as in Equation B.2. Large turbulent quantities on the other hand may increase the bottom shear stresses. Increased turbulence causes larger fluctuations in the flow velocity and therefore the threshold value for erosion is exceeded more often. it is hypothesized that bed shear stress values are larger near the edges of the sediment trap, and lower in the middle of the trap compared to the situation without trap. The effect of increased bed shear stress is expected to be significant for locations close to the edges of the sediment trap as flow deceleration may be significant there. The reduction in local flow velocity reduces the local bed shear stress at locations in the trap that are not close to the edges. For basins where sediment is continuously deposited and resuspended, this may play a significant role. The erosion deposition formulation would only be applicable for sediment trap locations where adequate flow velocities are present. If flow velocities are very low, the critical threshold for erosion would not be exceeded

and the mechanism is of minor importance. Sedimentation is expected to increase in the middle of the trap due to the low bed shear stresses, but at the same time sediment is expected to erode near the edges. Based on this hypothesis, it would be logical to assume that a longer sediment trap would function better.

The enhanced trapping of a sediment trap due to the erosion deposition mechanism is hypothesized to be significant for an adequate long sediment trap in a basin where tidal flow velocities are substantial.

3.3.3 Dense suspension flows

The dense suspension flows are driven by a gravity term. The creation of an overdepth by the installation of a sediment trap is therefore expected to result in larger trapping quantities. The sediment flows due to a density gradient in the direction of the trap. A question that rather rises is if these dense suspension flows or fluid mud flows are present at all times. Fluid mud is hypothesized to be caught almost entirely in the sediment trap, so dependent on if it is actually present this could be a very effective strategy. The shape and dimensions of the trap are thought to be of minor importance. Perhaps a more gradual shape would reduce the amount of resuspension from the dense layer in the water column, but this effect is hypothesized to be small. This result in the final hypothesis for the trappng mechanisms:

The enhanced trapping of a sediment trap due to capturing of dense suspension flows is hypothesized to be significant for any shape of sediment trap, given that it has an overdepth.

Chapter 4

Setup of hydrostatic Delft3D-FLOW online SED model

In this Chapter the setup of the numerical Delft3D model is treated. It is dedicated to answering the third research question: 'To investigate the balance between mechanisms that govern the trapping of sediment in the sediment trap, are we able to set up a numerical model?' The model is set up as a 2DV simplification of the Botlek south-west basin, where the sediment trap is currently installed. The idea of the model is to keep it simple to emphasize on dominant trapping processes. Step by step the model is built up to represent the governing mechanisms that trap sediment in the sediment trap as explained in Chapter 3 'Sediment trap dynamics'. First the grid dimensions are treated and why specifically these dimensions are chosen. Afterwards boundary conditions are imposed that govern the hydrodynamics of the model. Finally, sediment is added to the model. Once the model is up and running, a representative set of parameters is chosen to run simulations of various shapes with in Chapter 6 'Optimization of the sediment trap design'. This chapter focuses solely on the setup of the model. Hydraulic analyses, parametrization of sediment scenarios and the functioning of the sediment trap is treated in Chapter 5 'Analyses of trapping mechanisms'. Rome was not built in a day, and neither was this model. For the challenges that had to be faced and how these are solved, the reader is referred to Appendix G 'Model challenges'.

4.1 Setup of the model

4.1.1 Grid dimensions

The basin is modelled as a rectangular box, with 877 equidistant cells of 10 m in the x-direction (8770 m) and 2 equidistant cells of 128 m in the y-direction (256 m),

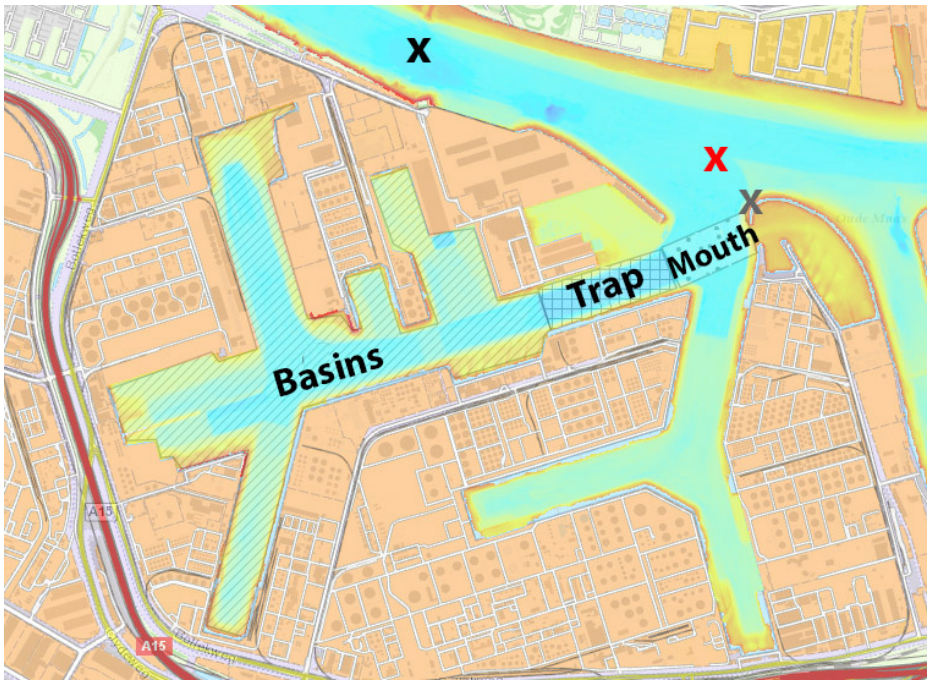

Figure 4.1: A depth coloured map (Port of Rotterdam, 2019) represents the setup of the model. The 3D areas 'Basins', 'Trap' and 'Mouth' have been transposed to a 2DV model. Crosses indicate the locations where the boundary conditions are taken from. The black cross indicates the location where sediment measurements done by (De Nijs, 2012) were done, which is the basis for the SPM time series. The grey cross indicates the location inside the Geulhaven where the water level is measured for the simulation period. The red cross shows the location from which the calculated salinity values from OSR are used.

excluding the dummy cells. The left boundary is an open boundary where water level, salinity and SPM concentration timeseries determine the hydrodynamics and transport of substances. The right boundary is a closed boundary. The first 4 cells are cells where no exchange of sediment with the bottom takes place and are added to prevent adaptation of the morphological change on the boundary conditions. The reference depth is chosen at 16.5 meters to represent the current Botlek depth corresponding with the input salinity and water level values. Depths inside the sediment trap area vary. The model domain can be seen as three areas, further referred to as areas 'mouth'. 'trap' and 'basins'. The first area 'mouth' is from cell 1 until 39 (0 to 390 m). Area 'mouth' represent the distance from the boundary conditions to the start of the sediment trap. The depth of this model area is 16.5 meters. The boundary conditions are the water level, salinity profiles are all based on simulations in the Geulhaven by the Operationeel Stromingsmodel Rotterdam (OSR) indicated with the red cross in Figure 4.1. The SPM boundary conditions are based on measurements from (De Nijs, 2012) at the location marked with the black cross. The second area 'trap' is the area from cell 40 until 119 (400 until 1190). This is the location where the sediment trap currently is located. This is the main area of interest where various

depth profiles can be tested. The third area 'basins' is the area from cell 120 to last cell 877 (1200 to 8770 m). This area behaves as the basin area behind the sediment trap and is required to obtain a similar tidal prism to the Botlek harbour case. It represents the storage area of the basins. The dimensions of the grid are chosen in such a way that the total exchange of water over the sediment trap equals that of the Botlek Harbour basin (Appendix A 'Dredging in the port of Rotterdam', Table A.1). The 2DV simulation grid cross-section then looks like Figure 4.2. In the figure the entire domain is shown, onward the domain of interest are the first 1500 m to enable higher resolution for the areas where the mouth and the trap are located. The computations were done with 20 vertical sigma-layers as vertical resolution is important to serve the goals of the numerical model. Table 4.1 shows the layer distribution, where resolution is increased towards the bottom as these layers are of major importance for the sediment transport within the water column and with the bed. The ratio between two adjacent sigma-layers is always well below the safe limit of 1.5 as advised in the Delft3D-FLOW manual (Delft Hydraulics, 2006).

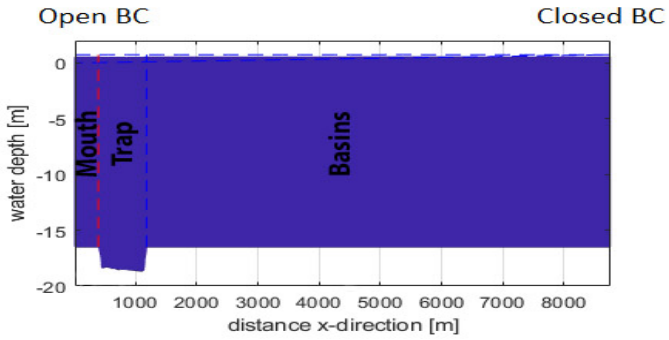

Figure 4.2: The 2DV grid used for the numerical model of the Botlek situation as in Figure 4.1. The left boundary represents the open boundary where the salinity, SPM and water level timeseries govern the water motion.

layer no.	thickness [%]	layer no.	thickness [%]	layer no.	thickness [%]	layer no.	thickness [%]
1	2.38	6	12	11	5.55	16	1
2	3.4	7	12	12	3.95	17	0.71
3	4.9	8	12	13	2.8	18	0.5
4	7	9	10	14	2	19	0.35
5	10	10	7.8	15	1.41	20	0.25

Table 4.1: The vertical layer distribution of the simplified Botlek model. Layer 1 is at the surface, layer 20 at the bed.

4.1.2 Hydrodynamic boundary conditions

The first step after dimensioning the grid is by imposing boundary conditions on the open boundary. The open boundary imposes tidal barotropic forcing in the form of

water level elevations, and baroclinic forcing due to salinity and SPM profiles. The SPM and salinity substances at the boundary are transported with the corresponding flow. Sediment will be stalled for now, and the focus lies on the hydrodynamics due to the barotropic tidal forcing and the baroclinic forcing due to salinity. The water level, given in Figure 4.3 consists of measurement done with a stationary measurement point inside Geulhaven, shown with the grey cross in Figure 4.1. The salinity profile originates from SDS-output files computed with the current OSR model for the period of 20th of August 2018 until 1st of September 2018, where the first 4 days are used to spin up the initial conditions of the 2DV model. The location of the calculation grid cell of the profile is indicated with the red cross in the figure. The water level in combination with 3D profiles of salinity imposed on the model are given in Figure 4.5. The spin-up is followed by 8 days of simulation with 16 tidal periods where morphological changes take place. The period is characterized by a below mean discharge of 800 $m3/s$ at Lobith compared to the average discharge of 23s00 $m3/s$ and a dry period, enabling the salt wedge to penetrate further inward and resulting in above mean salinity values. Largest salinity values are observed between 23th and 25th of August, The salinity levels are considerably high between 20th of August and 25th August, around 28th of August and around 30th of August. 28th of August corresponded with a spring-tide. Around the spring-tide a strong tidal forcing can be observed, which will be used later in the research. However, the spring-tide does not necessarily correspond with the largest salinity levels. As explained in Chapter 2 'Understanding the system' a larger river discharge suppresses the salt wedge, reducing its ability to penetrate further inside the harbour. The discharge in the Rotterdam Waterway is given in Figure 4.4. A large resemblance can be seen with the water level as the tide suppresses the fresh water discharge. Water actually flows in landward direction with each flood. Low river discharges are present for the period of 20th of August until 24th of August. For this period the salinity values in the boundary profile are large. From 25th of August and onward, the river discharge increases considerably, and salinity values are somewhat milder. We can see that the salinity profile is about 3 hours out of phase with the tidal forcing. A combination of tidal filling and density driven currents as explained in Chapter 2' Understanding the system' explains this exchange behaviour, but this is further assessed in the next chapter.

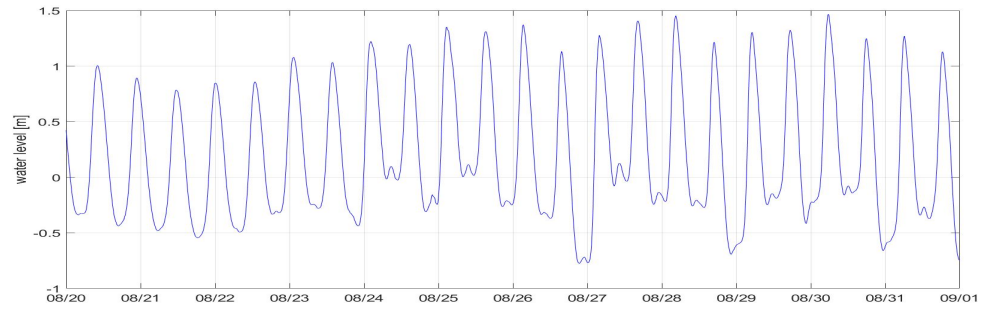

Figure 4.3: The water level boundary condition used at the open boundary. The boundary condition is from measurements done inside Geulhaven indicated with the grey cross in Figure 4.1 from 20th of August until the 1st of September.

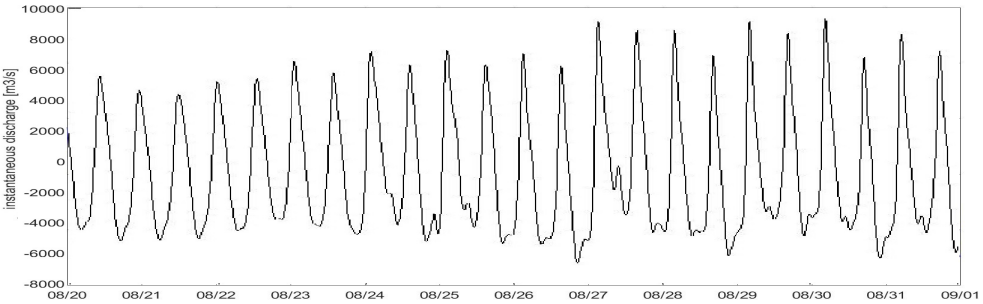

Figure 4.4: The calculated discharge as calculated by Operationeel Stromingsmodel Rotterdam (OSR) through the New Waterway for the simulation period from 20th of August until the 1st of September. A strong dependence on the tidal signal can be observed. The values are not used in the model, but show the dependence of the strength of the salt wedge on the river discharge.

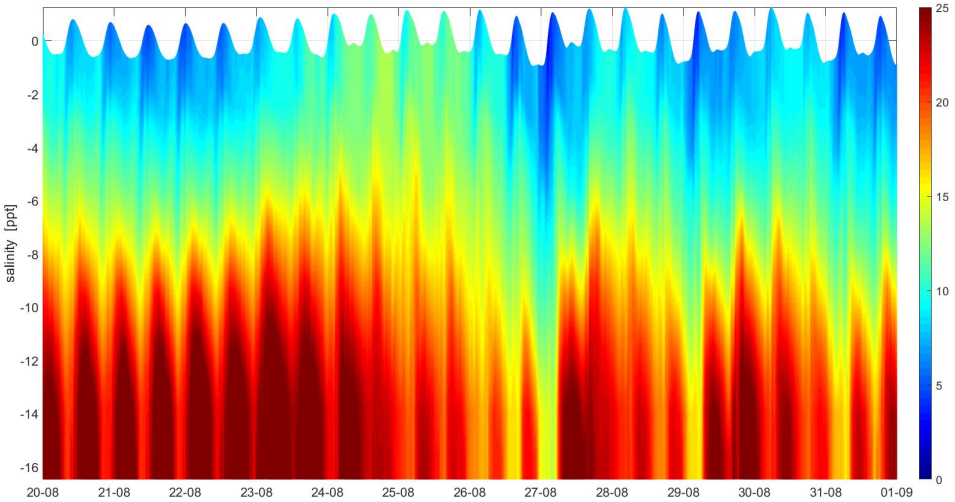

Figure 4.5: The imposed salinity 3D boundary condition. The simulation period from 20th of August until the 1st of September is calculated by OSR at the location indicated with the red cross in Figure 4.1.

4.1.3 Sediment

Now that the hydrodynamics are implemented, it is time to add sediment to the model. While the modelling of hydrodynamics is quite straightforward, modelling sediment transport correctly is rather difficult. Generally sediment studies show that actual results may differ quite much from the predicted simulations. Sediment transport may seem a stochastic process as it is influenced by many processes and characteristics. But also in the modelling practise many uncertainties hold. The determination of various parameters took many simulations and literature research. This is not included in the main report for brevity. The extensive determination of each of the parameters is provided in Appendix E 'Parameterization of the model'. Sediment is modelled as a one sediment fraction with a settling velocity of 0.6 mm/s, which is only transported as a suspended load. Other effects that influence the settling velocity such as flocculation and hindered settling are absent in the model. These processes may however influence the harbour siltation to quite a large extent, the main goal is to quantify sediment differences based on the dominant mechanisms explained in Chapter 3 'Sediment trap dynamics'. These are the density driven flows due to sediment content, vertical displacement due to turbulence and settling and erosion/deposition. For these mechanisms a crude approximation by just a single constant settling velocity suffices. To mimic the behaviour of the salt wedge with its corresponding ETM, the SPM time series at the open boundary are generated based on the measurements of De Nijs (2012). A Rouse profile for sediment is applied to the saline part of the water column for the salinity time series from OSR resulting in the variable SPM timeseries in Figure 4.6. Sediment is only present in large concentrations at the tip of the salt wedge as De Nijs argued and confirmed with his field surveys. No equilibrium conditions exist for the starved bed conditions and sedimentation transport is supply limited. Starved bed conditions imply that there is no initial sediment present in the bed, except for sediment that enters through the boundaries. Sediment is transported as washload and depends on the availability of sediments. Sediment enters the model domain through the left open boundary. Concentrations in the water column and sediment on the bed is limited by the sediment influx and outflux imposed by hydrodynamics. The transport of mud inside the domain is a delicate balance between the phasing of flow velocity and available sediment concentrations at the boundary. As the ETM is the main source of siltation of the Botlek harbour (De Nijs, 2012), its effect is modelled as closely as possible. Many modelling researches such as Van Kessel et al. (2011) and J. C. Winterwerp &

van Kessel (2003) impose a constant sediment boundary condition. Inflow of sediment with each tide may result in overestimation of sediment inflow. De Nijs (2012) emphasizes the dependence of sediment supply on the salt wedge. Measurement show that sediment is only present within a three hour time period corresponding with the salt wedge propagating inward. In Appendix D 'Generation SPM time-series' these measurement are used to generate a SPM time series as model input. The water and salinity profile closely resembles the profile from OSR. Since very little information about sediment profiles in the port of Rotterdam is known, the field data of De Nijs is used to generate a SPM time series. The concentrations are only available at NAP-3m near the surface and NAP-12m near the bed. The SPM time series is fit to have the same tidal phase dependency as the field data of De Nijs, and a Rouse profile is applied to the saline structure in the water column. The Rouse profile for a settling velocity of 0.60 mm/s results in a nearly homogeneous distribution over the water column. The upper part of the salt wedge over the vertical is set at 17 ppt. A Rouse profile has been applied to the concentration measurements of De Nijs until the pycnocline of the salt wedge to mimic trapping of large sediment concentration in the salt wedge. The resulting SPM time series then looks like Figure 4.6. A more extensive description of the generation of the variable SPM boundary condition as seen in the figure can be read in Appendix D 'Generation SPM time-series'.

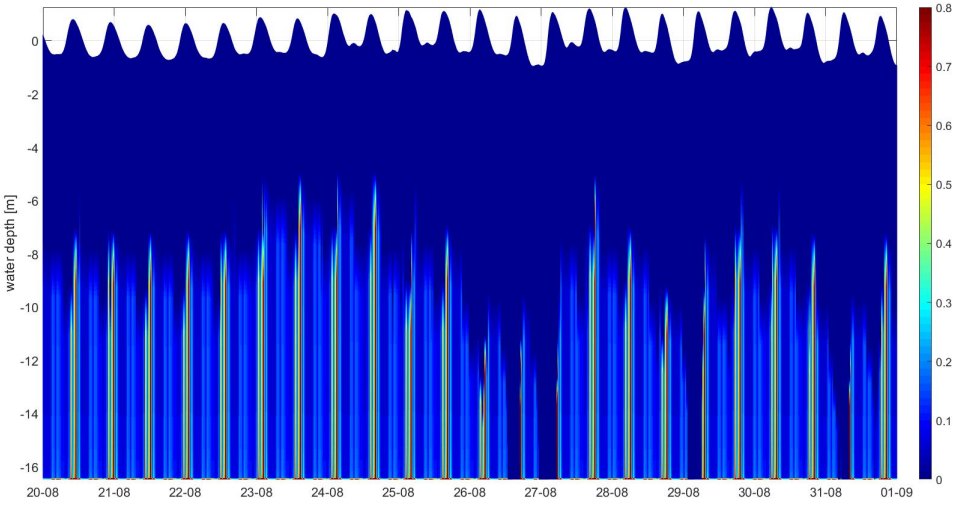

Figure 4.6: Suspended Particulate Matter (SPM) 3D boundary condition generated (Appendix D 'Generation SPM time-series') to correspond with the Estuarine Turbidity Maximum (ETM). Large concentrations of sediment are present during peak salinity values. Concentrations are in kg/m^3.

The main parameters for sediment were determined and we are left with unknowns for erosion/deposition, namely the erosion parameter M, critical shear stress for ero-

sion $\tau_{c,e}$, critical shear stress for deposition $\tau_{c,d}$ and deposition efficiency parameter DepEff for fluid mud. For the determination of critical shear stresses for erosion and deposition some nifty modelling applications are used based on advice of experts of Deltares. As determining critical shear stresses for erosion and deposition and the erosion parameters is a tough job without soil measurements, the amount of calibration parameters are minimized. The critical shear stress for deposition is set to a value of $\tau_{c,d} = 1000\ N/m^2$. In other words, sediment will always deposit as soon as it hits the bed as the critical shear stress for deposition is never exceeded. By using this method only the erosion parameter M and critical shear stress for erosion $\tau_{c,e}$ require calibration. The latter is done by first looking at determined critical shear stresses for erosion based on (van Rijn, 2005) for estuaries. A range of possible shear stress values is obtained for various degrees of consolidation in bed. For the dynamic environment described in the model, sediment is assumed to be moved regularly. The lower limit of the range is therefore analyzed with runs with hydrodynamics only for a simulation with and without trap. The frequency of exceedence for the entire simulation period of certain shear stresses are compared and a constant value of $\tau_{c,e} = 0.18\ N/m^2$ is used for the parameterization of the erosion parameter M. Please note that because of the constant value for the critical shear stress for erosion, consolidation effects have no influence on the shear threshold value. Whatsoever consolidation effects are not taken into account at all in the model. The critical shear stress is chosen as a constant value and the erosion parameter M is varied for the parameterization of erosion, because increasing erosion parameter M linearly increases the erosion, while this does not hold for varying the critical shear stress as can be seen in the formulation by Partheniades (1962) in Equation 3.10 in Chapter 3 'Sediment trap dynamics'. It is an easy and effective way to compare various erosion scenarios with each other. The same has been done for various 'fluid mud scenarios' as they are referred to from now on for various deposition efficiencies. Although they are called fluid mud scenarios, it is still a highly simplified form of fluid mud as only dense suspension flows and delayed deposition are taken into account. Processes such as flocculation and hindered settling are not taken into account. The fluid mud scenarios actually mean that a Deposition Efficiency DepEff is not equal to one. Sediment has a delayed deposition to the bed and dense suspension layers are formed in the lowest layers of the water column. According to the Equation of State in Chapter 3 'Sediment trap dynamics' the corresponding density of the flow increases and a density gradient in the horizontal is present, governing dense suspension flows. The parameterization of the erosion parameter M is done with $\tau_{c,e} = 0.18\ N/m^2$ for no, little, moderate, substantial and

lots of erosion with $M = 0, 0.0002, 0.0005, 0.0008, 0.020$, respectively. Varying these parameters change the behaviour of sediment to be more erosion driven or fluid mud driven. In Chapter 5 'Analyses of trapping mechanisms' the parameterization thus determination of these parameters is included. Here, also the impact of the sediment trap on settling/deposition only, erosion and fluid mud scenarios are treated.

During the parameterization, the variable SPM time series showed unpredictable results in the domain. This is undesired for the assessment of the various trapping mechanisms. This is more extensively treated in the next chapter. The variable SPM boundary condition has therefore been replaced with a constant distribution of sediment concentrations over the layers after the parameterization of erosion parameter M and fluid mud parameter DepEff. Although this results in a less realistic representation of reality considering the ETM, the results are more straightforward, less stochastic and the exchange of sediment with the boundary is dependent on the exchange of water due to the hydrodynamics. The new SPM boundary condition is given in Figure 4.7, which is basically an arbitrary Rouse profile (Appendix D 'Generation SPM time-series' for the given parameters to fit sediment quantities from the survey data.

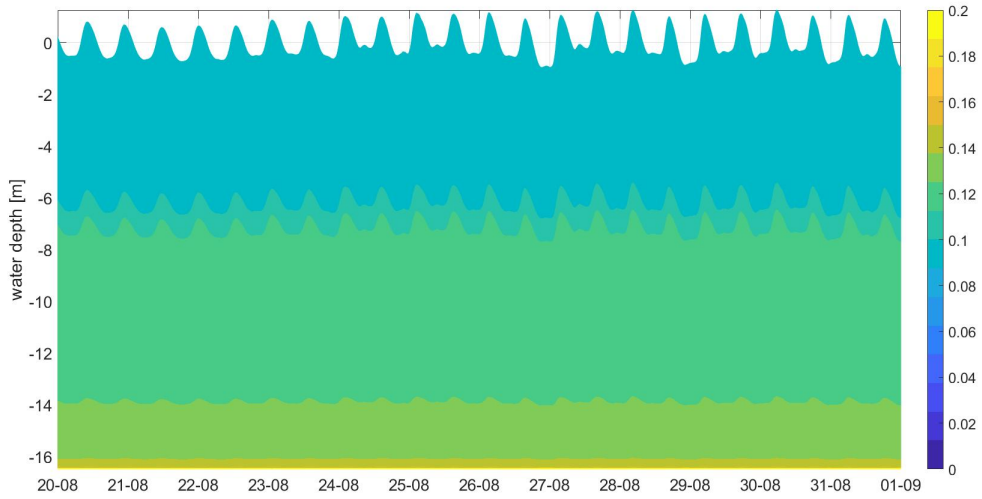

Figure 4.7: Suspended Particulate Matter (SPM) constant boundary condition to correspond with similar total sediment entering the domain as the variable SPM boundary condition. Concentrations are in kg/m^3.

4.1.4 Calibration

Every model is a simplified form of reality. To gain some insight in the representation of the model, e.g. the accumulation pattern, sediment quantities et cetera, the

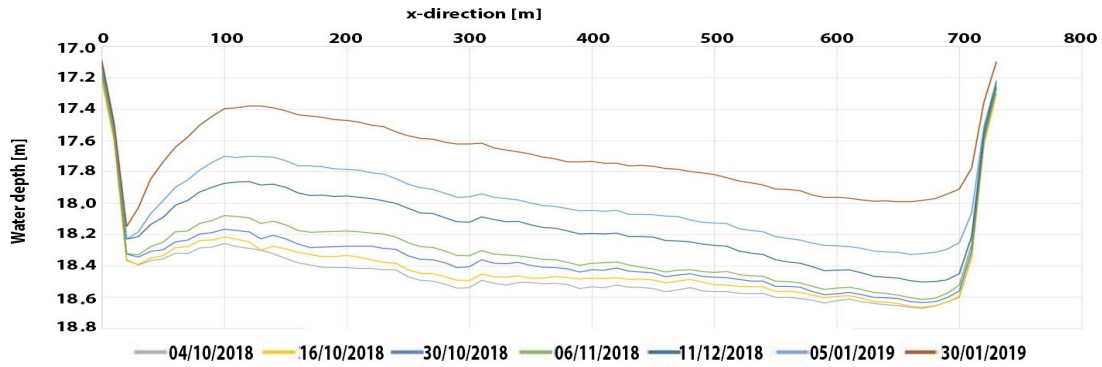

Figure 4.8: Averaged bathymetry profiles for each of the bathymetry surveys for the polygon as given in A.2 in Appendix A 'Dredging in the port of Rotterdam'.

following calibration possibilities are used:

- A 2-4 weeks repeating Echosounder Multibeam survey over a period of 118 days of the Botlek Harbour.
- Maintenance dredging quantities of the Botlek Harbour over the years 2015 - 2017 when no interventions were executed.

A 118 days survey with a frequency of 2 to 4 weeks was done for the Botlek sediment trap. A 118-day Echosounder Multiebeam survey of the Botlek harbour was executed when no dredging activities were executed and accumulated sediment can be described to natural sedimentation only. A rectangle polygon was drawn over the sediment trap and values were averaged over the width to result in a 1D updating bottom over the survey time period, shown in Figure 4.8. More information about this survey can be found in Appendix A 'Dredging in the port of Rotterdam'. Remind that the x-direction is way larger than the y-direction so the actual slopes are not as steep as they seem in the figure. The pattern shows a sort of natural stacking of sediment. Fluid mud behaviour, where sediment would distribute more evenly over the trap, seems to be minimal. A large drop directly after the left edge is observed and another minima is observed near the outer edge. This may be due to regular settling of sediment and may be enhanced by erosion. The pattern will be used to conclude on the settling/deposition only, erosion and fluid mud scenarios.

To correspond with the survey period of 118 days, the simulation of 8 days is multiplied by a morphological factor of 14.75. The three scenarios, i.e. one for settling and deposition only, one that also includes erosion and one that also includes fluid mud behaviour, can be assessed independently on how the trap contributes to the trapping of sediment for that mechanism. However, no insight is provided whether

the scenario is actually realistic. Therefore, also a look is taken at the maintenance dredging quantities over the year 2015 - 2017. These years no interventions were executed at the Botlek harbour and dredged material corresponds with naturally accreted sediment only. The dredged material is divided by the empirical bulking factor of 1.25 to get an idea of the accumulated sediment over the basins. The areas that correspond with the model domain are described to the three areas mouth, trap and basins and scaled to correspond with a similar value of accretion as the 118-day survey period. The approach is considered rough, yet every piece of knowledge is useful for the crude calibration of this model setup. The numerical values of the maintenance dredging data are provided in Table 4.2. A more elaborate approach to this table is given in Appendix A 'Dredging in the port of Rotterdam'.

Period	**Trap**	**Acc. Sed. Mouth**		**Acc. Sed. Trap**		**Acc. Sed. Basins**		**Acc. Sed. Total**	**Favourable sediment**
[days]	[yes / no]	[m3]	[% of total]	[m3]	[% of total]	[m3]	[% of total]	[m3]	[%]
118	Not maintained	80,230	28	90,445	31	117,330	41	288,005	59

Table 4.2: The amount of accumulated quantities are calculated for the areas used in the simulation for a 118 day period based on the dredged quantities of years 2015 - 2017 in Table A.2. This is a rough estimation as the dredged quantities are divided by the bulking factor of 1.25. The quantities may however give a rough estimation of what the model results should produce.

Chapter 5

Analyses of trapping mechanisms

This chapter treats the fourth research question: 'How much do the mechanisms contribute to the trapping of sediment in the sediment trap?'. First the hydrodynamics are analyzed for the simulation with and without trap. Theory treated in Chapter 3 'Sediment trap dynamics' is applied to the model setup of Chapter 4 'Setup of hydrostatic Delft3D-FLOW online SED model'. A look is taken at The hydrodynamics of the system by looking at the mechanisms described in Chapter 2 'Understanding the system'. To assess the functioning of the sediment trap, a more detailed approach is used. The mechanisms that describe the hydrodynamics around the sediment trap as described in Chapter 3 'Sediment trap dynamics' are looked at.

5.1 Analysis of hydrodynamics

In this subsection the hydrodynamics of some main mechanisms are explained that are considered important for the understanding of the system. No sediment particles are present in this model study yet. The model grid is similar as that in Figure 4.2. However, the post-processing focuses on the area between 0 and 1500 m. Most of part of area 'basins' is not shown in the results, while it did participate in calculations. This buffer area is not considered and the resolution of the dynamics near the trap are increased to emphasize on certain processes around the sediment trap. The results are assessed based on a dashboard of simulation videos. Snapshots of the graphs of the dashboard are shown to explain relevant processes. The dashboard consists of eight graphs that show the results. An entire tidal phase has been analyzed by use of the dashboard, and the results are presented in Figure 5.1. For high water (HW), ebb, low water (LW) and flood the graphs are presented from left to right, respectively. The hydrodynamics are analyzed in the next section. When relevant, the start of the sediment trap is shown with a vertical red dashed line with the letter 'S' next to it.

Similarly, the end of the sediment trap is shown with a vertical blue dashed line with the letter 'E' next to it. The graphs that are presented are:

- The **water level** elevation is shown as a function of time, indicated with a red marker to show the progress in the simulation. The signal represents tidal signal imposed at the boundary. The varying surface elevation results in barotropic forcing that governs tidal flow due to a horizontal pressure gradient. This is explained in Appendix C 'Hydrodynamics by Delft3D-FLOW'.

- **Salinity** distributions are shown in the third graph with a dark red colour for high salinity values and a dark blue colour for low salinity values. Larger salinity values in the flow increase the corresponding density of the flow according to the Equation of State as explained in Chapter

- **Turbulence** is shown as the turbulent eddy viscosity. Absence or very little amounts of turbulence are shown with a dark blue colour. Larger quantities of turbulent eddy viscosity are given with a green colour.

- **Bottom shear stress** is shown with the black line, where values are positive for flood flow and negative for ebb flow. The bottom shear stress are important for the amount of erosion that occurs during the simulations. When a certain threshold value is exceeded, sediment is able to resuspend. Averaged values are given by a dashed red line for flood flow and a dashed blue line for ebb flow.

- **Velocity** distributions are given in basin-directed indicated with positive values and the colour red, and river-directed indicated with negative values and the colour blue. The horizontal velocity magnitudes are governed by various mechanisms, such as tidal filling and density driven currents. 3 'Sediment trap dynamics'. The horizontal density gradient induced by the variation of salinity governs a horizontal density current.

- The **Richardson number** as explained in Chapter 3 'Sediment trap dynamics' is given to express the stability of the stratified flow. The values $\mathrm{Ri} < \frac{1}{4}$ are shown with a red colour, indicating instabilities in the stratification.

- The squared **composite Froude number** calculated for two layered flow is shown with the solid black line in the 6th graph. The dashed line shows the squared internal Froude number of the top layer, while the dotted line shows the squared internal Froude number of the bottom layer. The composite Froude

number tells us what the internal hydraulic state of the flow is, i.e. supercritial, critical or subcritical for values $G^2 > 1$, $G^2 = 1$ or $G^2 < 1$, respectively. The calculation method of this dimensionless number is explained in Chapter 3 'Sediment trap dynamics'. Even if sediment is absent in the simulation, it still provides information about sedimentation and erosion patterns. Please note that the composite Froude number can only be calculated when a two-layered flow is present. If not, the values of the number is set to -0.25 (no supercritical flow).

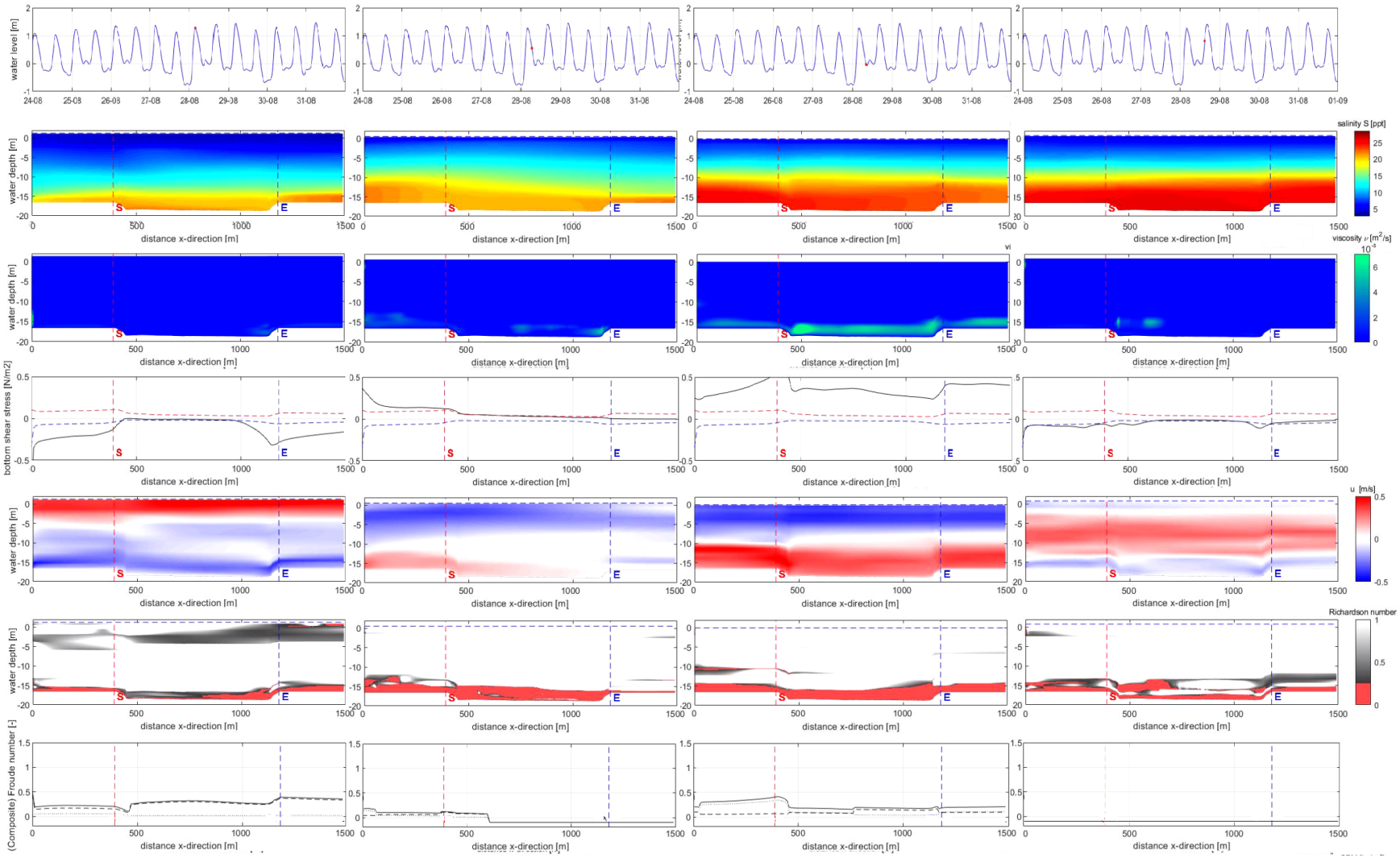

Figure 5.1: The 2DV hydrodynamics around the sediment trap for four distinctive moments in the tidal signal. From left to right, high water (HW), ebb, low water (LW) and flood are presented, respectively. The graphs indicate the water level, salinity, turbulence, bottom shear stress, velocity, Richardson number and composite Froude number from top to bottom, respectively.

5.1.1 Exchange of water with the boundary

The dominant mechanisms as treated in Chapter 2 'Understanding the system' are analyzed for the imposed hydrodynamics in the model. The mechanisms of tidal filling, salnity induced density currents and horizontal exchange are explained in the chapter. Horizontal exchange of water is not considered in this 2DV model.

5.1.1.1 Tidal filling

One of the main exchange mechanisms in harbour basins is tidal filling as explained in Chapter 2 'Understanding the system'. If the exchange of water between the basin and the river is entirely dominated by tidal filling and density plays no significant role, the exchange is quite straightforward. Rising water (flood) for $\delta\zeta/\delta t > 0$ would increase the water in the basin by a positive flow velocity $\delta u_{i,j}/\delta t > 0$ over the entire water column, where ζ is the water level at the boundary and u the flow velocity at any arbitrary location (i, j). Falling water (ebb) for $\delta\zeta/\delta t < 0$ would decrease the water in the basin by a negative flow velocity $\delta u_{i,j}/\delta t < 0$ over the entire water column. However if we look at the hydrodynamics of a maximal increasing water level $\delta\zeta/\delta t > 0$ in the fourth column of Figure 5.1, this does not occur. The flow velocity does however not have the same sign over the water column. The density of the water is not homogeneous over the vertical, neither over the horizontal. Density difference due to salinity govern the vertical distribution of the flow patterns. The barotropic forcing does drive a pressure gradient that governs inflow of water in the domain. The rising water level drives a net increase of water in the basin. For the rising tide, even an outflow of water is observed near the bed. This is due to the salinity concentrations present in the domain. Apparently, the density of the water in the basin is larger than at the river (boundary), a current is driven by density gradient $\delta\rho/\delta x > 0$. We can see a slight increase when looking at the salinity profile at the graph. Density changes are purely due to salinity levels, as temperature is set as a constant and sediment is absent in the model. The density gradient drives a two-directional layered flow, inward in the upper part of the water column and outward in the lower part of the water column.

Mechanism 'Tidal filling' alone does not describe the hydrodynamics that govern the exchange of water with the harbour basin.

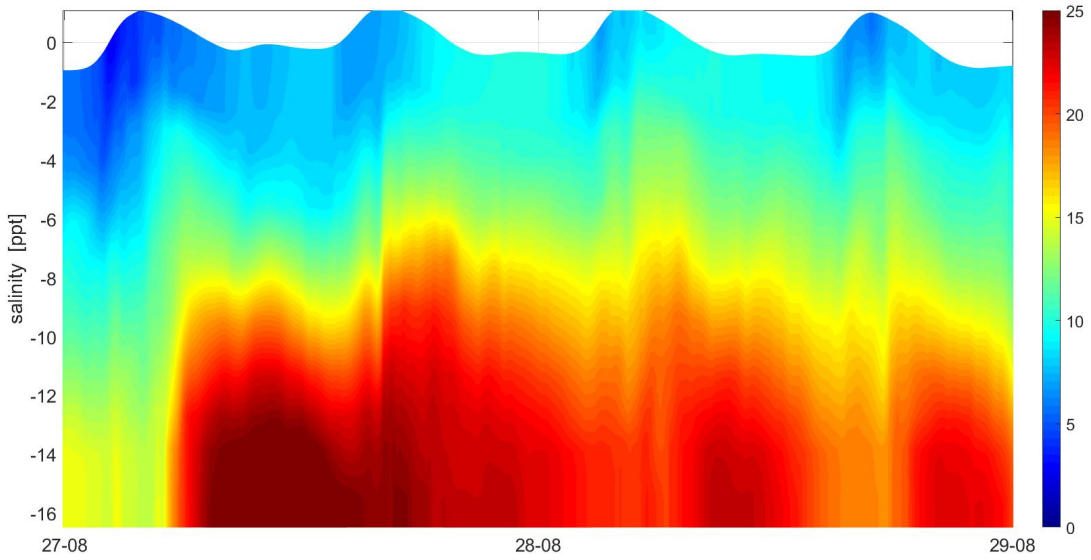

Figure 5.2: The imposed salinity 3D boundary condition is shown in the figure similarly as in Figure 4.5. Only the dates from 27th of August until the 29th of August are shown. The simulation period from 20th of August until the 1st of September is calculated by OSR at the location indicated with the red cross in Figure 4.1.

5.1.1.2 Density driven currents by salinity

We have seen that tidal filling is not the only mechanism governing flow in the harbour basin. Salinity drives a two-layered bidirectional stratified flow in the basin. The behaviour of the flow over the depth is largely governed by the density gradients due to the salinity. The rising and falling tidal elevation does govern a net transport of water. The peak salinity values that correspond with the salt wedge can be seen in Figure 4.5 and have a phase delay with the tidal forcing as explained in Chapter 2 'Understanding the system'. To get a better insight of the phase delay the salinity boundary condition of Figure 4.5 is zoomed in on the analysis dates of Figure 5.1, namely 28th of August. This is shown in Figure 5.2. From the figure we can see that the peak in salinity levels has a phase delay with the high water peak. The delay is somewhere between 1.5 and 3 hours. It varies per tidal cycle. It is hypothesized this is due to the tidal forcing strength and the freshwater discharge of river Meuse. Measurements of De Nijs in Appendix D 'Generation SPM time-series' show a phase delay of 1.5 hours between the high water peak and salinity peak. The frequency of the salt wedge follows the tidal period. One of these distinctive peaks in flow velocity due to salinity is shown in the third column of Figure 5.1. While the peak salinity values occur at the boundary between 1.5 and 3 hours after HW, the maximum salinity induced density current magnitudes occur during LW, around 6 hours after HW for the case in Figure 5.1. As this current is dependent on the density gradient, the

timing of the maximum density current is dependent on the storage of salinity concentrations in the basin. This in turn is dependent on salt intrusion of the previous tidal cycles. This sums up to our first conclusions considering hydrodynamics:

The net exchange of water is governed by the tidal filling mechanism. Density currents caused by salinity differences govern the vertical flow velocity distributions. The phase difference between high water and salinity peak values is between 1.5 and 3 hours.

5.1.2 Sediment trap dynamics

The sediment trap dynamics as explained in Chapter 3 'Sediment trap dynamics' will be treated in the section according to the imposed hydrodynamics on the model. An in-depth analysis of the local flow velocity, local turbulent kinetic energy, bed shear stress, Richardson number, composite Froude number are provided according to Figure 5.1 and averaged values over the entire simulation period. Exactly this tidal signal with an emphasis on the third column is chosen for a few reasons. The first is that this signal shows one of the largest near bed flow velocities during inflow. The extremes of the simulation yield a solid base for various parameters, e.g. maximum composite Froude number or occurring bed shear stresses. It proves to be a useful example for the treatment of the theory about sediment trap dynamics. The second reason is that during these large flow velocities the flow pattern shows a strict two layered flow. Assumptions made considering two layered flow are likely to hold for the strong pycnocline.

5.1.2.1 Local flow velocity

The density gradient due to salinity values govern the horizontal flow in the domain. The horizontal flow velocity magnitude seems to diminish some in the water column above the trap. To emphasize this difference, absolute values of the flow velocity, averaged over the entire simulation period, are compared for a simulation with and without trap in Figure 5.3. This is also done for the turbulent eddy viscosity for turbulence and the bottom shear stress for the erosion and deposition. In the figure indeed a lower average flow velocity can be observed in the water column above the trap (right) compared to the situation without trap. On some locations, this difference may be significant. For example look at the location of $x = 700m$. The averaged flow velocity reduces from approximately 0.18 m/s to 0.10 m/s, which is a significant reduction. We can therefore confirm our hypothesis regarding the flow velocity above

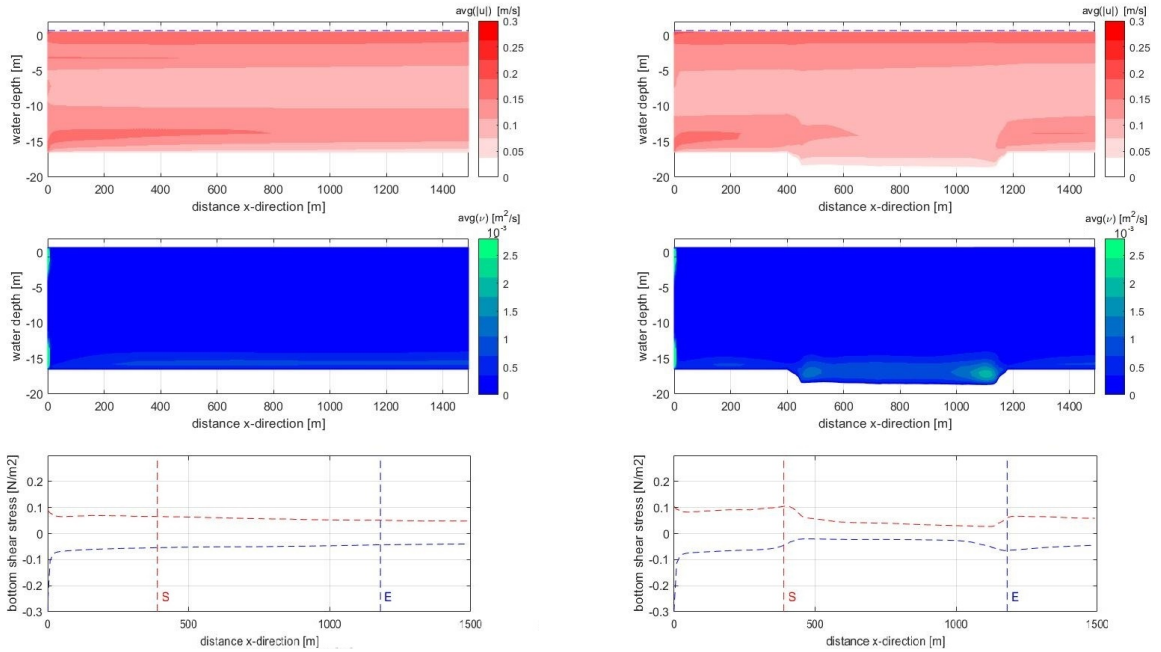

Figure 5.3: Average values are shown over the entire simulation period of the absolute average flow velocity, average turbulent eddy viscosity and average bed shear stress basin directed (red dashed) and river directed (blue dashed) from top to bottom, respectively. The left column shows the simulation without trap, the right column the simulation with sediment trap.

the sediment trap and draw our first conclusion based on hydrodynamics only:

The theoretical statement that the flow expansion caused by the sediment trap would reduce the flow velocity locally has been confirmed by the numerical model.

5.1.2.2 Local turbulent kinetic energy

In Figure 5.1 the largest turbulent eddy viscosities are observed for large flow velocities. For low velocities turbulence seems to be small. When we look at the third column, turbulence is observed for a large amount in the water column just above the sediment trap. The expectation would be that this increase in turbulence would be largest just after the flow expansion and diminish over the trap. The largest turbulence values are indeed observed near the flow expansion at $x \approx 500m$. The values however seem to diminish less rapidly than expected. When we look at averaged turbulent eddy viscosity values in row 2 in Figure 5.3, we see that the sediment trap indeed governs turbulence production. The average turbulent eddy viscosity is significantly higher for the simulation with trap compared to the simulation without trap, i.e. $2.3 * 10^{-3}$ compared to $1.3 * 10^{-3}$. An interesting phenomenon is however that the average turbulent eddy viscosity is larger near the second edge of the sediment trap,

that is the one that is farthest away from the river. A strong resemblance between theory hypothesis and the model hydrodynamics are observed regarding the flow expansion:

The theoretical statement that the flow expansion caused by the sediment trap would increase the turbulence locally has been confirmed by the numerical model.

5.1.2.3 Bed shear stress

Also the bed shear stress has been assessed in Figure 5.1. A strong resemblance between the occurring flow velocities and bed shear stress can be seen as discussed in Chapter 3 'Sediment trap dynamics'. Large flow velocities increase the bed shear stress to values of the order 0.5 N/m^2 and erosion is likely to be present at these values. The effect of turbulence on the bed shear stress is however hard to read from the figure. A reattachment point 5-7 times the height downstream of the step should experience to the most severe attack on the bottom due to turbulence according to the theory of (Blom & Booij, 1995) in Chapter 3 'Sediment trap dynamics'. With the height of the trap of 2.5 meters, this point would lie around 15 meters after the expansion. With the dimensions on the x-axis in Figure 5.3 this is hard to read. The edges of the trap have been zoomed in to in Figure 5.4. The slope is not sufficient to see a flow separation. 15 meters behind the start of the flow deceleration, we would still be on the sloping part of the edge. In the left column of Figure 5.4 we can however see a slight peak after 15 meters of the flow deceleration. Also for ebb flow in the right column of Figure 5.3, a slight increase is observed for the bed shear stress for ebb flow (blue dashed line). It is however quite small. Therefore, the influence of the turbulence levels on the average bed shear stress can be observed to be small and only near the decelerating flow. Since the large dimensions of the trap, the bed shear stress seems to be determined by the occurring flow velocities dominantly. The shear stresses are on the other hand somewhat higher. Therefore we would conclude the following:

The hypothesis that the bed shear stress would increase near the edges of the sediment trap, but decreases inside the sediment trap has been confirmed by the numerical model.

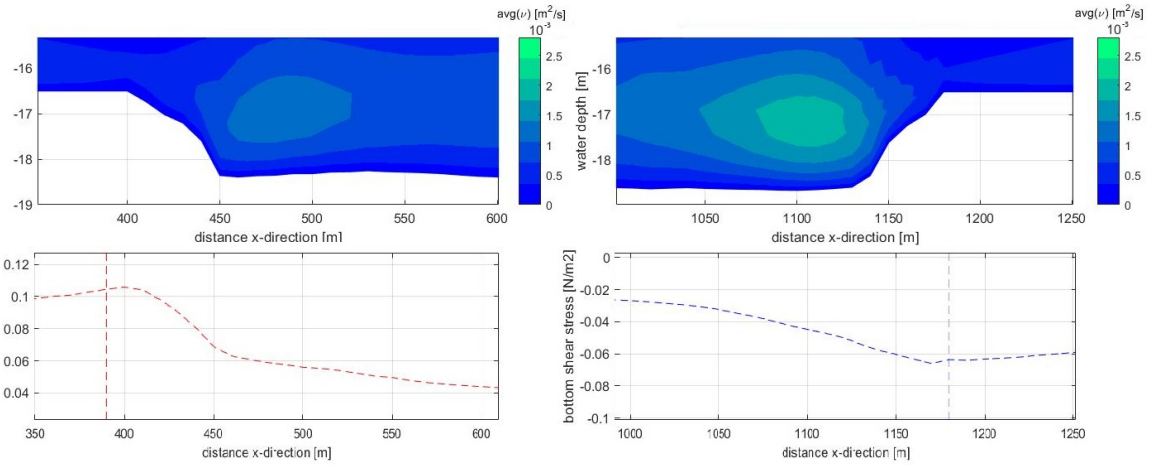

Figure 5.4: The influence of the increased turbulence near the edges of the sediment trap are assessed in the figure. Values are the same as in Figure 5.3.

5.1.2.4 Stratified flows

An interesting graph is that of the Richardson number in Figure 5.1. The graph shows the spatial distribution of the Richardson number $\text{Ri} = \frac{g}{\rho}\frac{\delta\rho}{\delta z}/|\frac{\delta u}{\delta z}|^2$. The number expresses the ratio between the buoyancy term and flow shear term as explained in Chapter 3 Sediment trap dynamics. For strong density gradients over the vertical or for location with large shear velocities due to strong gradients in the vertical, the Richardson number may result in low values and tell us something about the stability of the flow. For values $\text{Ri} > 0.25$ the flow is considered stable and the hydrostatic pressure assumption is considered valid. However, for values $\text{Ri} < 0.25$ the flow may be unstable and Kelvin-Helmholtz instabilities may develop. In that case non-hydrostatic effects may be important. Unstable flow may be expected near the bed, as the bed induces large shear values on the flow. Generally, during the simulation the Richardson number is above 0.25 for the entire domain expect for the lowest layers. However, during the peak velocities as can be seen in Figure 5.1 the flow is unstable above the sediment trap. Non-hydrostatic pressure effects may be of importance in this region. Exactly this moment is of the utmost importance, because these layers are expected to carry sediment. This leads to the following conclusion regarding modelling choices:

Large flow velocities governed by the density gradient due to salinity differences may lead to an unstable stratification. The non-hydrostatic instabilities caused by this phenomenon are not included in the hydrostatic model.

Another graph that we look at to determine something about the hydraulic internal structure is the composite Froude number. The bottom graphs of Figure 5.1 show the calculated internal Froude numbers from the top (dashed), bottom (dotted) and the composite Froude number (solid). Please note that some composite Froude numbers are not shown. This is due to the fact that the flow is not exactly bidirectional but varies several times in direction over the vertical. Because this mainly occurs for small flow velocities, the hydraulic state will definitely be subcritical so no further attention has been paid to this phenomenon. Even for the large velocities depicted for the analyses, the composite Froude numbers are well below one. The composite Froude number have been analyzed for the entire simulation signal and are below 1 at all times. This suggests that we are dealing with a subcritical internal flow structure at all times. No hydraulic jumps are expected to be present in the simulation. An effect that may occur are the lee waves for a small obstacle for absolutely subcritical flow as introduced by Long in Chapter 3 'Sediment trap dynamics'.

By further analyzing the hydrodynamics of the simulations, the conclusion was made that the flow has to be supercritical when looking at the third column of Figure 5.1. Apparently, the theory for the hydraulic state of two-layered flow by Armi (1986) does not suffice for the density profile present in the simulations. The theory for a continuous stratification by Winters & Armi (2012) as explained in Chapter 3 'Sediment trap dynamics' is therefore applied to a similar flow pattern as the third column. This is shown in Figure 5.5. This moment in the simulation is chosen, because it is convenient and used for further analyses of various depths in Chapter 6 'Optimization of the sediment trap design'. In the figure an acceleration is observed near the left corner of the sediment trap. At this location the flow switches to supercritical as the internal Froude number is above one. At this location the flow is stable, and no turbulence is observed, as one would expect ofr supercritical flow. Once the flow decelerates, a jump is experienced. The flow layer expands, turbulence is present and salinity is distributed higher over the water column. This may have a significant effect on the distribution of sediment. This effect will be further illustrated in Chapter 6 'Optimization of the sediment trap design'. The following is concluded:

Numerical simulations confirm that the sediment trap changes the properties of the internal flow, which may change the hydraulic state of the flow resulting in large instabilities and even an internal hydraulic jump.

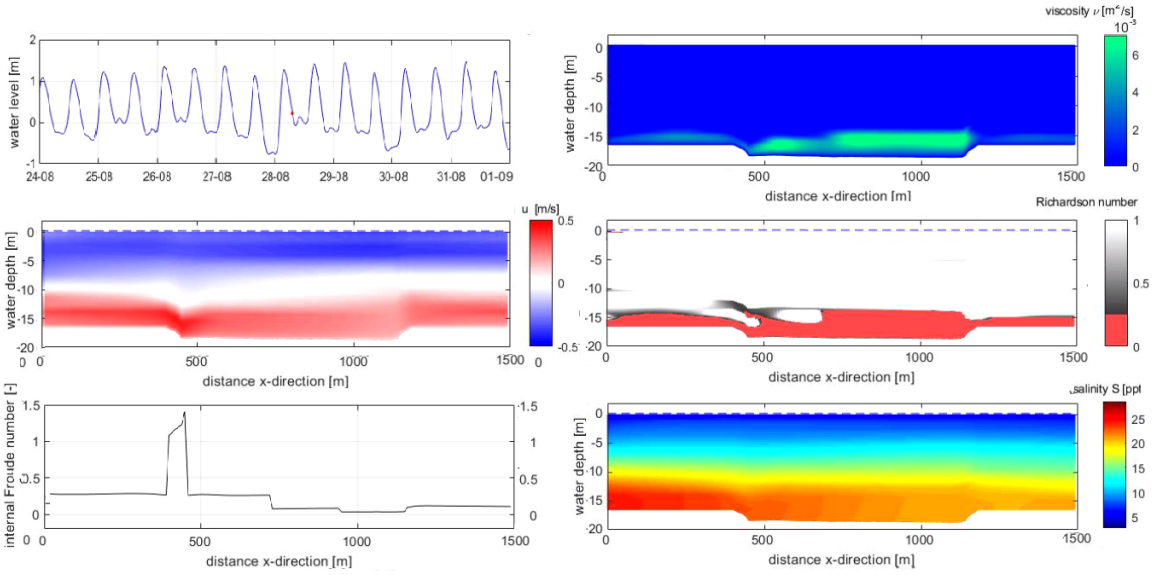

Figure 5.5: A snapshot of the simulation shows that according to the theory of Winters & Armi (2012) for a continuous density gradient, the hydraulic state of the flow switches from supercritical to subcritical and an internal hydraulic jump can be observed. Graphs show the water level, turbulent viscosity, flow velocity, Richardson number, internal Froude number and salinity from top left to bottom right, respectively.

5.2 Sediment

5.2.1 Distinguish trapping mechanisms

Now that the hydrodynamics are assessed and a distinction has been made between the case with and without the sediment trap, it is time to see how these differences in bed shear stress, local flow velocity, turbulent eddy viscosity and overdepth affect sediment. To do this a look is taken at the three scenarios to represent the trapping mechanisms in Chapter 3 'Sediment trap dynamics'. For each of the scenarios, a representative setting is approached by varying the erosion parameter M for erosion and fluid mud parameter DepEff for fluid mud. For settling and deposition, only one scenario is tested. Each of the scenarios is run with the simulation where the boundary conditions of the SPM time series is variable and represents the ETM. Each simulation uses the exact same set of parameters (except for the one parameterized), boundary conditions and bathymetry profiles distinguishing with and without a sediment trap. The results are assessed on the proportional distribution of accumulated sediment at the end of the simulation. A dinstinction is made between sediment that has accumulated in the mouth from 0 m to 390 m, the sediment trap from 400 m to 1190 m and the harbour basins from 1200 m to 8770 m. Entire accumulation patterns and tabled values are included in Appendix E 'Parameterization of the model'. For brevity, here only the results of the parameterization are shown and the sedimentation

patterns of the chosen parameter sets.

5.2.1.1 Settling and deposition

First a simulation is run where only settling and deposition are present. In this simulation erosion parameter $M = 0$ and fluid mud parameter DepEff $= 1.0$. Sediment settles as soon as it hits the bed and once in the bed it does not leave anymore. Without any erosion or fluid mud behaviour, the influence of the reduced local flow velocity and the turbulent eddy viscosity on the sedimentation of fines can be assessed. A reduced local flow velocity does also reduce the local bed shear stress. The process of settling is shown in Figure 5.6. Erosion is however not present so this does not influence accumulated sediment. The accumulation quantities at the end of the simulation are shown at the top of Table 5.1.

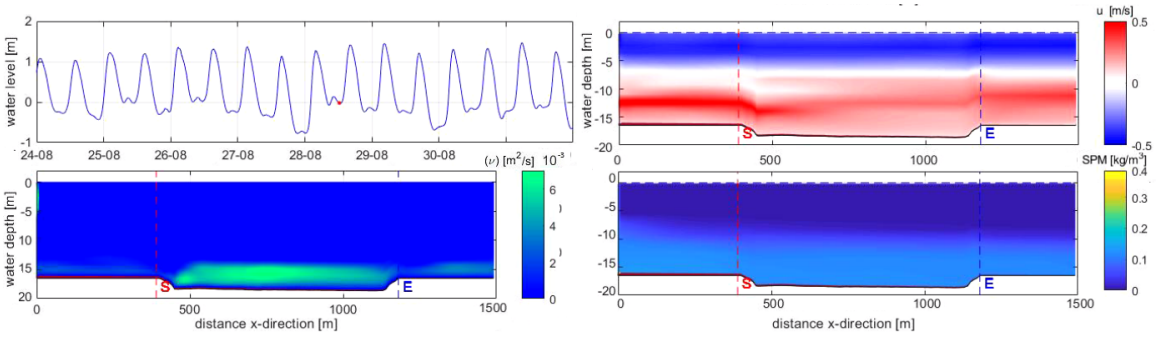

Figure 5.6: The process of settling is determined by the settling velocity of the sediment and the upward turbulent forces. In the horizontal sediment is transported by the flow velocity.

We see that for the simulation without trap a large decrease of 7% in net accumulation is present for the simulation with sediment trap. This is a rather large difference for only a difference in bathymetry and also counter-intuitive. Because of the large differences in total accumulation of sediment, we look at the proportional distribution of accumulated sediment for all simulations. In both simulations 35 % of the sediment has accumulated in the trap. The trap reduced the accumulation in the basins by 6 % (34 % to 32 %). Accumulation in the harbour mouth increased by 6 %. For the simulation that only includes settling/deposition, little use of the sediment trap was noticed. The accumulation pattern and tabled values are given in the top figure of Figure E.2 (Appendix E 'Parameterization of the model') and Table 5.1. For further research, it has only been used as a comparison and the following is concluded:

A numerical simulation with sediment trap where only settling and deposition is present results in marginal improvements compared to a simulation without sediment

trap.

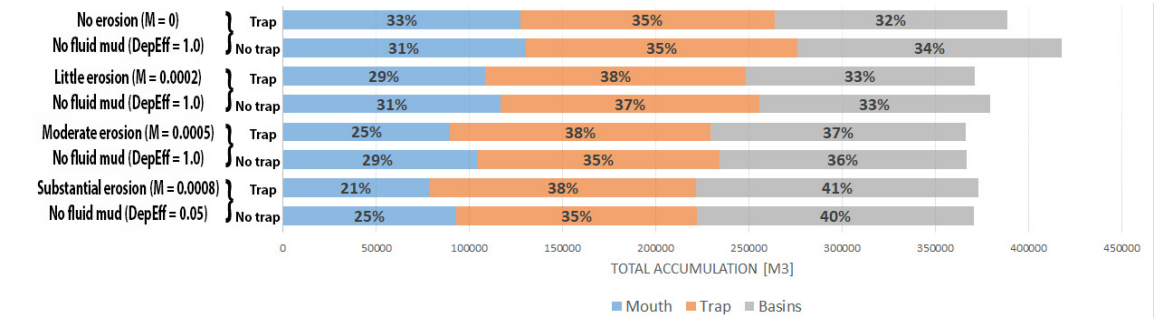

Table 5.1: Parameterization of erosion parameter M based on the accumulation quantities of sediment for a variable boundary condition for SPM (ETM). Each simulation is run with and without trap for the exact same parameters except M, boundary conditions and bathymetry (trap/no trap).

5.2.1.2 Erosion scenario

Erosion is gradually added to the model to see how this influences the distribution of sediment. It would be nice to include some erosion in the model and see how the shape of the sediment trap influences this process. It is however a large unknown. The process of erosion in the numerical model can be seen in Figure 5.7.

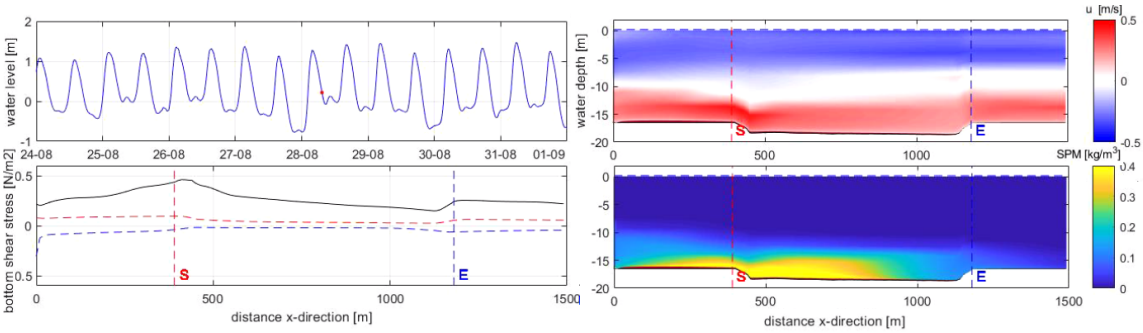

Figure 5.7: The process of erosion is determined, on top of the settling processes, by the bottom shear stress. When the critical shear stress of 0.18 N/m^2 is exceeded, erosion occurs as seen in the figure. This simulation is run with moderate erosion values of $M = 0.0005$

The effect of erosion is assessed by running simulations with the same hydrodynamics for various erosion parameters M. Comparing these runs gives an indication of how important the erosion/deposition mechanism is for the trapping of sediment in the sediment trap. Each of the runs is done for the situation with and without a sediment trap. Five erosion settings are run. The parameterization of the erosion parameter M is done with $\tau_{c,e} = 0.18 N/m^2$ for no, little, moderate, substantial and lots of erosion with $M = 0, 0.0002, 0.0005, 0.0008, 0.020$, respectively. The results of

accumulated sediment are given in Table 5.1. Erosion increases from top to down. If we look at the trends, we see that the total accumulated sediment differs for different erosion values. A 7 % decrease for the simulation without erosion (top table) is followed by a 2 % decrease for little erosion, negligible difference for moderate erosion and an increase of 1 % for substantial erosion. Also a run with lots of erosion was simulated, but this run hit the bottom grid disabling any further erosion. This could be solved by adding initial sediment to the model. It is however considered unrealistic and left out of further research. When a look is taken at the proportional distribution of sediment in Table 5.1 a trend can be seen for increasing erosion values. For increasing erosion values sediment seems to gather deeper in the domain. A shift from the mouth to trap and basins can be observed. The trap seems to hold on to more sediment for increasing erosion. The amount of sediment caught in the trap increase 0 % (35 % to 35 %) for no erosion, 3 % for little erosion (37 % to 38 %), 9 % for moderate erosion (35 % to 38 %) and also 9 % for substantial erosion (35 % to 38 %). Unfortunately, most of this sediment originates from the mouth. Sediment in the mouth has a cheap disposal cost, just like the sediment trap. Sediment accumulated in mouth and trap is further labeled as 'Favourable sediment', while the sediment in the basins is unfavourable. When a look is taken at the accumulated quantities in the basins, less improvements are observed. For no erosion the presence of the sediment trap leads to a decrease of 6 % (34 % to 32 %), little erosion leads to a negligible decrease (33 % to 33 %), moderate erosion even leads to an increase of proportional accumulation in the basins of 3 % (36 % to 37 %) and substantial erosion leads to an increase of 3 % (40 % to 41 %). This leads to the following conclusion:

Based on numerical simulations that include erosion with a varying SPM boundary condition, erosion enhances the trapping of sediment in the sediment trap. Most of this sediment originates however from the sediment mouth. In the harbour basins the presence of a sediment trap may even increase the accumulation of sediment. There is no significant contribution on the maintenance dredging costs by the installation of sediment traps in an environment where erosion is important.

The representative parameterset for erosion is chosen to be the simulation with moderate erosion with $M = 0.0005$. This set shows the largest correspondation with the accumulated quantities of the maintenance dredging data in Table 4.2. The accumulation pattern of this parameterset is given in the middle in Figure E.2 (Appendix E 'Parameterization of the model') with numerical values in Table 5.1.

5.2.1.3 Fluid mud scenario

The simulations with fluid mud were a bit harder to assess. Therefore, some extra simulations are run to conclude on model results. Fluid mud behaviour is approached by varying the DepEff coefficient. The fluid mud is a simplified form as only dense suspension flows and delayed deposition are taken into account. Flocculation, hindered settling and various consolidation layers are not taken into account. A varying DepEff results in a delayed deposition by a fraction, i.e. parameter DepEff, to the bed and dense suspension layers are formed in the lowest layers of the water column. Sediment increases According to the Equation of State in Chapter 3 'Sediment trap dynamics' the corresponding density of the flow increases and a density gradient in the horizontal is present, governing dense suspension flows. The process of fluid mud in the numerical model can be seen in Figure 5.8. The lowest layer shows a high suspended sediment concentration.

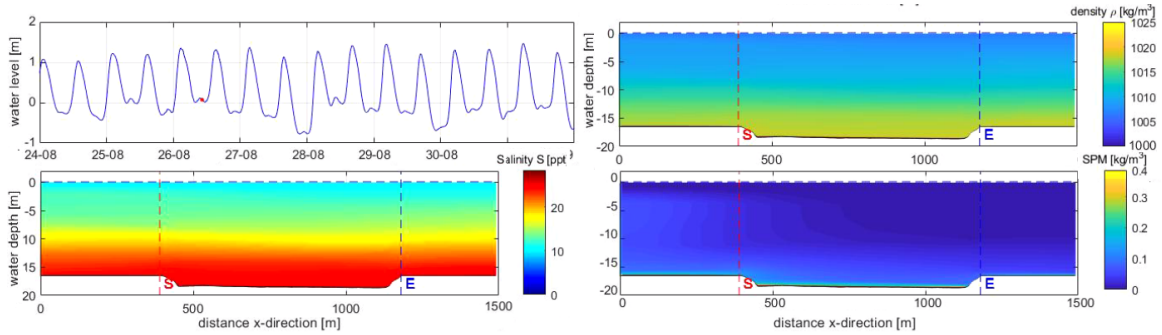

Figure 5.8: The process of fluid mud is determined, on top of the settling processes, by the reduced deposition due to the DepEff. A small layer of suspended sediment is formed above the bed, increasing the density of the water and driving density driven flows. This run has typical substantial fluid mud values with DepEff = 0.2.

Fluid mud is gradually added to the model by reducing the DepEff to see how this influences the distribution of sediment. Comparing these runs gives an indication of how important the fluid mud mechanism is for the trapping of sediment in the sediment trap. Each of the runs is done for the situation with and without a sediment trap. Six fluid mud settings are run. The parameterization of the fluid mud parameter DepEff is done for no, little, moderate, substantial, lots and extreme fluid mud behaviour with DepEff $= 1.0, 0.7, 0.5, 0.2, 0.1, 0.005$, respectively. The results of accumulated sediment are given in Table 5.2. Fluid mud behaviour increases from top to bottom. Here, some interesting and unpredictable differences are observed. We see that the total accumulated sediment differs for different fluid mud values. There is however no trend to be distinguished. A 7 % decrease for the simulation without fluid mud (top table) is followed by a similar decrease of 7 % for little fluid mud, a

2 % increase for moderate fluid mud, followed by an enormous decrease of 9 % for substantial fluid mud, a decrease of 5 % for lots of fluid mud and a minor increase of 1 % for extreme fluid mud behaviour. The large variations confirm the speculations obtained by the analysis of the settling and erosion scenario that the variable SPM boundary condition is not a right way to vary scenarios with each other. The minor changes in hydrodynamics due to the variation of a certain parameter or shape would result in tremendous differences (up to 9%) in imported sediment from the boundary into the domain. For erosion the trend could be seen, but for fluid mud the quantities of sediment in the domain seemed rather random. The following is concluded:

The application of a varying SPM boundary condition over time with a very occasional supply of sediment to mimic the ETM at the boundary, results in a highly sensitive model regarding sediment quantities on the hydrodynamics in the domain.

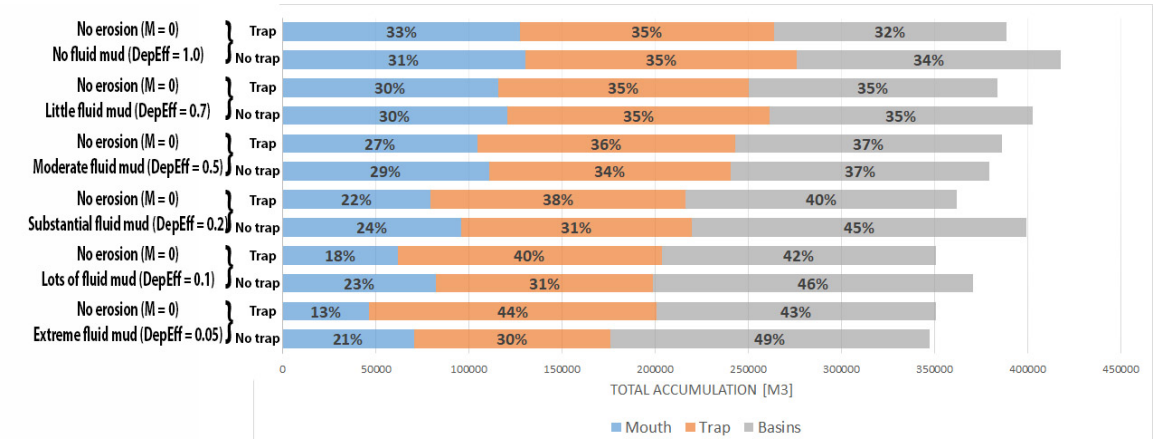

Table 5.2: Parameterization of fluid mud parameter DepEff based on the accumulation quantities of sediment for a varying boundary condition for SPM (ETM). Each simulation is run with and without trap for the exact same parameters except DepEff, boundary conditions and bathymetry (trap/no trap).

However, the parameterization is finished based on this simulations. A strong trend can be observed for the proportional accumulation of sediment. When a look is taken at the proportional distribution of sediment in Table 5.2 a trend can be seen for increasing fluid mud values. Just like with erosion, for increasing fluid mud values sediment seem to gather deeper in the domain. A shift from the mouth to trap and basins can be observed. The trap seems to hold on to a lot more sediment for increasing fluid mud. The amount of sediment caught in the trap increases 0 % (35 % to 35 %) for no fluid mud, 0 % for little erosion (35 % to 35 %), 6 % for moderate fluid mud (34 % to 36 %), 23 % for substantial fluid mud (31 % to 38 %), 29 % for

lots of fluid mud and an impressive 47 % for extreme fluid mud behaviour. Just like the erosion scenarios, for fluid mud also some of this sediment originates from the mouth. The amount of favourable sediment (mouth and trap) however did increase for simulation with increasing fluid mud .When a look is taken at the 'unfavoured sediment', i.e. accumulated quantities in the basins, also improvements are observed. For no fluid mud the presence of the sediment trap leads to a decrease of 6 % (34 % to 32 %), little fluid mud leads to a negligible decrease (35 % to 35 %), moderate fluid mud also leads to a negligible decrease (37 % to 37 %) and substantial fluid mud leads to an decrease of 13 % (45 % to 40 %) of accumulated sediment in the basins, lots of fluid mud to a decrease of 10 % (46 % to 42 %) and extreme fluid mud to a decrease of 14 % (49 % to 43 %). This leads to the following conclusion:

Based on numerical simulations with fluid mud behaviour and a varying SPM boundary condition, fluid mud enhances the trapping of sediment in the sediment trap. A decrease of accumulation in the mouth was observed, a significant increase in the trap and a significant decrease in the basins. There is a significant contribution to the maintenance dredging costs by the installation of sediment traps in an environment where fluid mud is present. The decreased amounts of accumulated sediment in the basin for at least substantial fluid mud behaviour may vary between 10 % and 14 %, depending on how aggressively this fluid mud behaviour is modelled.

The representative parameterset for fluid mud is chosen to be the simulation with substantial fluid mud for DepEff = 0.2 This set shows the largest correspondation with the accumulated quantities of the maintenance dredging data in Table 4.2. The accumulation pattern of this parameterset is given in the bottom figure in Figure 5.9 with numerical values in Table 5.3.

5.2.2 Three scenarios

Based on the three mechanisms, for each mechanism a representative parameterset is chosen. The three scenarios based on the dominant trapping mechansisms extensively described in Chapter 3 'Sediment trap dynamics' are:

- Only settling and deposition - No erosion ($M = 0$) and no fluid mud behaviour (DepEff = 1)
- Erosion - Moderate erosion ($M = 0.0005$, $\tau_{c,e} = 0.18\ N/m^2$) and no fluid mud behaviour (DepEff = 1)

- Fluid mud - No erosion ($M = 0$) and substantial fluid mud behaviour DepEff $= 0.2$

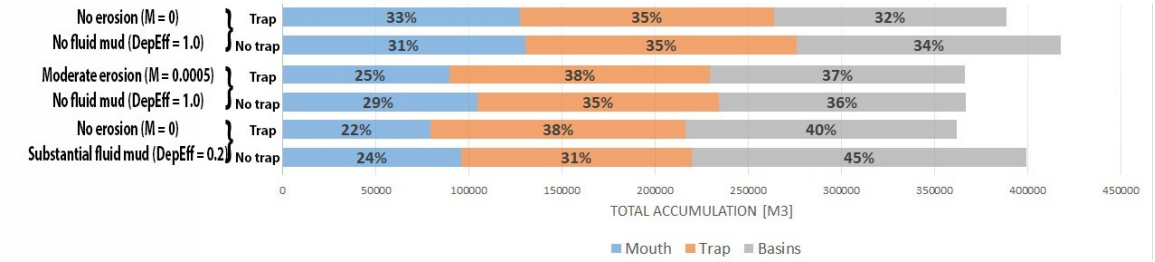

Table 5.3: Three scenarios are used based on the parameterization of erosion parameter M and fluid mud parameter DepEff based on the accumulation quantities of sediment for a varying boundary condition for SPM (ETM). Each simulation is run with and without trap for the exact same parameters except M and DepEff, boundary conditions and bathymetry (trap/no trap).

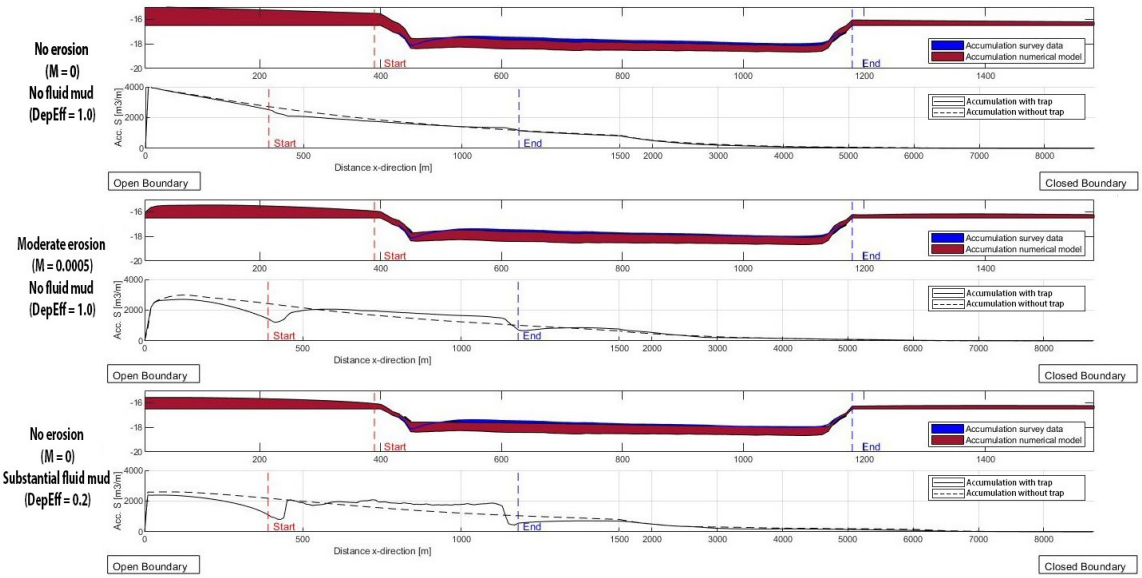

Figure 5.9: Three scenarios are assessed for a simulation with (solid line) and without (dashed line) trap for a varying SPM boundary condition (ETM) over time. The top figure of each scenario shows the accumulation pattern of the model (red) and the accumulation pattern of the survey (blue) for the case with sediment trap. The bottom figure of each scenario shows the magnitude of accumulation of sediment over the entire domain. Please note the non-equidistant x-axis. The first 1500 m have a higher resolution as it is the domain of interest.

The results are given in Table 5.3 and their sedimentation patterns are shown in Figure 5.9 for the end of the simulation. For each scenario, the top figure shows the accumulation of sediment (dark red) compared to the survey data pattern (blue) at the sediment trap location. The bottom figure shows where the sediment is accumulated over the entire domain for situation with and without a sediment trap. Table E.1 in Appendix E 'Parameterization of the model' gives an overview of the values of the simulations of the figure. We must ask ourselves which scenario is actually realistic. Therefore the available calibration data is used:

- The sedimentation pattern of the accumulated sediment in the model compared to the survey data (Appendix A 'Dredging in the port of Rotterdam")
- Sediment distribution over the three areas mouth, trap and basins compared to the maintenance dredging quantities for a not maintained sediment trap over 2015-2017 provided by (Port of Rotterdam, 2019) (Appendix A 'Dredging in the port of Rotterdam').

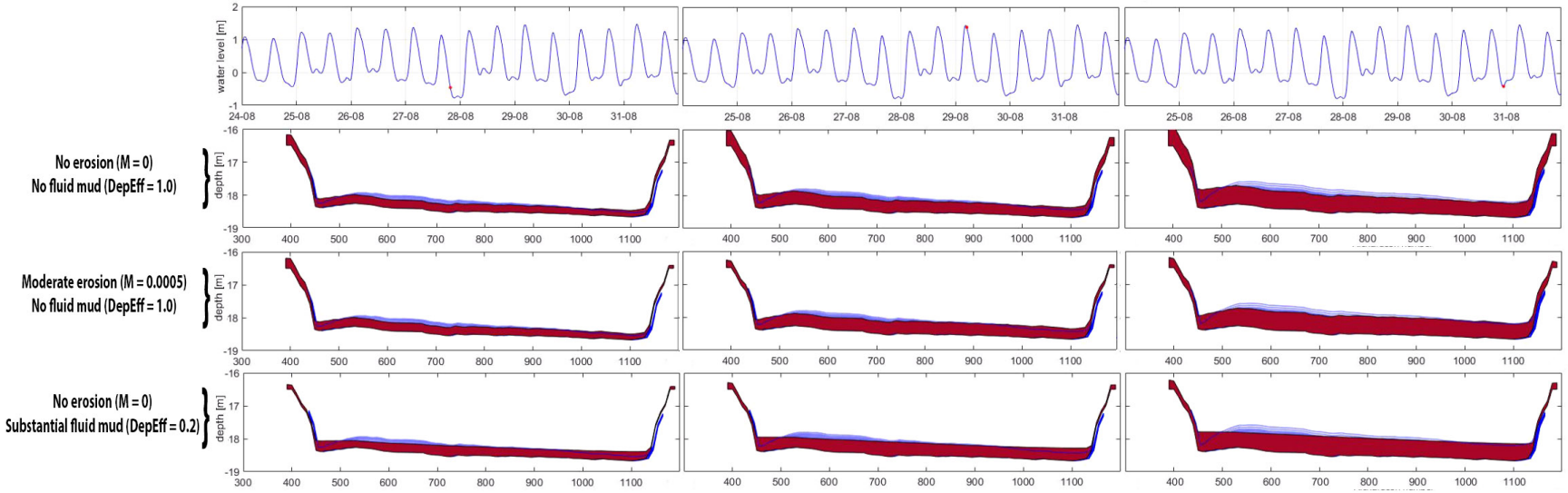

Figure 5.10: The progression of accumulation of sediment (constant b.c.) for three timesteps. The differences between the three scenarios are shown: settling only, erosion and fluid mud. The top row shows the three timesteps indicated with a red marker on the tidal signal of the simulation. Rows two to four show the numerically calculated accumulation in dark red and the linearly interpolated survey data in striped blue.

In Figure 5.10 the progression of sedimentation is shown for the three scenarios. The top accumulation figure shows the accumulation of the settling scenario. Sediment gradually settles and a large overprediction of settling on the left edge and the left corner can be observed. The middle accumulation figure shows the erosion scenario. Progressing from the left to the middle column, a small decrease of sediment on the edge can be observed. This is due to the erosion that took place. The pattern mimics the survey data reasonably well. The last figure shows the accumulation of sediment for fluid mud. The sediment is spread out evenly over the bottom. This shape does not represent the survey data. For the three scenarios, the second scenario in Figure 5.9 seems to mimic the survey data the best. The scenario where no erosion nor fluid mud is present results in a overprediction of accumulation just near the left edge of the sediment trap. Presumably also a overprediction of sediment in the mouth is present. A decrease in accumulation is observed just after the left edge and the rest of the pattern corresponds quite accurately with the survey data. Sediment seems to gather further in the basin as one would expect for erosion scenarios. For a simulation where a trap is included even more sediment erodes from the mouth for a simulation without trap. For the simulation with fluid-mud behaviour sediment seems to spread out over the basin as one would expect. The trap is homogeneously filled and the accumulation pattern follows the shape of the bottom of the trap. Although this mechanism may contribute largely to the trapping of sediment, it does not correspond very well with the survey data. Before we continue with the constant SPM boundary, the following is concluded:

An erosion scenario seems to represent the sedimentation pattern of the Echosounder Multibeam surveys the best.

We continue to look at the proportional sediment distribution in Table 4.2 in Chapter 4 'Setup of hydrostatic model' based on the maintenance dredging data provided by Port of Rotterdam (2019). A sedimentation distribution of 28 %, 31 % and 41 % is expected over the mouth, trap and basins, respectively. Of course, this is highly dependent on also other parameters that are assumed to be fixed in the numerical model, e.g. the settling velocity. The maintenance dredging also considers data for a not maintained sediment trap. The results should therefore maintain between the simulations with and without trap. The low trapping efficiency of 31 % is the bottom line of all those scenarios for substantial fluid mud without trap. Perhaps the settling velocity of $w_S = 0.6mm/s$ is a small overprediction of the settling velocity.

The scenario for settling only is considered to be too unrealistic for sedimentation. Lots of sediment gathers in the mouth of the harbour and no increase of sedimentation in the sediment trap is observed. However, if we take a look at the accumulation of sediment in the Botlek Harbour in Figure 2.4 in Chapter 2 'Understanding the system', definitely can be noticed that an increase in sedimentation should be observed in the sediment trap, even for a not maintained one. Therefore, the settling only scenario is not used for further research. The remaining scenarios for moderate erosion and substantial fluid mud are used for the assessment of different shapes for the sediment trap in Chapter 6 'Optimization of the sediment trap design'.

The maintenance dredging data provided by Port of Rotterdam *(2019) gives a good impression of the quantities of accumulated sediment, but no dominant trapping mechanism can be assigned based on this data. The data shows an increased accumulation rate in the sediment trap. This is observed for both the erosion and fluid mud scenarios, but not for the settling only scenario.*

5.2.2.1 Two dominant scenarios

Apparently the varying SPM time series at the open boundary is very sensitive to the hydrodynamics in the first cells of the model. A small change in flood or ebb magnitude results in large variations in the sediment quantities in the domain. Luckily, this problem revealed during the parameterization of the model. The results do give us some plausible conclusions. Erosion plays a limited effect on the capturing of sediment in the sediment trap. For all erosion parameters no significant increase in capturing of sediment is observed. The conclusion that the presence of fluid mud increases the capturing of sediment is also considered plausible. For small Deposition Efficiencies, which mimic a strong fluid mud behaviour, very favourable results were observed and the sediment trap could be an efficient mitigation measure. Our survey data does not confirm the sedimentation pattern on the other hand. For this reason, simulations are continued with two sets of parameters: One for erosion and one for fluid mud. The variable boundary condition for SPM will be replaced by a constant boundary condition as can be seen in Figure 4.7 in Chapter 4 'Setup of the hydrostatic model'.

5.2.3 Confirmation of previous conclusions

We have just concluded that the variable SPM boundary conditions result in too large uncertainties. The simulations of the three scenarios for settling only, erosion and fluid mud are therefore run again. This time with the constant SPM boundary conditions as in Figure 4.7. The results are presented in Table 5.4 and Figure 5.11. Numerical values are given in Table E.3 in Appendix E 'Parameterization of the model'. The results are comparable for the simulation with the variable boundary conditions. For the settling only scenario, a variable SPM boundary condition resulted in no extra sedimentation in the trap (35 % to 35 %) and a decrease of 6 % (34 % to 32 %) in the basins was concluded for the simulation with the sediment trap. For the constant SPM boundary condition these number are a slight increase of 3 % (32 % to 33 %) for the trap and a decrease of 5 % in the basins. The results are very similar. For the simulation with the moderate erosion scenario, the simulations with a variable SPM boundary condition resulted in an increase of 9 % in the trap (35 % to 38 %) and also an increase in the basins of 3 % (36 % to 37 %). For the constant SPM bounndary condition, the increase in the trap is 9 % (32 % to 35 %) and in the basins a decrease of 2 % (49 % to 48 %). The results, again, are very similar. Although the situation has slightly improved, no significant contribution is observed. For the simulation that has substantial fluid mud, the simulations with a variable SPM boundary condition resulted in an increase of 23 % in the trap (31 % to 38 %), and a decrease of 13 % (45 % to 40 %) of accumulated sediment in the basins. For the constant SPM boundary condition the result are an increase of 21 % in the trap (28 % to 34 %), and a decrease of 6 % (54 % to 51 %) in the basins. These results are somewhat less favourable for the installation of sediment trap. It is hypothesized this is due to the constant supply of sediment, less dense suspensions are able to form. The resulting density gradient will be smaller than for a situation where large concentrations enter the domain. This is the exact mechanism that drives the dense suspension flows. Another thing that is interesting is the amount of sediment accumulated in the domain. The constant boundary condition was applied to diminish differences in imported sediment in the domain. For the variable SPM boundary condition, the presence of the trap resulted in a decrease of 7 % for a settling only scenario, a similar sediment count for a moderate erosion scenario and a large decrease of 9 % for the substantial fluid mud scenario. For the contant SPM boundary condition, the differences are an 8 % decrease for settling, a 4 % decrease for moderate erosion and a 3 % decrease for fluid mud. It can be concluded that there are still some significant differences in accumulation of sediment for a constant SPM boundary condition. This leads to the following conclusions.

Simulations with a constant boundary condition yield the same results considering the dominant mechanisms for the trapping of sediment in the sediment trap. Settling only and erosion scenarios show little contribution, while the fluid mud scenario shows a significant contribution to the trapping of sediment in the sediment trap. Even for constant SPM boundary conditions, still large variations up to 9 % are observed between exactly the same simulation due to a difference in bathymetry. Apparently, the presence of the sediment trap influences the hydrodynamics to such an extent that it may even result in less import of sediment.

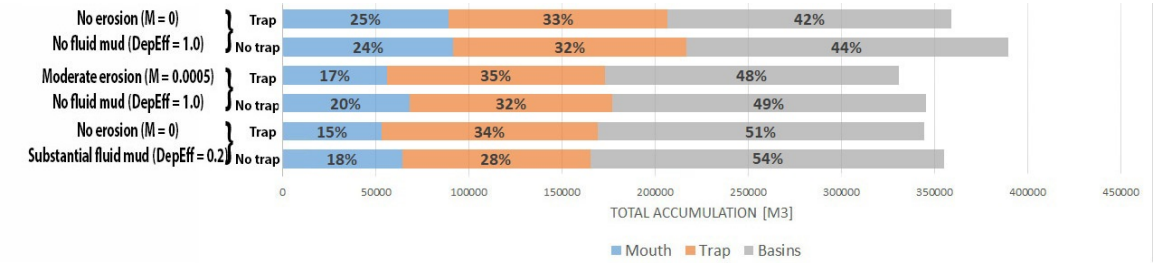

Table 5.4: Three scenarios are used based on the parameterization of erosion parameter M and fluid mud parameter DepEff based on the accumulation quantities of sediment for a constant boundary condition for SPM. Each simulation is run with and without trap for the exact same parameters except M and DepEff, boundary conditions and bathymetry (trap/no trap).

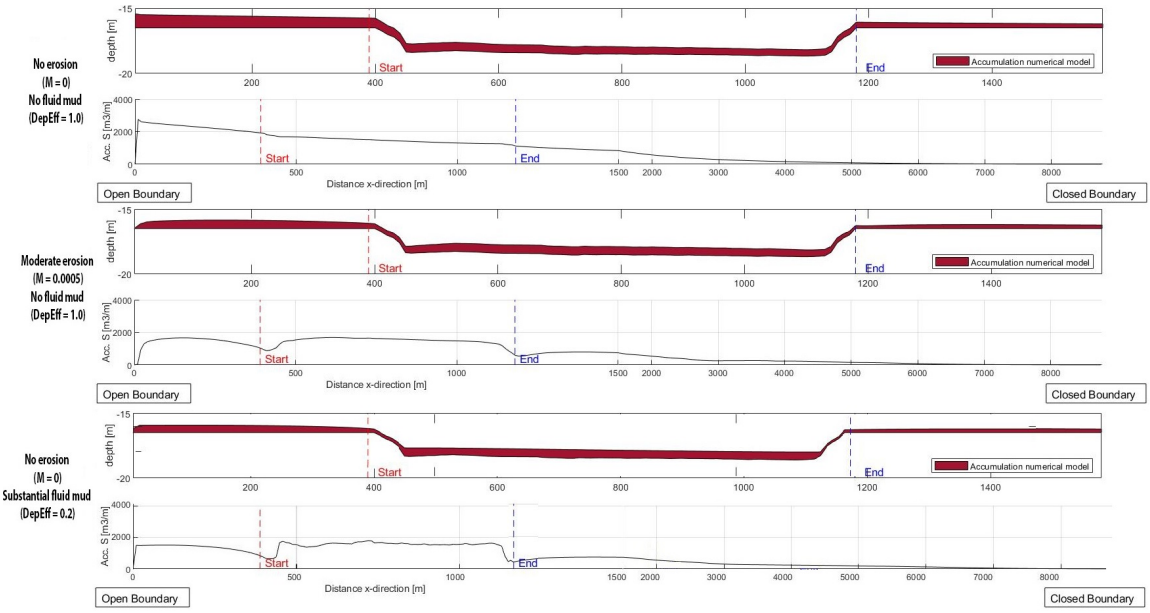

Figure 5.11: Three scenarios are assessed for a simulation with (solid line) and without (dashed line) trap for a constant SPM boundary condition (ETM) over time. The top figure of each scenario shows the accumulation pattern of the model (red) and the accumulation pattern of the survey (blue) for the case with sediment trap. The bottom figure of each scenario shows the magnitude of accumulation of sediment over the entire domain. Please note the non-equidistant x-axis. The first 1500 m have a higher resolution as it is the domain of interest.

Chapter 6

Optimization of the sediment trap design

In this chapter the final research question is answered: 'What shape and volumes result in an ideal design for sediment traps?'. Various shapes have been designed. The hydrodynamics of the shapes are assessed first and hypotheses about these shapes are provided. Afterwards, the shapes are tested on sediment by adding the constant SPM boundary condition. The two scenarios, i.e. erosion and fluid mud, of Chapter 5 'Analyses of trapping mechanisms' are used to check the hypotheses previously stated. Conclusions are drawn about improving the sediment trap shape.

6.1 Hydrodynamics and accumulation of sediment

Straightforward design adaptations are used to test various sediment shapes. On top of the simulations without trap and with trap, now called 'basic trap', also a trap twice as deep '2x deep', a trap half as deep '2x shallow', a trap twice as short '2x short', a trap twice as long '2x long', a gradual declining trap 'V-shape' and a sill are implemented in the model. The trap twice as long is treated in a separate section, because each of the sections 'Mouth', 'Trap' and 'Basins' has to be reclassified to enable comparison between simulations. First, the influence of different sizes of overdepth is treated to see if the overdepth has a significant influence on the internal hydraulic state of the flow. Then we switch to a more crude approximation of hydrodynamics. Each of the shapes is analyzed by means of the averaged hydrodynamics compared to the simulation with the basic trap. Accumulation quantities of the sediment follow up for both the erosion and fluid mud scenario. The simulations without trap and with the basic sediment trap have already been analyzed so are not treated in this chapter. The accumulation quantities of each of the shapes are given in Figure 6.1

and Table 6.1 for erosion, and in Figure 6.2 and Table 6.2 for fluid mud. Numerical values of these figures are found in Appendix F 'Supporting tables optimization'.

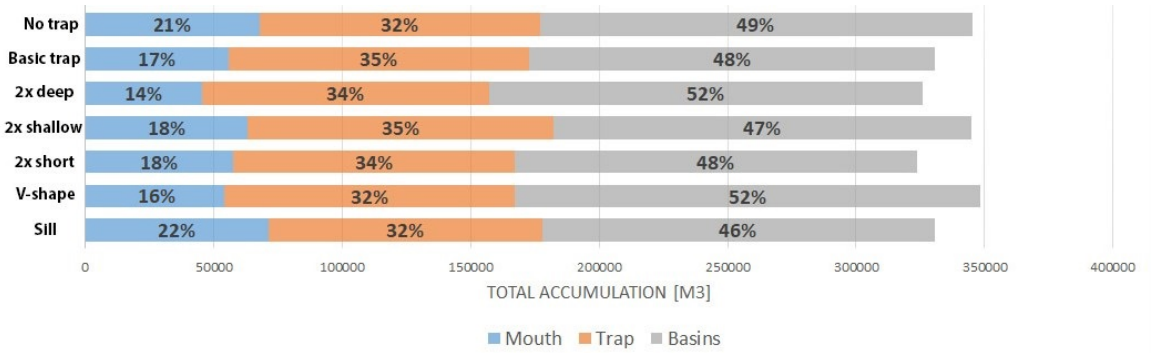

Table 6.1: Each of the sediment trap designs is simulated on a moderate erosion scenario with a constant SPM boundary condition. The table shows the quantities and proportions of accumulation in the mouth, trap and basin at the end of the simulation.

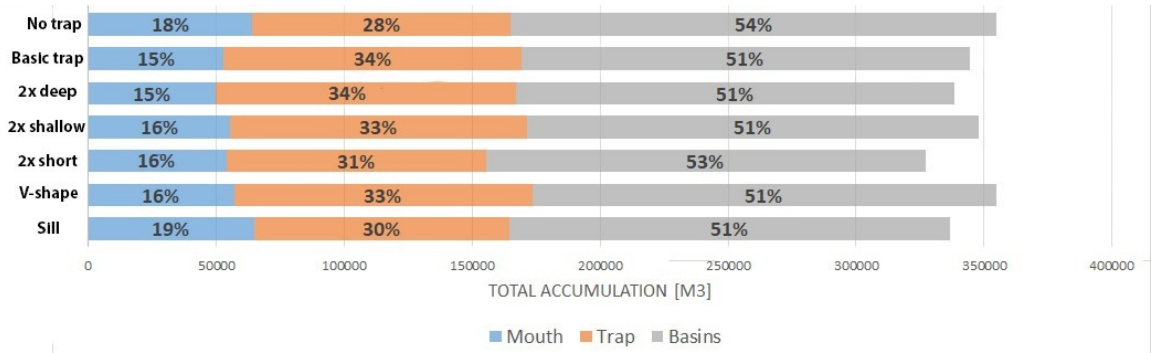

Table 6.2: Each of the sediment trap designs is simulated on a substantial fluid mud scenario with a constant SPM boundary condition. The table shows the quantities and proportions of accumulation in the mouth, trap and basin at the end of the simulation.

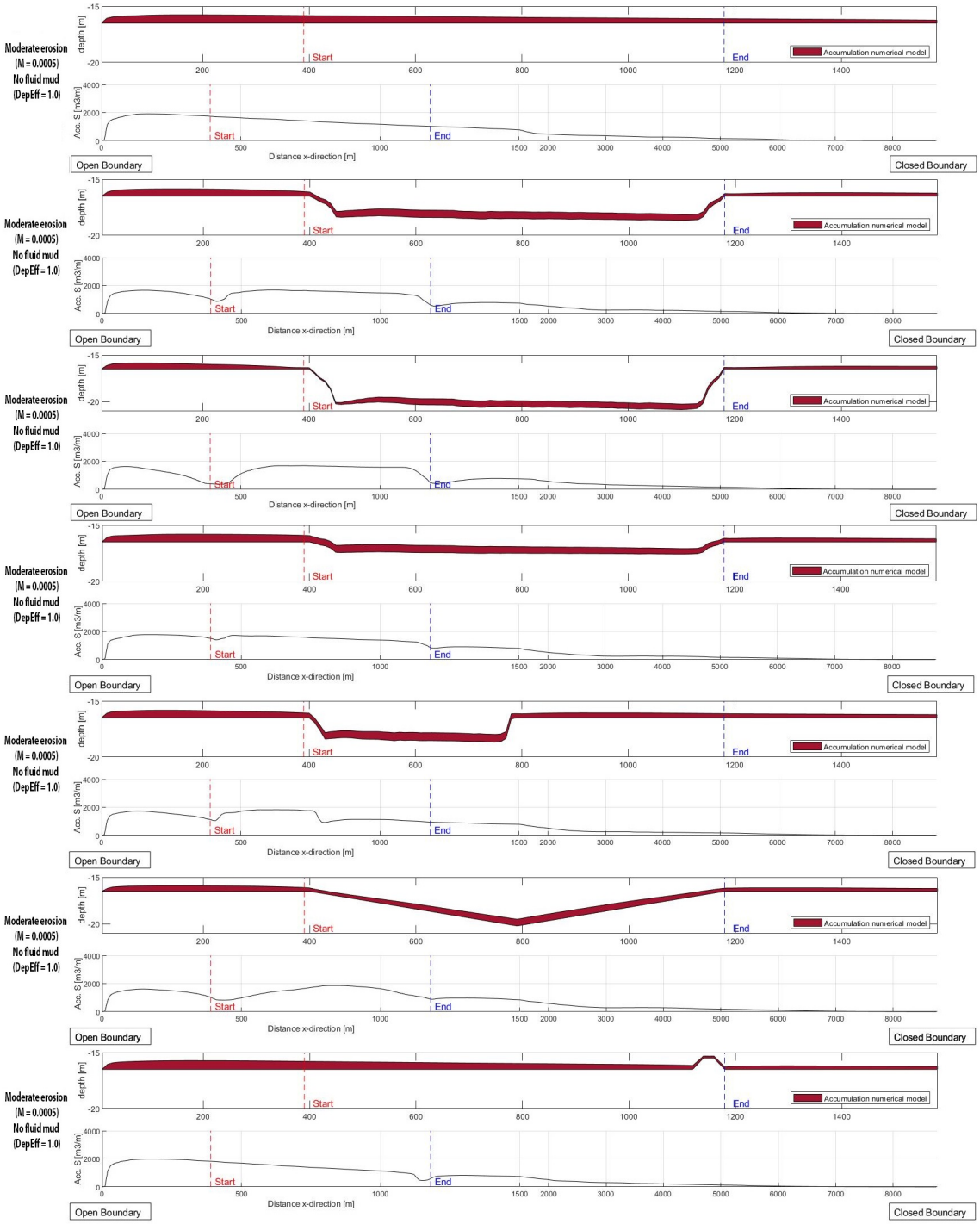

Figure 6.1: Each of the sediment trap designs is simulated on a moderate erosion scenario with a constant SPM boundary condition. The top figure of each scenario shows the accumulation pattern of the model (red). The bottom figure of each scenario shows the quantity of accumulation of sediment over the entire domain. Please note the non-equidistant x-axis. The first 1500 m have a higher resolution as it is the domain of interest.

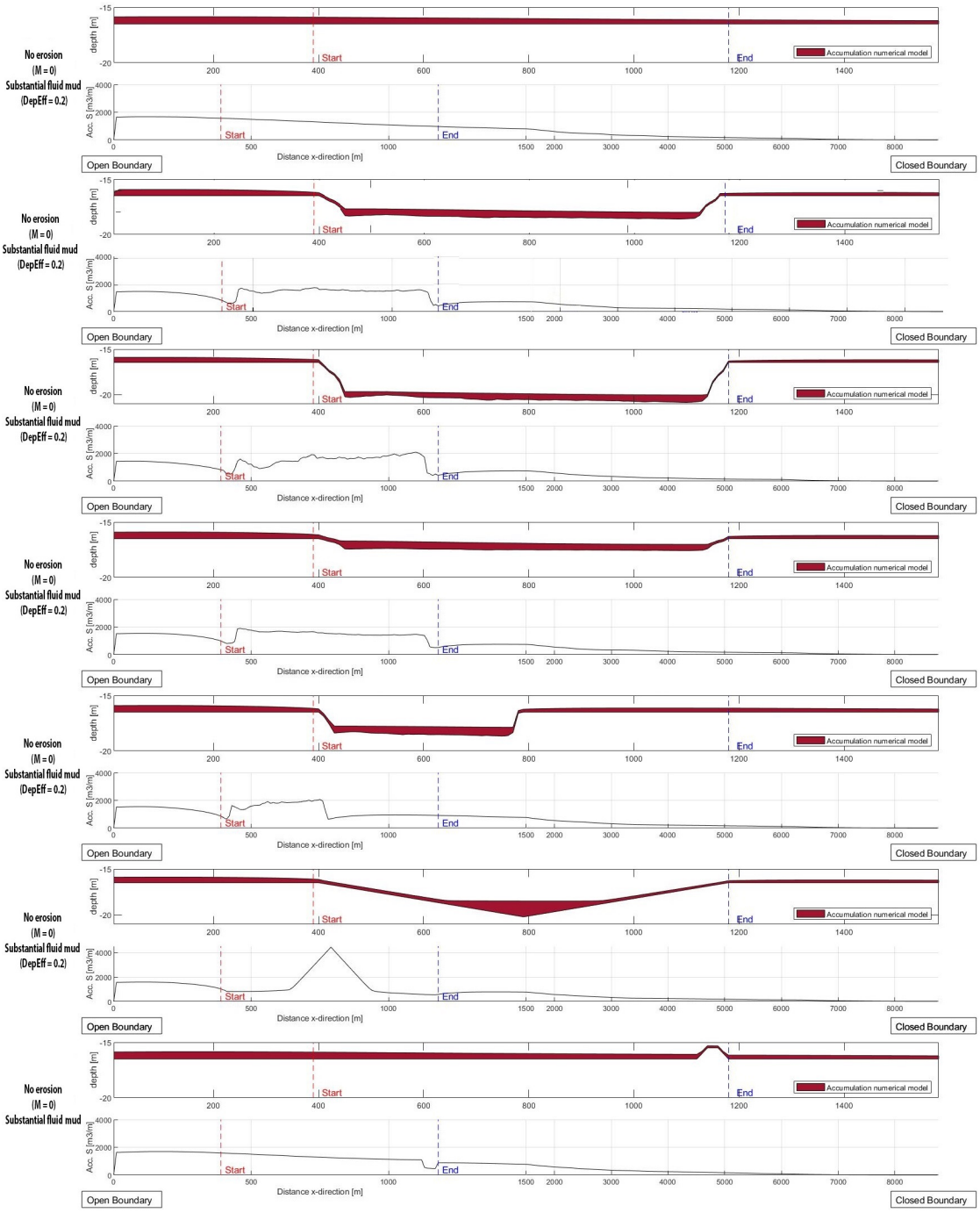

Figure 6.2: Each of the sediment trap designs is simulated on a substantial fluid mud scenario with a constant SPM boundary condition. The top figure of each scenario shows the accumulation pattern of the model (red). The bottom figure of each scenario shows the quantity of accumulation of sediment over the entire domain. Please note the non-equidistant x-axis. The first 1500 m have a higher resolution as it is the domain of interest.

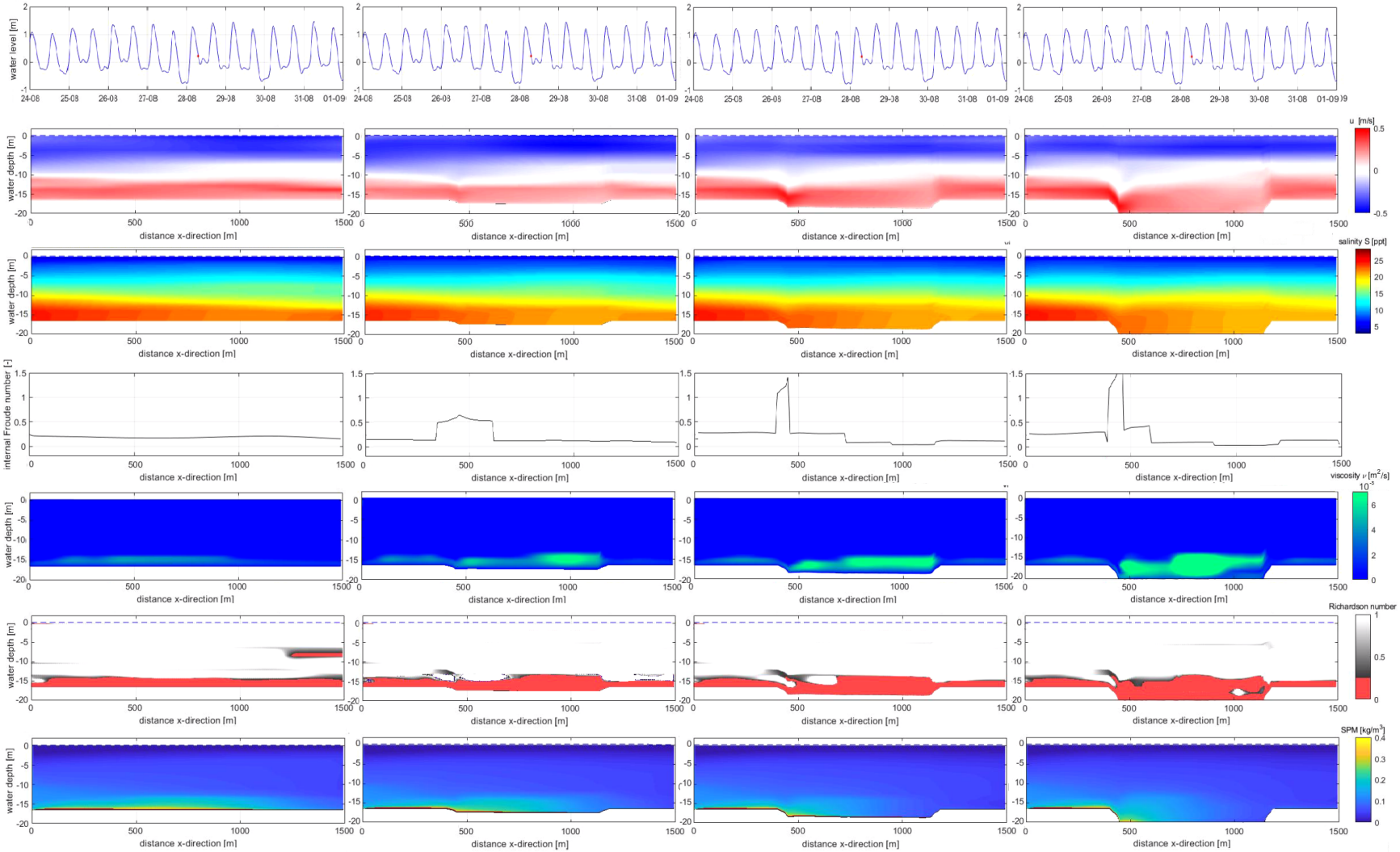

Figure 6.3: The 2DV hydrodynamics around the sediment trap for four distinctive overdepths for the exact same moment in the simulation. From left to right, no sediment trap, trap twice as shallow, regular trap and trap twice as deep are presented, respectively. The graphs indicate the water level, flow velocity, salinity, internal Froude number for a continuous density gradient, turbulence, Richardson number and Suspended Particulate Matter (SPM) from top to bottom, respectively.

6.1.1 Internal flow dynamics

We have seen in Chapter 3 'Sediment trap dynamics' that an obstacle changes the internal wave properties and may even change the hydraulic state of the internal flow. Chapter 5 'Analyses of trapping mechanisms' confirms this behaviour according to the theory for internal flow properties of flow with a continuous density gradient by Winters & Armi (2012). In this section the hydrodynamics of the internal flow are treated for various bathymetries. The influence of the depth of sediment trap on the hydrodynamics and sediment is shown in Figure 6.3. The figure shows a snapshot of the exact same moment in the simulations for no sediment trap, a trap half as deep, the regular trap and a trap twice as deep. The graphs for the regular trap have already been provided in Chapter 5 'Analyses of trapping mechanisms' to show that the hydraulic state of the flow could indeed change. The graphs show the water level, flow velocity, salinity, internal Froude number for a continuous density gradient, turbulence, Richardson number and SPM from top to bottom, respectively. Something interesting happens for the various depths in the figure. For the left column, where no trap is present, the salinity gradient drives a horizontal flow which is undisturbed. The internal Froude number shows that the internal flow is absolutely subcritical. Not much turbulence is present and the flow is only unstable near the bottom according to the Richardson number. This is expected due to the bottom shear stress. SPM is gathered in the lower parts of the water column.

When we look at the second row for a trap twice as shallow, we can see that the salinity gradient is very similar to the simulation without trap. The flow seems to slightly accelerate over the left edge of the trap, but no significant increase is observed. The flow still remains absolutely subcritical and no internal hydraulic jump is observed. Some increased turbulence is observed when the flow decelerates again further into the trap. At the location of increased turbulence the Richardson number indicates the stratification is not entirely stable. Sediment seems to be slightly higher redistributed in the water column, indicating that turbulence cause uplift forces on the sediment.

The third column for the regular sediment trap has been treated in the previous chapter already. A strong acceleration is observed at the edge of the trap, while the salinity density gradient is similar as the other simulations. The internal Froude number increases to values larger than one, indicating that the internal hydraulic state of the flow switches to supercritical. Later, this switches back to subcritical and an internal hydraulic jump is observed. At the supercritical part of the flow, turbulence is absent what we would expect for supercritical flow. Once the flow switches to

subcritical, the flow is unstable according to the Richardson number. Substances in the water column, e.g. salinity and SPM, experience an uplift and are distributed higher in the water column quite abruptly.

The final column that shows the trap twice as deep experiences the same phenomena as the third column. The difference is that the acceleration is stronger, just as the internal Froude number. Therefore, also the internal hydraulic jump is stronger. Substances are distributed higher in the water column. The following important conclusion is drawn:

An overdepth in the bathymetry changes the internal flow properties. This may change the internal hydraulic state of the flow, resulting in an internal hydraulic jump. Numerical simulations show that a deeper sediment trap has a larger acceleration, thus a larger internal Froude number. Shallower traps result in smaller accelerations. If an internal hydraulic jump occurs, the uplift of substances, e.g. salinity and SPM, is influenced by the strength of the jump.

An important note is that we've used an arbitrary timestep in the simulation to visualize the influence of the overdepth. For the entire simulation, there may be times all shapes experience subcritical flow or that also the trap twice as shallow experiences supercritical flow. Figure 6.3 shows that the magnitude of the depth actually may influence the internal flow structure largely. This does not always have to be the case. In the following (averaged) analyses, this effect must be kept in mind. For each of the scenarios, this definitely plays a role but is not seen in the averaged hydrodynamics.

6.1.2 Various shapes

6.1.2.1 Twice as deep

The first trap that is simulated is the '2x deep' trap. The trap twice as deep is expected to result in a larger flow deceleration, increased turbulence levels and a reduced bed shear stress. To quantify these hypotheses, the values of these parameters are averaged over the entire simulation period. Averaged hydrodynamics of the simulation are shown in Figure 6.4. The deeper trap indeed shows increased turbulence levels, even further reduction of flow velocities and a more extreme definition of the bed shear stress. Bottom shear stress are larger near the edges and even smaller in the rest of the sediment trap. Figure 6.3 shows that the acceleration for the trap twice as deep is the largest of all depths. Expectations are that internal hydraulic

jumps occur more often and are stronger of character. This will have a negative effect on the trapping of sediment.

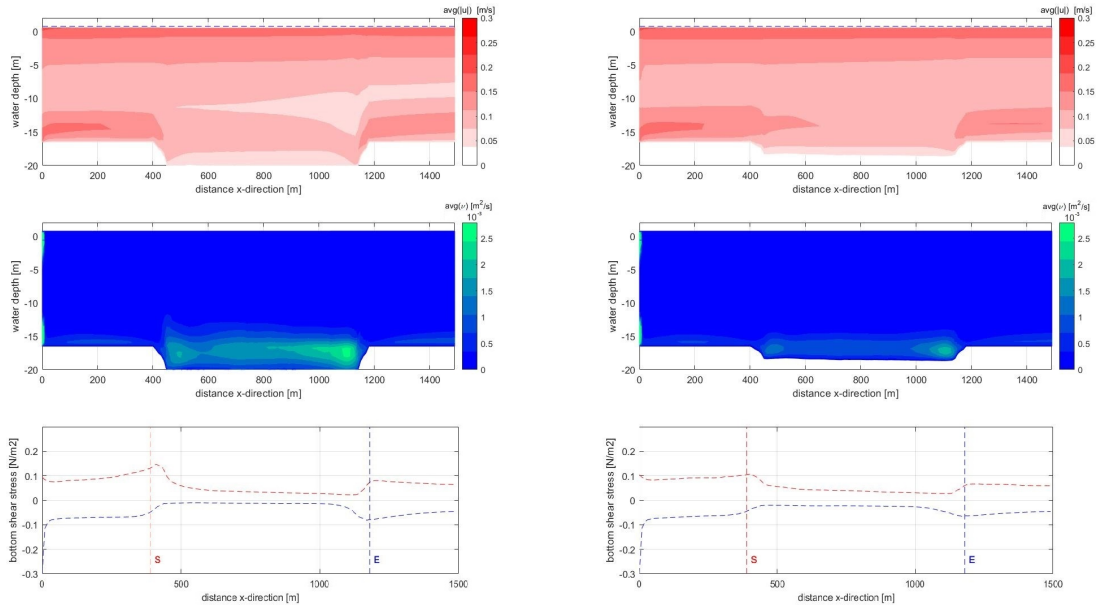

Figure 6.4: Averaged values are shown over the entire simulation period of the absolute average flow velocity, average turbulent eddy viscosity and average bed shear stress basin directed (red dashed) and river directed (blue dashed) from top to bottom, respectively. The left column shows the simulation with a trap twice as deep, the right column the simulation with the basic sediment trap.

By common sense one would think that a deeper trap catches sediment better. If a look is taken at the hydrodynamics, this thought is altered. A significant increase in turbulence increases the upward forces on the sediment in combination with a more frequent presence of hydraulic jumps. Eroded sediment is easily transported upward by the turbulent forces and fluid mud layers are broken down by the turbulence. The increased overdepth would catch dense suspension flows just as well as a regular trap. A look is taken at the accumulation quantities. The erosion scenario shows indeed worse results than the basic trap. Even more sediment is eroded from the mouth, a decrease of 3 % (35% to 34%) of accumulated sediment in the trap is seen and an increase of 8% (48 % to 52%) in the basins. This is even worse than the situation without trap. For the fluid mud scenario exactly the same is observed as for a basic trap. The proportional distributions are the same over the mouth, trap and basin. The deepening of the trap resulted in a net decrease of sediment of 6% for the erosion scenario and a decrease of 2% for the fluid mud scenario.

Deepening the sediment trap further is not desired for the trapping of sediment. For

simulation with a constant SPM boundary condition an increase of accumulation of 8% was observed for the erosion scenario in the basins and no increase was observed for the fluid mud scenario compared to the simulation with a basic sediment trap.

6.1.2.2 Twice as shallow

The second trap that is simulated is the '2x shallow' trap. The trap half as deep is expected to result in a smaller flow deceleration, smaller turbulent eddy viscosities and an increased bed shear stress compared to the simulation with a basic trap. Also for this simulation, hydrodynamics are analyzed based on averaged values over the entire simulation period. Averaged hydrodynamics of the simulation are shown in Figure 6.5. The shallower trap indeed shows decreased turbulence levels. The reduction in flow reduction is almost diminished and smaller turbulence levels are observed. The trap is expected to result better for the erosion scenario, but it is questioned whether it will catch the fluid mud flows correctly or that some might pass due to the small overdepth. Figure 6.3 shows that the acceleration for the trap twice as shallow is small compared to toher depths. Expectations are that internal hydraulic jumps occur less often and are not as strong of character if they are present. This will not have a significant effect on the trapping of sediment.

If we look at the accumulated sediment for erosion, an improvement can indeed be noticed. A minor increase of accumulation is observed in the mouth, similar accretion in the trap and a minor decrease of 2 % (48 % to 47 %) in the basins compared to the simulation with a basic sediment trap. The fluid mud flows seems to be caught just as well as for the regular trap. A little bit more sediment is accumulated in the mouth, the trap shows therefore a minor decrease of 3 % (34 % to 33 %), but the same proportional amount of sediment is accumulated in the basins.

A shallow sediment trap shows similar results as a regular sediment trap. While it is the common assumption that a shallower sediment trap fulfills the trapping function to a lesser amount, this is not the case. For the erosion scenario it even results in a small decrease of accumulation in the basins of 2% for moderate erosion. The fluid mud scenario results in the same quantity of accumulation in the basins.

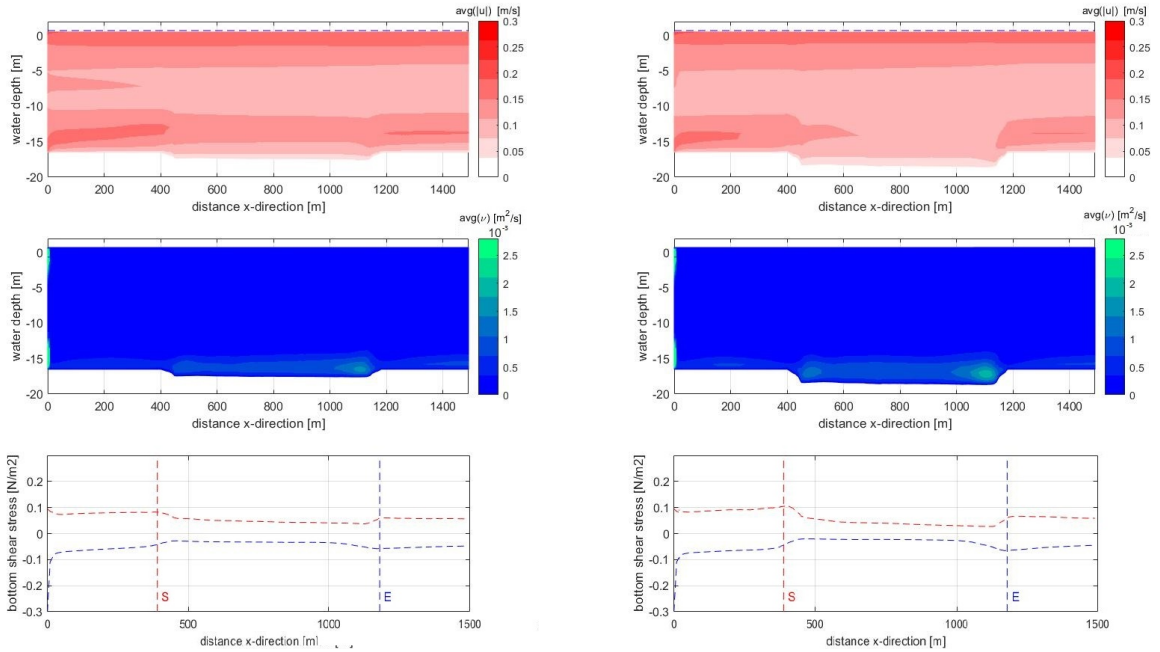

Figure 6.5: Averaged values are shown over the entire simulation period of the absolute average flow velocity, average turbulent eddy viscosity and average bed shear stress basin directed (red dashed) and river directed (blue dashed) from top to bottom, respectively. The left column shows the simulation with a trap half as deep, the right column the simulation with the basic sediment trap.

6.1.2.3 Twice as short

A trap twice as short is simulated to see if the length of the trap influences the trapping of the sediment trap. The hydrodynamics are expected to be kind of similar to the regular trap. The turbulence levels are expected to be a little bit higher, because the edges are reached by both ebb and flood current related turbulence. The bottom shear stress is expected to be influenced in a negative matter, i.e. larger average bed shear stress. A larger proportion is closely located to the edges and a smaller proportion is covered by the sediment trap. The flow velocity reduced for a similar amount, but for a smaller area. These effects are indeed confirmed by the averaged hydrodynamics over the entire simulation as can be seen in Figure 6.6. The trap twice as short is expected to have similar internal flow properties as the regular sediment trap. This is not further investigated.

The accumulation of the short sediment trap is divided in the same three regions mouth (0 m to 390 m), trap (400 to 1190 m) and basins (1200 m to 8770 m) as the above simulations to be able to compare the accumulation of these simulations with each other. Some of the sediment included in the region 'trap' will therefore actually be behind the trap. Although inconvenient for the actually definition, it is

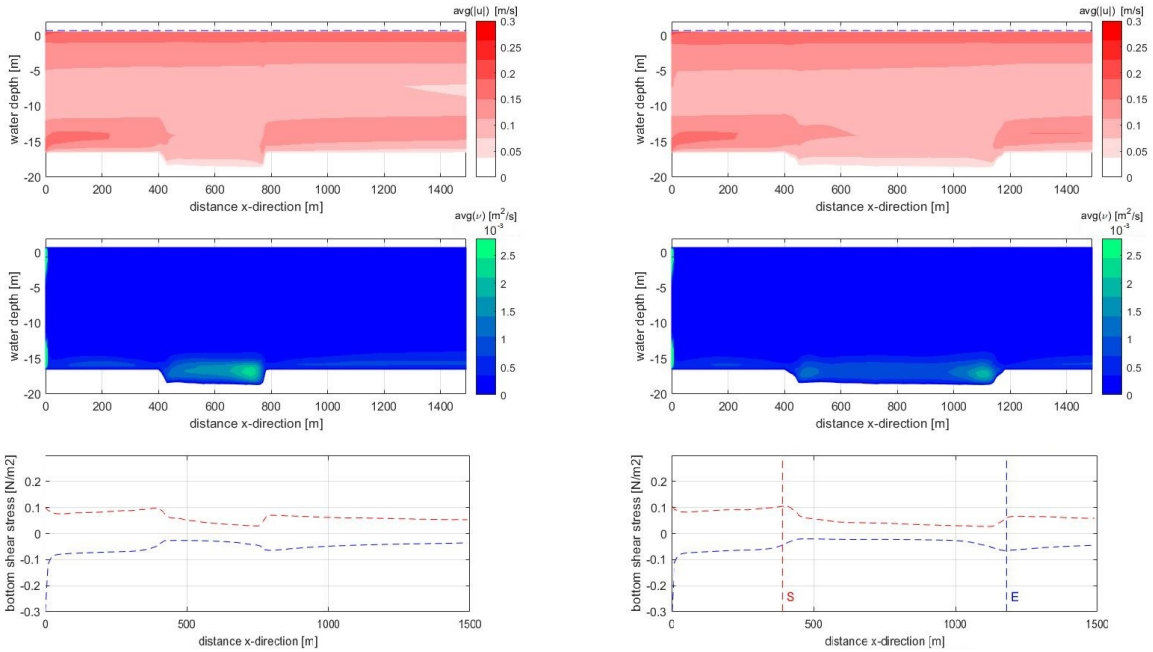

Figure 6.6: Averaged values are shown over the entire simulation period of the absolute average flow velocity, average turbulent eddy viscosity and average bed shear stress basin directed (red dashed) and river directed (blue dashed) from top to bottom, respectively. The left column shows the simulation with a trap twice as short, the right column the simulation with the basic sediment trap.

convenient to be able to compare the simulations this way. If we look at the accumulated sediment for erosion, a small increase in proportional amount of sediment is accumulated in the mouth. The trap shows a small decrease of 3% (35 % to 34 %) of accumulated sediment and the basins show a similar number as the regular trap. For the fluid mud scenario, the trap twice as short showed a proportional increase of 13 % (15% to 17%) in the mouth, a decrease of 9 % (34 % to 31 %) in the (regular sized) sediment trap area and an increase of 4 % (51 % to 53 %) in the basins.

A shorter sediment trap seems unfavourable for the trapping of sediment. For the erosion scenario, no improvement nor deterioration was observed compared to the regular sized trap. For the fluid mud scenario, an increase of 4% of accumulation of sediment was observed in the basin area.

6.1.2.4 Twice as long

A trap twice as long is simulated to see if the length of the trap influences the trapping of the sediment trap. The hydrodynamics are expected to be kind of similar to the regular trap but for a longer domain. Therefore, a larger distance is covered with

a lower flow velocity and increased turbulence levels. The bottom shear stress is expected to be influenced in a favourable way. A large distance is covered by a lower flow velocity thus lower bottom shear stress. Averaged hydrodynamics as given in Figure 6.7 confirm these hypotheses partially. The flow velocity reduction is less over the entire distance than was expected.

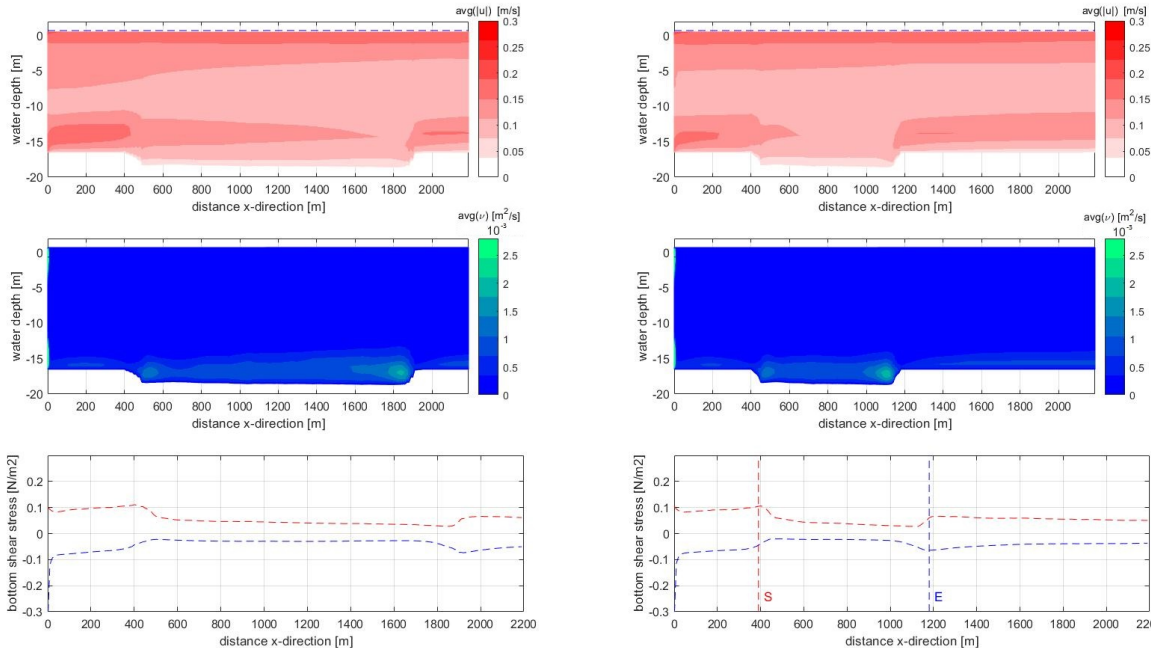

Figure 6.7: Averaged values are shown over the entire simulation period of the absolute average flow velocity, average turbulent eddy viscosity and average bed shear stress basin directed (red dashed) and river directed (blue dashed) from top to bottom, respectively. The left column shows the simulation with a trap twice as long, the right column the simulation with the basic sediment trap. Please note the values at the x-axis are increased compared to other comparisons.

The trap is expected to result in considerable improvement compared to the regular trap or no trap. Because of the increased length and the necessity to compare with other situations, the three areas have been redivided for this simulation. The mouth is still the same from 0 to 390 m. The sediment trap thus starts at the same location. The area of the sediment trap is increased to 400 to 1960 m. Proportional distribution will therefore greatly be influenced. This has no influence on the functioning of the sediment trap. To confirm this, the simulation with a regular sediment trap and without trap have also been added to the tables. The basins area is from 1970 m to 8770 m. Accumulation quantities for these adapted areas are given in Table 6.3 and in Appendix F 'Supporting tables optimization' for numerical values. Accumulation patterns for erosion and fluid mud for the simulation without trap, with trap and trap twice as long for these adapted areas are given in Figure 6.8.

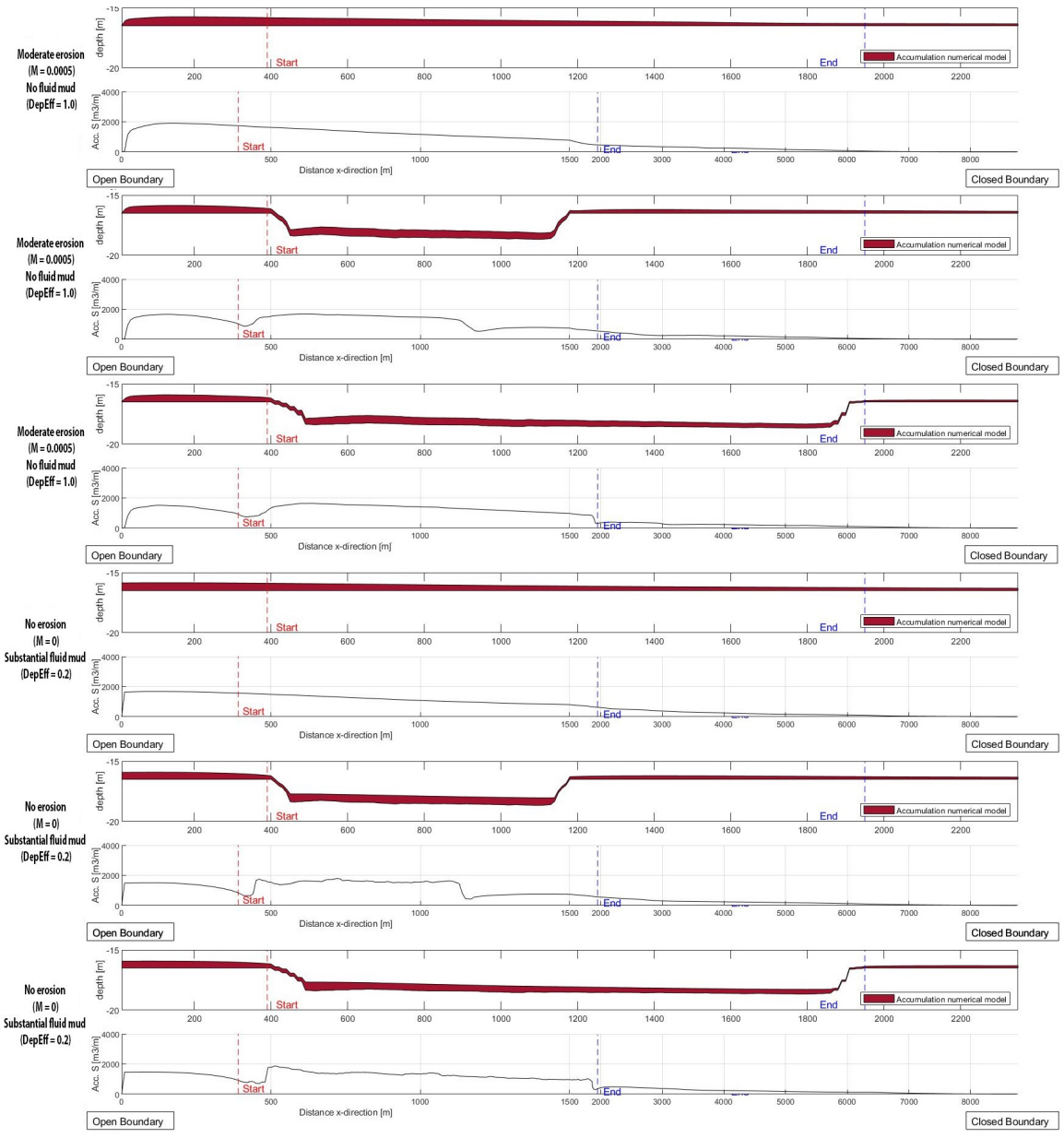

Figure 6.8: The trap twice as long design is simulated on a moderate erosion and substantial fluid mud scenario with a constant SPM boundary condition. To compare the simulation with other simulations, the mouth, trap and basin areas are redefined. Also the simulation without trap and with the regular trap are added for comparison. The top figure of each scenario shows the accumulation pattern of the model (red). The bottom figure of each scenario shows the quantity of accumulation of sediment over the entire domain. Please note the non-equidistant x-axis. The first 1500 m have a higher resolution as it is the domain of interest.

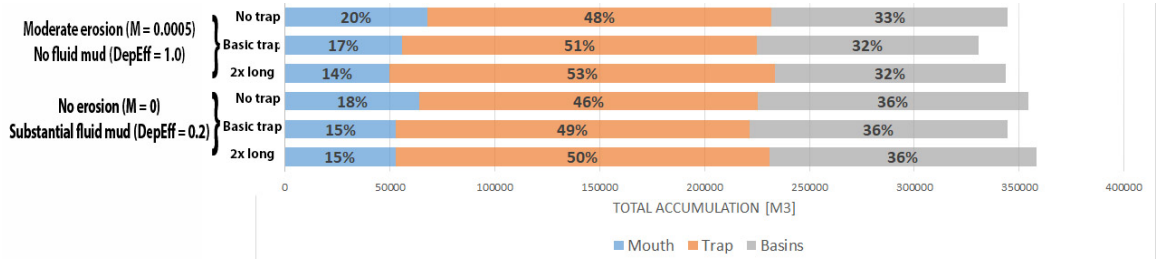

Table 6.3: The trap twice as long design is simulated on a moderate erosion and substantial fluid mud scenario with a constant SPM boundary condition. To compare the simulation with other simulations, the mouth, trap and basin areas are redefined. Also the simulation without trap and with the regular trap are added for comparison. The table shows the quantities and proportions of accumulation in the reclassified mouth, trap and basin at the end of the simulation.

The accumulation quantities do not confirm our hypothesis, but neither dissaprove them either. No significant improvement in trapping of sediment compared to the simulation with a regular sediment trap is observed. While some more sediment is caught in the trap, it originates from the harbour mouth. For both the erosion and fluid mud scenario, a similar proportional amount of sediment accumulates in the basin area. Another thing that is interesting, is that an increase of total accumulation has been noticed compared to both a simulation with regular trap and without trap.

Although hypothesized, a longer sediment trap does not significantly improve accumulation of sediment compared to a regular sediment trap. For both the erosion and fluid mud scenarios, similar proportions accumulated in the harbour basins.

6.1.2.5 V-shaped sediment trap

The next shape that is assessed is the v-shaped sediment trap. The idea of this trap is to create as little turbulence as possible by slowly declining the bottom of the sediment trap. Dimensions were chosen in such a way that the volume in the trap is similar to that of the regular sediment trap. When a look is taken at the hydrodynamics, a distinctive reduction in turbulence levels is not found. The main difference is that there are not two maxima near the edges as is the case for a regular sediment trap, but there is only one maximum in the middle of the trap. The bottom shear stress seems to be larger on the left slope, so some more accretion on the right slope is expected. The flow velocity reduction is not considerable. The trap is expected to not shown a significant improvement compared to the basic sediment trap. The V-shaped sediment trap shows some serious deceleration so the internal flow properties

are expected to be similar to that of a trap twice as deep, i.e. strong and frequent internal hydraulic jumps. This is however not investigated further.

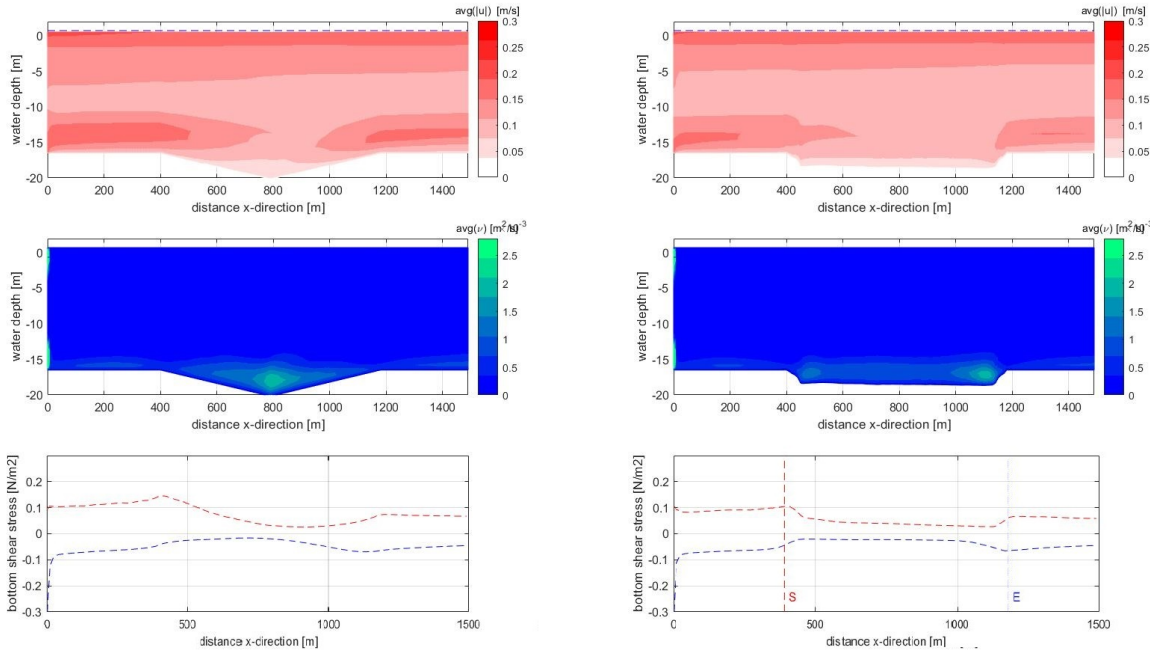

Figure 6.9: Averaged values are shown over the entire simulation period of the absolute average flow velocity, average turbulent eddy viscosity and average bed shear stress basin directed (red dashed) and river directed (blue dashed) from top to bottom, respectively. The left column shows the simulation with a V-trap where the depth gradually decreases and increases, the right column the simulation with the basic sediment trap.

Accumulation quantities confirm this hypothesis. The trap increases the accumulation in the basins for the erosion scenario with a tremendous 13 % compared to a simulation with trap. This is even significantly worse than the simulation without trap. There is an increase of turbulence, but no significant decrease in flow velocity. For the fluid mud scenario the v-shaped trap functions similarly as the simulation with a regular trap. A small difference is in the distribution between mouth and trap.

A gradual declining sediment trap seems unfavourable for the trapping of sediment. Increased turbulence levels are still present, while the flow velocity reduction is considerably reduced. For fluid mud similar trapping quantities as for a regular sediment trap are observed. For the erosion scenario, an increase of 13 % of accumulation was observed in the basins.

6.1.2.6 Sill

The sill is an experiment that came to mind after a few field observations were made. Increased accumulation was observed toward an underwater sill, while locations deeper in the basin were merely touched. The idea of the sill is to repulse density driven currents. It is expected that for the erosion no significant increase can be observed, but for the fluid mud simulation a significant reduction of accumulation in the basins is present. When a look is taken at the hydrodynamics in Figure 6.10, flow velocities are very similar to a simulation without trap. Compared to the simulation with a regular trap, flow velocities have increased, turbulence levels have decreased and the bottom shear stress has a constant value (therefore slight increase) over the domain. A sill would be desirable regarding the internal flow properties. No accelerations due to the bathymetry are present so no significant change is present in the internal flow properties.

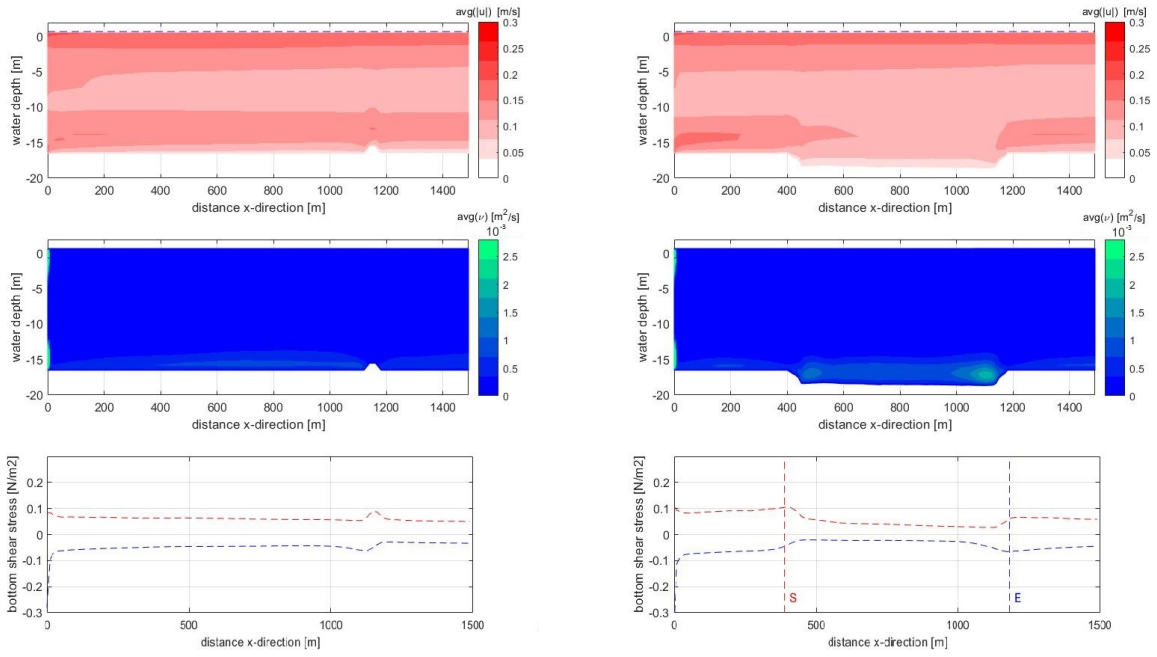

Figure 6.10: Averaged values are shown over the entire simulation period of the absolute average flow velocity, average turbulent eddy viscosity and average bed shear stress basin directed (red dashed) and river directed (blue dashed) from top to bottom, respectively. The left column shows the simulation with a sill, the right column the simulation with the basic sediment trap.

The sill did however have some interesting results. While no significant improvement was expected for the erosion scenario, this was actually the case. A lot more sediment is accumulated in the mouth, namely an increase of 29 % (17 % to 22 %). The accumulation at location of the trap is reduced by 9 % (35 % to 32%) and in the

basins a reduction compared to the simulation with the trap was observed of 4% (48 % to 46 %). This results in a reduction of 6% accumulation in the basins compared to the simulation where no trap in present. For the fluid mud scenario compared to the simulation with trap similar results are observed for the accumulation in the basin, both result in 51% accumulation in the basins. For the simulation with the sill, more of the remaining sediment is located near the mouth.

Installation of a sill yield favourable results for the trapping of sediment. A small sill may reduce sedimentation in the basins by 6 % compared to a simulation without sill or trap for an environment where erosion is important. For an environment where fluid mud is present the sill functions as good as a sediment trap, but the sediment is located in larger quantities in the mouth instead of the trap.

6.2 General conclusions

Now that all the shapes have been analyzed separately, some trend can be distinguished over all simulations.

6.2.1 Internal flow dynamics

We have seen that the internal flow characteristics play a signifcant part in the trapping of sediment. An overdepth in the bathymetry changes the internal flow properties. This may change the internal hydraulic state of the flow, resulting in an internal hydraulic jump. Numerical simulations show that a deeper sediment trap has a larger acceleration, thus a larger internal Froude number. Shallower traps result in smaller accelerations. If an internal hydraulic jump occurs, the uplift of substances, e.g. salinity and SPM, is influenced by the strength of the jump. This effect is strongly represented by the accumulation patterns. Shallow traps seem desirable, while deep traps seem to hinder the goal of the sediment trap.

The overdepth of the sediment trap has serious consequences regarding the internal hydraulic state of the flow. Internal hydraulic jumps seem to influence the trapping of considerably. Numerical simulations confirm the hypotheses that shallow sediment traps result less frequent jumps and weaker jumps compared to deeper sediment traps. This effect is hypothesized to be the main cause for the advantageous results of a sediment trap twice as shallow c.q. the disadvantageous result of a trap twice as deep.

6.2.2 Erosion

For the erosion scenario, no straightforward conclusions can be drawn. The creation of an overdepth has shown to result in a marginal improvement in the capturing of sediment in an environment where erosion is important. A regular sediment trap decreases accumulation for an environment with moderate erosion in the harbour basins by 2%. A shallow trap may increase this amount to 4%, but deepening the trap further may even enhance accumulation in the basins. A shorter or longer trap did not improve the situation. Installation of a sill did however result in a decrease of 6 % compared to situation without trap. The following is therefore concluded.

In an environment where erosion is important, the length of the trap has no significant influence on reducing accumulation in the harbour basins. A too large overdepth results in the undesired effect of increasing accumulation in the basins, while a shallow trap slightly reduces the amount of sediment trapped in the basins. A sill was found to be the best measure, by reducing the sedimentation in the basins by 6% for a simulation with moderate erosion.

6.2.3 Fluid mud

An interesting phenomenon is observed when looking at Figure 6.2. For all simulation with an overdepth the same proportional amount of sediment accumulated in the basins. The size of this overdepth seems to be of no importance. For all simulation with the same length trap the same amount of sediment would accumulate in the basins. For the trap twice as short, more sediment accumulated in the basins. The following is concluded.

The presence of an overdepth has shown to result in a significant improvement in the capturing of fluid mud flow. For the trapping of substantial fluid mud layers, an overdepth results in 6% less sediment in the harbour basins no matter the depth or shape of the trap. The length of the sediment did influence the accumulation in the basins. A trap twice as short showed an increase of 4 % of accumulation in the basins compared to a regular trap. A trap twice as long or installation of a sill resulted in similar accumulation in the harbour basins as a regular trap.

6.2.4 Total accumulation

The total accumulation of sediment in each of the simulation is still a big question-mark in this thesis. By replacing the variable SPM boundary time series with a constant boundary condition, expected was that no signifcant difference would be present in terms of total accumulation. This is however still the case. It even seems that for deeper traps the total accumulation decrease, while the port is deepened. This is highly counter-intuitive and possibly an interesting topic for further research. If for such similar runs the hydrodynamics change the import of sediment up to 8% (2x shorter compared to no trap), this might be interesting to look in to. The following is concluded.

Even for the constant SPM boundary condition the accumulated sediment quantities in the domain differ significantly. The same trend can however be observed for erosion and fluid mud scenarios. A counter-intuitive conclusion is drawn that for deeper traps the sediment that enters the domain reduces. The V-shaped and trap twice as long resulted in an increase in imported sediment, while the trap twice as short resulted in the largest decrease of accumulated sediment in the domain.

6.2.5 Sediment trap as mitigation measure

This finally leaves us with the remaining research objective: 'Is the sediment trap an effective mitigation measure to significantly reduce maintenance dredging costs?'. So far, three scenarios have been distinguished. The settling scenario resulted in a marginal improvement in accumulation of sediment, but was considered to be too divergent from field data. The erosion scenario resulted in quite different results. The sediment trap only seems to be an effective measure if it is shallow. A too deep sediment trap would actually increase sedimentation in the basins. The scenario did however reproduce the survey data very well. For the fluid mud scenario, each type of sediment trap is an effective mitigation measure. A longer sediment trap results in less accumulation in the basins than a short one. The main point is however that any type of overdepth would result in improvement of the maintenance dredging costs significantly. The problem is however that we do not exactly know what mechanism is dominant at this point. Different measurements such as daily bathymetry measurements could provide this answer. The available bathymetry measurements do

not provide enough information to know whether fluid mud, settling or erosion transported the sediment in the basins. Increasing the frequency to have a bathymetry of each tidal cycle would suffice.

Whether a sediment trap is an effective mitigation measure depends on the type of sedimentation in the harbour basin. For fluid mud flows, any type of overdepth decreases accumulation of sediment considerably. The amount of overdepth or the shape does not influence this in the numerical model. The length of the trap should be sufficient. A too short trap results in a smaller decrease of accumulation in the basins compared to a regular trap. For erosion enviroments, only shallow sediment traps have proven to reduce accumulation in the basins. Too deep traps actually increase accumulation in the basins. A sill has proven to be the best measure for both mechanisms. If overdepth is desirable for navigation a shallow sediment trap would be advised. For both erosion and fluid mud scenarios a reduction of accumulation in the harbour basins are observed.

Chapter 7

Conclusions

This chapter discusses the results and the entire research. First the 'Discussion' explains the significance of the results in the context of the report and the wider literature on the topic. Results are explained and feedback is given on the questions proposed in the Introduction. Finally, the relevance of the results to wider engineering problems is provided. A short review of the findings of the numerical simulations is given in the 'Conclusions'. The conclusions about the results are linked back to the original aims and objectives of the research. Finally, outlook for further research is included in 'Recommendations'.

7.1 Discussion

The research focuses on answering the research question whether sediment traps are an effective mitigation measure for the reduction of maintenance dredging costs. The research question was translated to the aim of quantifying the reduction of accumulation in harbour basins by the installation of sediment traps with numerical model simulations.

The setup of a numerical model inevitably results in errors. To determine the boundary conditions, some creativity had to be used. A measured water level time series was combined with a calculated Operationeel Stromingsmodel Rotterdam (OSR) time series for salinity to describe hydrodynamics as shown in Figure 4.5 (Port of Rotterdam, 2019). The salinity time series have been assumed to be correct, but this is not further investigated. The philosophy to keep the model as simple as possible paid off, but still some assumptions were too radical. First there was the assumption of sediment concentrations. This was a large uncertainty and the measurements of De Nijs (2012) were the only literature that was available at the subject. The varying Suspended Particulate Matter (SPM) boundary condition in Figure 4.6 was

generated in Appendix D 'Generation SPM time-series' to represent the Estuarine Turbidity Maximum (ETM) resulted in large variations in accumulation of sediment in the domain. Although this behaviour is plausible, no linear trend was observed between scenarios in Tables 5.1 and 5.2 for erosion and fluid mud, respectively. Quantities of sediment seemed to vary for each simulation almost randomly, especially for the fluid mud scenarios. The philosophy to keep the model as simple as possible was left. Accumulation was not only determined by the adaptations of the bathymetry, but minor hydrodynamics changes resulted in large accumulation differences.

A constant SPM boundary condition should solve this error. Although this is less realistic, it is a common practice in modelling studies such as J. C. Winterwerp & van Kessel (2003). Luckily the variable SPM time series was only used for the parameterization of the erosion and fluid mud parameter and no serious delay was experienced. Differences in accumulated sediment were still observed, but did not show a stochastic character anymore. The assumption of hydrostatic pressure has been analyzed by means of the Richardson number, expressing the ratio between the buoyancy term to the flow shear term (Pietrzak, 2017). The assumption does not always hold. The vertical mixing may therefore be slightly underestimated. While this should not be too large a problem, the moments that this happens were the exact moments that large flow velocities occurred thus sediment would be present in the water column. This could be solved by solving the momentum equation in the z-direction, on top the x and y-direction. This possibility is however only included in Delft3D for z-layers, while σ-layers are used in the model. With these shortcomings in mind, the result was a rigid, simple model with no effects other than the bathymetry on the accumulation of sediment. Strong linear trends can be seen between sediment traps with increasing depths, i.e. '2x shallow', 'basic' to '2x deep', and traps with increasing lengths, i.e. '2x short', 'basic' to '2x long', in Tables 6.1 for erosion and 6.2 for fluid mud.

When we try to give meaning to the results with a theoretical background, it is hard to include all possible potential influences. To answer our main research question 'Is the sediment trap an effective mitigation measure for the reduction of maintenance dredging costs?' we intend to quantify results. By changing bathymetries and analyzing as many relevant processes as possible, e.g. velocity distributions, turbulence levels, stratified flows, internal hydraulic states of the flow, bathymetry, sediment characteristics, we try to understand as thorough as possible what is happening with each bathymetry change. Lots of processes are analyzed that could challenging enough for research on its own. The subject is rather broad and although

the research question might sound straightforward, many individual influences could be investigated in more detail.

With that in mind also some assumptions have been made in the case study. Use has been made for a single (dry) period for a single location, i.e. the Botlek harbour. The geometry is adjusted to 2DV to fit this exact location. Conclusions that are drawn may only be applicable to this exact setup. Conclusions should not be seen as normative in terms of numbers, each harbour basin has its own flow characteristics, salinity intrusion, tidal prism and sediment supply. Even for the Botlek harbour, results may vary considerably for seasonal changes. A stronger river discharge influences the salt intrusion considerably. Conclusions should rather be seen as the influence of certain processes and mechanisms on the sedimentation in the sediment trap.

Unfortunately, recognition that the internal hydraulic state of the flow plays such a large part in the sedimentation around sediment traps was one of the final findings of the research. Theoretical hypotheses are confirmed by the model results. This is however only treated for various depths of the sediment trap. If this was recognized earlier, research could have a larger scope towards the subject.

That capturing dense suspension flows is a dominant mechanism that enhances the trapping of sediment is clear from the research. The shape of the overdepth should be determined by looking at the internal flow properties. Shallow traps seem to reduce the internal hydraulic jump frequency and strength. Whether that is actually happening in reality is another question. While the numerical simulations are able to assess the different mechanisms very well, they do not provide a direct link to the in situ case. The numerical simulations provide an excellent indication whether and what type of sediment trap would be advisable for various types of environments and that the sediment trap may be an effective mitigation measure for reducing maintenance dredging costs.

7.2 Conclusions

The conclusions of the report are used to answer the main research objective: 'Determine if the sediment trap is an effective mitigation measure to significantly reduce maintenance dredging costs.' This research objective is treated by answering five research questions:

1. What are the dominant processes that drive harbour siltation?

2. What is the most relevant mechanism that determines the trapping of sediment in sediment traps?

3. To investigate the balance between mechanisms that govern the trapping of sediment in the sediment trap, are we able to set up a numerical model?

4. How much do the mechanisms contribute to the trapping of sediment in the sediment trap?

5. What shape and volumes result in an ideal design for sediment traps?

Chapter 2 'Understanding the system' helps us understand what processes and mechanisms drive harbour silation by asnwering the first research question. The port of Rotterdam is located in an estuarine system where sediment is supplied by the river and sea. The marine sediment is eroded by waves and currents. When a stratification is present, suspended sediment confines below the pycnocline (Geyer, 1993). River sediment is transported as suspended material over an oscillating salt wedge that is forced by the tidal signal. The strong pycnocline in this salt wedge has a turbulence destructing character and SPM is accumulated in the tip of the salt wedge. This ETM exchanges large sediment quantities with harbours in the port of Rotterdam (De Nijs, 2012). Dominant processes that govern the exchange of water with harbour basins are the mechanisms tidal filling, density driven currents by salinity and horizontal exchange by turbulent shear (Langendoen, 1994). The scenarios contribute to harbour siltation by exchanging sediment rich water into the basin and sediment poor water out.

To increase the trapping of sediment locally, the installation of sediment traps is considered. By increasing the bathymetry locally, an increase of local accumulation is expected and a decrease of accumulation of sediment deeper in the harbour basin. The deepening of the bathymetry affects the hydrodynamics in the basin. The flow expansion caused by the sediment trap theoretically reduces the flow velocity (van Rijn, 2005), but increases the turbulent kinetic energy locally (Nakagawa & Nezu, 1987) (Blom & Booij, 1995). The sediment trap changes the properties of the internal flow, which may theoretically change the hydraulic state of the flow resulting in large instabilities. To investigate the dominant mechanism for the trapping of sediment in the sediment trap, a distinction is made between three trapping mechanisms. These are treated in Chapter 3 'Sediment trap dynamics' that answers the second research question. A settling and deposition scenario is considered where the sediment is advected by the hydrodynamics and the vertical distribution of sediment

over the water column is determined by the downward settling velocity and upward turbulent kinetic energy only. The sedimentation of fines due to this mechanism is expected to not significantly improve by installation of a sediment trap. A second mechanisms that is investigated is the trapping of the sediment due to the erosion and deposition mechanism. On top of the settling scenario, a reduction of bottom shear stress inside the sediment trap leads to a reduction of erosion and enhance the trapping of sediment. The enhanced trapping of a sediment trap due to this mechanism is hypothesized to be significant for an adequate long sediment trap in a basin where tidal flow velocities are substantial. The third mechanism that is investigated is the capturing of dense suspension flow. Large concentrations of sediment increase the density of the water according to the Equation of State resulting in a density gradient in the horizontal. The density gradient governs the dense suspension flow, which is caught by the sediment trap. The enhanced trapping of a sediment trap due to capturing of dense suspension flows is hypothesized to be significant for any shape of sediment, given that it has an overdepth.

To investigate the balance between mechanisms that govern the trapping of sediment in the sediment trap, a numerical model is set up. Chapter 4 'Setup of hydrostatic Delft3D-FLOW online SED model' discusses the decisions made in the setup of the model and treats research question 3. A simple rectangular 2DV basin with an open and closed boundary is set up to represent the Botlek Harbour. Variations due to the curvature of a river bend are averaged out over the width. By imposing a salinity and water level time series and a constant SPM boundary condition, the behaviour of above described mechanisms could be simulated reasonably well. Mechanism 'Tidal filling' alone does not describe the hydrodynamics that govern the exchange of water with the harbour basin. The net exchange of water is governed by the tidal filling mechanism. Density currents caused by salinity differences govern the vertical flow velocity distributions. The phase difference between high water and salinity peak values is between 1.5 and 3 hours. The theoretical statement that the flow expansion caused by the sediment trap would reduce the flow velocity and increase the turbulence locally has been confirmed by the numerical model. The bed shear stress increases near the edges of the sediment trap, but decreases inside the sediment is concluded from the numerical model. Large flow velocities governed by the density gradient due to salinity differences may lead to an unstable stratification with Richardson numbers smaller than $\frac{1}{4}$ (Miles, 1961). The non-hydrostatic instabilities caused by this phenomenon are not included in the hydrostatic model (Delft Hydraulics, 2006).

The hypothesis that the sediment trap changes the properties of the internal flow has been shown to be of influence according to the theory of (Winters & Armi, 2012) for a continuous density gradient. Numerical simulations confirm that the sediment trap changes the properties of the internal flow, which may change the hydraulic state of the flow resulting in large instabilities and even an internal hydraulic jump. An overdepth in the bathymetry changes the internal flow properties. This may change the internal hydraulic state of the flow, resulting in an internal hydraulic jump. Numerical simulations show that a deeper sediment trap has a larger acceleration, thus a larger internal Froude number. Shallower traps result in smaller accelerations. If an internal hydraulic jump occurs, the uplift of substances, e.g. salinity and SPM, is influenced by the strength of the jump. The overdepth of the sediment trap has serious consequences regarding the internal hydraulic state of the flow. Internal hydraulic jumps seem to influence the trapping of considerably. Numerical simulations confirm the hypotheses that shallow sediment traps result less frequent internal hydraulic jumps and weaker jumps compared to deeper sediment traps. This effect is hypothesized to be the main cause for the advantageous results of a sediment trap twice as shallow c.q. the disadvantageous result of a trap twice as deep.

Research question 4 is treated in Chapter 5 'Analyses of trapping mechanisms'. First a parameterization is done to see what influences various degrees of erosion and fluid mud have on the sediment. Later on representative values are chosen to continue analyses of various shapes. During the parameterization the scenarios settling and deposition, erosion and fluid mud were investigated. The parameterization has been done with a variable SPM boundary conditions to represent the behaviour of the ETM. This resulted in a very occasional supply of sediment. The model was therefore highly sensitive to hydrodynamics regarding sediment quantities in the domain. Some conclusions about the parameterization were still considered valid, while conclusions on the quantities of sediment are not used. Numerical simulations where only settling and deposition are present result in marginal improvements with sediment trap compared to a simulation without trap. Based on numerical simulations with a strong erosion influence, erosion enhances the trapping of sediment in the sediment trap. Most of this sediment originates however from the sediment mouth. In the harbour basins the presence of a sediment trap may even increase the accumulation of sediment. There is no significant contribution on the maintenance dredging costs by the installation of sediment traps in an environment where erosion, i.e. settling, deposition and erosion, is important.

Based on numerical simulations that include fluid mud behaviour, fluid mud enhances the trapping of sediment in the sediment trap. A decrease of accumulation in the mouth was observed, an increase in the trap and a decrease in the basins. There is a significant contribution to the maintenance dredging costs by the installation of sediment traps in an environment where fluid mud is present. The decreased amounts of accumulated sediment in the basin for substantial to lots of fluid mud behaviour may vary between 10 % and 14 %, depending on how this fluid mud behaviour is modelled.

The representation of the three scenarios is assessed based on a bathymetry survey and maintenance dredging quantities. The sedimentation pattern of the accumulated sediment in the model for each scenario is compared to a 118 day Echosounder Multibeam survey with a frequency of 2-4 weeks. During this period no temporal storage or dredging activities took place and all sedimentation can be assigned to natural sedimentation. The sedimentation is also compared with maintenance dredging data of the years 2015 - 2017. During these years no project-based dredging, e.g. the deepening of the basins, took place. The erosion scenario seems to represent the sedimentation pattern of the Echosounder Multibeam surveys the best. The maintenance dredging data gives a good impression of the quantities of accumulated sediment, but no dominant trapping mechanism can be assigned based on these data. The data show an increased accumulation rate in the sediment trap. This is observed for both the erosion and fluid mud scenarios, but not for the settling only scenario. Therefore we have only continued with a scenario for moderate erosion and a scenario for substantial fluid mud behaviour. To investigate the influence of various shapes of the sediment trap, the varying SPM boundary condition has been replaced by a constant boundary condition. Simulations with a constant boundary condition yield the same results considering the dominant mechanisms for the trapping of sediment in the sediment trap. Settling only and erosion scenarios show little contribution, while the fluid mud scenario shows a significant contribution to the trapping of sediment in the sediment trap. Even for a constant SPM boundary condition, considerable variations up to 9 % are observed between exactly the same simulation due to a difference in bathymetry. Apparently, the presence of the sediment trap influences the hydrodynamics to such an extent that it may even result in less import of sediment.

Many shapes are tested in Chapter 6 'Optimization of the sediment trap design', treating research question 5, to assess the influence of different sediment trap designs. Many shapes such as twice as deep, shallow, short and long, but also a v-shape and a sill were investigated. A distinction is made between a erosion and fluid mud

scenario. For the erosion scenario, quantities seem to be entirely driven by the internal flow properties. The creation of an overdepth has shown to result in a marginal improvement in the capturing of sediment in an erosion environment. A regular sediment trap decreases accumulation for a moderate erosion environment in the harbour basins by 2%. A shallow trap may increase this amount to 4%, but deepening the trap further may even enhance accumulation in the basins. A shorter or longer trap did not improve the situation. Installation of sill did however result in a decrease of 6 % compared to the situation without trap.

The presence of an overdepth has shown to result in a significant improvement in the capturing of fluid mud flow. For the trapping of substantial fluid mud layers, an overdepth results in 6% less sediment in the harbour basins no matter the depth or shape of the trap. The length of the trap did influence the accumulation in the basins. A trap twice as short showed an increase of 4 % of accumulation in the basins compared to a regular trap. A trap twice as long or installation of a sill resulted in similar accumulation in the harbour basins as a regular trap. But also an interesting thing happened for the total accumulation of sediment in the domain for each scenario. Even for the constant SPM boundary condition the accumulated sediment quantities in the domain differ significantly. The same trend can be observed for erosion and fluid mud scenarios. A counter-intuitive conclusion is drawn that for deeper traps the sediment that enters the domain reduces. The V-shaped and twice as long trap resulted in an increase in imported sediment, while the twice as short trap resulted in the largest decrease of accumulated sediment in the domain.

That leaves us with our main research objective: 'Determine if the sediment trap is an effective mitigation measure to significantly reduce maintenance dredging costs.' Whether a sediment trap is an effective mitigation measure depends on the type of sedimentation in the harbour basin. For fluid mud flows, any type of overdepth decreases accumulation of sediment considerably. The amount of overdepth or the shape does not influence this in the numerical model. The length of the trap should be sufficient. A too short trap results in a smaller decrease of accumulation in the basins compared to a regular trap. For environments where erosion is important, only shallow sediment traps have proven to reduce accumulation in the basins. Too deep traps actually increase accumulation in the basins. The reason for this is the internal wave structure. Deep traps may increase the frequency and strength of hydraulic jumps, negatively impacting sedimentation. A sill has proven to be the best measure for both mechanisms. If a certain Nautical Guaranteed Depth (NGD) is restrictive

for navigation a shallow sediment trap is advised. For both erosion and fluid mud scenarios a reduction of accumulation in the harbour basins is observed.

7.3 Recommendations

This chapter is assigned to conduction of further research. During the setup of the numerical model, there were a few things that could have improved the set up greatly.

Any model needs calibration. The calibration data, i.e. the maintenance dredging data and Echosounder survey, were sufficient to suffice as a preliminary study for sediment traps. The survey that was carried out on a frequency of 2-4 weeks gave a nice indication of the sedimentation quantity and pattern. Yet, a daily survey provides information on how sediment moves over a tidal period. This will help greatly to distinguish which trapping mechanism is dominant for the sediment trap. We do not know hwo often these fluid mud layers are present or at what bottom shear stress sediment is resuspended. More measurements should be performed to confirm the results of the numerical simulations. Research has concluded that sediment traps work under certain circumstances, whether these circumstances are actually present needs to be investigated further. But also other measurement could greatly contribute to research in the port of Rotterdam. If three stationary suspended sediment monitors are installed at the New Waterway, Old Meuse and in the New Meuse the boundary conditions of the system can be closed. For the simulation of the port of Rotterdam the sediment concentrations can be improved considerably by calibration of the model. Also measurements about the soil strength and density of the sediment layers will help significantly.

Maybe the most important recommendation is to investigate the internal flow structure further. In this research we have proven that hydraulic jumps may play a significant role in the sedimentation in sediment traps. Unfortunately, this has only been discovered at a late stage in the research and therefore feels a little bit rushed. To exactly determine when these jumps occur, under what circumstances, and what would ideally be the best design for various harbours is a very interesting outlook.

A recommendation is to conduct a research on the influence of bathymetry on the hydrodynamics and accumulation of sediment. Even for this simple model with a constant boundary condition, accumulation rates varied up to 8 % which is quite considerably for small depth variations. Perhaps by varying the bottom a larger decrease of accumulation can be observed due to differences in hydrodynamics.

We have used a hydrostatic numerical model. By analyzing the Richardson number, it could be concluded that the stratification was not stable at all times. Non-hydrostatic instabilities should be present, but are not correctly represented in this hydrostatic numerical model. Running a non-hydrostatic model, that solves the momentum equations in z-direction, to include these effects is recommended, for example with Delft3D-FLOW online SED with z-layers.

In the report we distinguish between erosion and fluid scenarios. It would be interesting to investigate how these scenarios interacts with each other. Reality likely is a combination of the two. Neither is it only erosion driven, nor only fluid mud driven. The harbour is now modelled to a situation where either erosion or fluid mud is present. In reality, both may be present and they may even interact. Eroded sediment exchanges with the fluid mud layer and the presence of fluid mud decreases the critical shear stress for erosion.

Various processes have not been considered in this model such as flocculation, consolidation effect and hindered settling. While including these processes in such a numerical model require a better understanding of the system as a whole, they can not be neglected. Each of these processes could be investigated separately.

Unfortunately, the implementation of the most successful sediment trap design were not implemented in the SIMONA-FLOW and Delft3D WAQ model. It would seem logical to recommend this for further research. However, since only the fluid mud scenario seems to significantly contribute, it is not advised to run the simulations in an offline SED model. Density currents have proven to be the most promising capturing mechanism for the sediment trap. These currents are not included in any offline model, therefore results would be disappointing. This effect is quantified in Appendix G 'Model challenges'.

Also the approximation of a single cohesive sediment with a constant settling velocity is quite a crude approximation. Various sediment types could be included to further investigate the sediment trap. Each of the simulation is run without initial sediment in the domain. The sediment was completely dependent on the sediment supply. Perhaps simulations where initial sediment is present would give interesting results about the accumulation within the harbour basin. Simulations are done with a basic Partheniades-Krone formulation for erosion and deposition. More advanced layers have shown to improve fine sediment modelling. One of these systems is the two-layer system by Van Kessel et al. (2011) in Appendix H 'Two-layer system'.

The Botlek harbour lies in a river bend. It is known that the inner bend attracts more sediment than the outer bend due to flow velocity differences. In this model

every simulation is 2DV modelled. Investigating the 3D effects such as this river bend behaviour and horizontal exchange may enhance the trapping of sediment in the sediment trap if a well-thought location is chosen.

The model runs for a single (dry) period. Seasonal variations may have a tremendous influence on hydrodynamics and sediment supply in the Botlek harbour. It is recommended to conduct further research on the impact of this seasonal variation on the sediment traps.

Appendix A

Dredging in the port of Rotterdam

This chapter supports the main chapters with figures and values for the port of Rotterdam and specially for the Botlek Harbour.

A.1 Maintenance dredging in the port of Rotterdam

The port of Rotterdam has seen an increasing quantity of dredged material due to maintenance dredging. Figure A.1 shows the trend of maintenance dredging quantities within the areas maintained by Port of Rotterdam. A side note with these figures is that the amount of dredged material does not equal sedimentation quantities directly. The quantity of dredged material depends on various other factors such as dredging strategy and available budget. Years with little budget result in smaller maintenance dredging quantities, while years with a larger budget result in large maintenance dredging quantities while a buffer is built up. This buffer can be expressed in an extra dredged depth below NGD, allowing sedimentation for a longer period until maintenance dredging is necessary again. The cubic meters of dredged material does not equal the cubic meters consolidated silt. During dredging the material is mixed with water and the cubic meters are measured with the 'half sphere'-method, where dredged material is measured to have a density of at least 1.2 tons/m^3. Port of Rotterdam is responsible to keep the harbour basins at a navigable depth, while Rijkswaterstaat is responsible for the New Waterway and New Meuse. For the period of 1982 until early 2000 this amount has been quite constant, although fluctuating between three and seven million cub meters per year. Since the construction of Maasvlakte 2 in 2013 this amount increased to a fluctuation between eight and twelve million cubic meters per year.

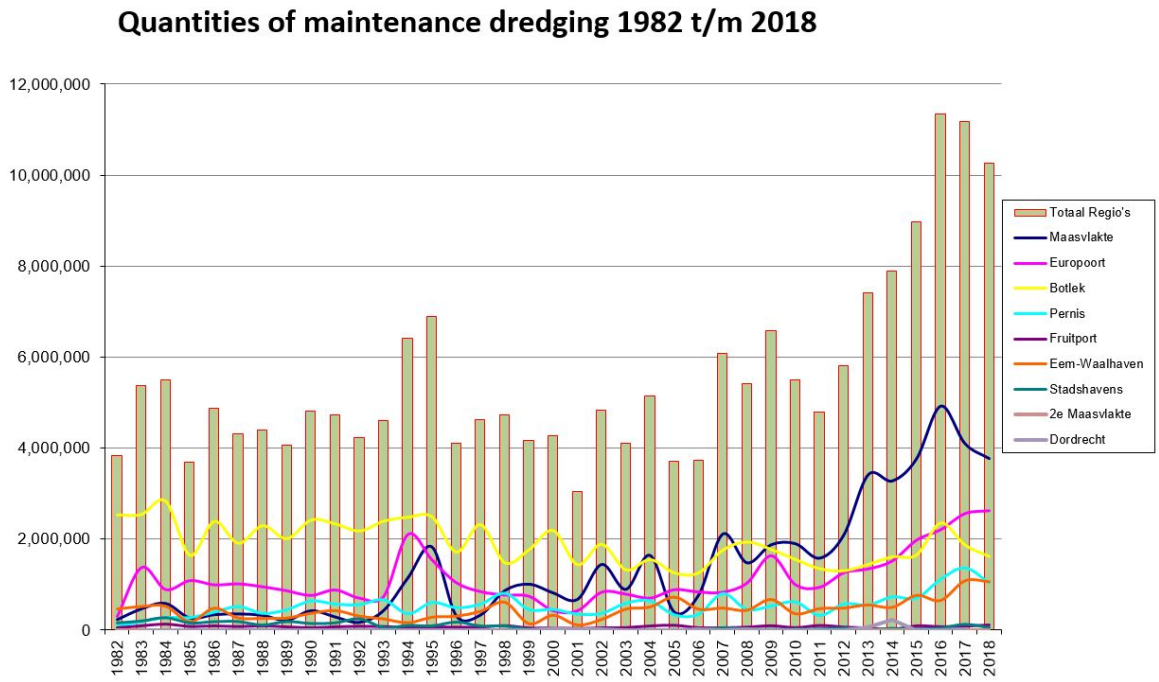

Figure A.1: Amount of maintenance dredging in m^3, and therefore costs, has increased greatly over the past years (Port of Rotterdam, 2019).

A.2 Dredging in the Botlek Harbour

This section discusses the developments around the Botlek Harbour. Quantities of maintenance dredging and the areas are defined in Figure 2.4 in Chapter 2 'Understanding the system'. The Botlek Harbour can be described as a partially mixed to stratified environment. It has a meso-tidal character, is located 20km from the North Sea and has larger siltation rates than other inland harbours as can be seen in Figure A.1.

A.2.1 Events

Two recent events that took place in the Botlek harbour are the removal of 'De Doorn' and an increase of the NGD.

In August 2014 the underwater sill 'De Doorn' was removed. Here, the depth increased from -5.60 meter to -14.50 meter NAP. This sill had a positive effect on the sedimentation. The bottom flow was repulsed by this sill and deflected back into the river Meuse. As a result, less sediment would enter the basins due to its presence. It was however not desirable for navigation, After the sill was removed larger ships were able to enter the Botlek basins. Also, shipping and navigation was easier and more safe.

In September 2018, the Botlek's NGD is increased from NAP - 14.50 m to NAP - 15.90 m to allow mooring of larger vessels. After realization of this new depth, the sediment trap in the Botlek was emptied and used for observation of this research. The actual depth after the hoppers have passed is around NAP - 16.50 m to allow for some buffer.

A.2.2 Dredging records

An overview of the dredged material is given in Figure 2.4. The tabled values are shown in Table A.1. Each dredging field is classified according to the amount cubic metres dredged per surface area per year. More easily this can be interpreted as meters per year dredged sediment. Only the data between 2015 and 2017 is considered here, as during this time the study area has not changed. In the years before 2015, 'De Doorn' greatly affected the sedimentation patterns. After 2017, a general increase of the NGD was implemented in the Botlek harbour, therefore more activities contaminate the data. On top of that, not all data of the year is available yet. Within the years between 2015 and 2017 the dredging records depend solely on the accretion of sediment and temporal storage in areas ABF, ABG and ABJ. The NGD through the main channels of the Botlek is 14.50 m during this period. Dredging records can be used to give a rough indication of the amount of accretion of sediment. It is considered a rough indication, because many uncertainties are involved. The amount of dredged material is influenced by dredging strategies, temporal dumping of sand in sediment traps (which is filtered out here, but is hypothesized to reduce the amount of accretion), but also dredging itself has a quite large uncertainty.

			Amount of dredging 2015 - 2017 [m3]				Temporal storage of sand IN [m3]			Natural accretion [m3]		
Area name	**Code**	**Surface area [m2]**	**2015**	**2016**	**2017**	**Total**	**2015**	**2016**	**2017**	**Total**	**Amount m3 / m2 for 2015 - 2017**	**m3/m2/year**
BOTLEK CENTRALE GEUL VAK 4	ABF	251819.3131	80,635	162,668	135,326	378,629	27,660			350,969	1.394	0.465
BOTLEK CG, VAK 2, WELPLAATHAVEN	ABG	262,680	49,708	189,701	32,582	271,991		155,045	27,930	89,016	0.339	0.113
BOTLEK MONDING	ABH	158,128	161,580	249,544	64,478	475,602				475,602	3.008	1.003
BOTLEK DOORN	AOZ	95,801	125,707	284,456	161,908	572,071				572,071	5.971	1.99
BOTLEK SCHEURKADE	ABI	62,712	75,953	48,562	14,769	139,284				139,284	2.221	0.74
BOTLEK SLIBPUT	ABJ	98,269	267,782	274,126	507,219	1,049,127	137678	6750	170454	734,245	7.472	2.491
BOTLEK ZWAAIKOM	ABK	184,084	225,279	430,686	274,669	930,634				930,634	5.055	1.685
BOTLEK Vak 4 GEM	ACM	369,219	92,521	29,549	48,870	170,940				170,940	0.463	0.154
CHEMIEHAVEN	ABV	292,209	9,221	30,808	11,780	51,809				51,809	0.177	0.059
3E PETROLEUMHAVEN CENTRALE GEUL	AAM	250,802	86,744	147,069	138,414	372,227				372,227	1.484	0.495
3E PETROLEUMHAVEN WEST TAK	AAN	283,946	55,676	174,022	58,312	288,010				288,010	1.014	0.338
3E PETROLEUMHAVEN ZUID TAK	AAO	329,658	136,978	172,805	106,025	415,808				415,808	1.261	0.42
ST. LAURENSHAVEN	AFO	327,770	62,668	37,363	85,742	185,773				185,773	0.567	0.189
AVR haven - ST. LAURENSHAVEN	AAW	47,371	0	0	0	0				0	0	0
TORONTOHAVEN	AFR	90,254	33,334	23,478	27,100	83,912				83,912	0.93	0.31
WELPLAATHAVEN	AJE	64,046	0	0	5,075	5,075				5,075	0.079	0.026
1e WERKHAVEN	AAF	184,747	38,607	0	48,510	87,117				87,117	0.472	0.157
2e Werkhaven	AAL	241,915	53,995	76,493	82,363	212,851				212,851	0.88	0.293
GEULHAVEN	ACN	232,667	23,615	0	0	23,615				23,615	0.101	0.034

Table A.1: Overview of the calculated dredging cubic meters per surface area per year for each dredging field. Data from dredging records is kept track of by Port of Rotterdam.

A.2.3 Rough estimation survey data

However, a first assumption can be made when we look at the quantities and the way the numerical model is set up in Chapter 4 'Setup of hydrostatic Delft3D-FLOW online SED model'. If a look is taken at Figure 2.4 in Chapter 2 'Understanding the system', we can compare the dredging areas with the model setup. The dredging area that correspond with area A 'Mouth' is given by dredge area 'ABH'. The area that corresponds with area B 'Trap' is given by area ABJ. Finally, the areas that are part of area C 'Basins' are 'ABF', 'ABG', 'ACM', 'ABV', 'AFO', 'AAW', 'AFR', 'AJE' and 'AAL'. We can take a look at the tabled values in Table A.1 to get a first estimation of how the model should represent accumulation of sediment over the simulation period. A look is taken at the quantity of dredged material over the years 2015 - 2017 for these three model areas A 'Mouth', B 'Trap' and C 'Basins'. The results are given in Table A.2. The results are given in hopper capacity and not in accumulated material. (Port of Rotterdam, 2019) uses an empirical factor of 1.25 to distinguish between hopper volume and in situ volume. As sediment is diluted, the density decreases with this factor. To be able to use the values of Table A.2 as a rough calibration for the model results, the total of the years 2015 - 2017 are divided by the bulking factor of 1.25 and multiplied by $\frac{118}{3*365}$ to account for the same simulation time as the survey data. The results are given in Table 4.2.

Year	**Trap**	**Dredged. Sed. Mouth**		**Dredged. Sed. Trap**		**Dredged. Sed. Basins**		**Dredged. Sed. Total**	**Trapping efficiency**
[-]	[yes / no]	[m3]	[% of total]	[m3]	[% of total]	[m3]	[% of total]	[m3]	[%]
2015	Not maintained	225,279	26	267,782	31	382082	44	875,143	41
2016	Not maintained	430,686	34	274,126	22	550060	44	1,254,872	33
2017	Not maintained	274,669	23	507,219	42	428838	35	1,210,726	54
2015-2017	Not maintained	930,634	28	1,049,127	31	1360980	41	3,340,741	44

Table A.2: The amount of dredged quantities are calculated for the areas used in the simulation based on the dredged quantities of years 2015 - 2017 (Port of Rotterdam, 2019). Please note that this is the amount in hopper capacity and not in accumulated sediment.

A.2.4 Surveys Botlek

To gain an idea of sedimentation rates within a sediment trap a field measurement is set-up. The Botlek sediment trap as seen in location 2.4 is emptied, last dredging activities took place at September 10, 2018, and not used for temporal storage. Echosounder multibeam survey have taken place on October 4, 16 and 30, November 6, December 11, and January 5 and 30. The multibeam measures at a density of 1.03 tons/m^3, therefore reflecting at the top of the fluid mud layer. An example of a bathymetry measurement is shown in Figure A.2. For the area within the red

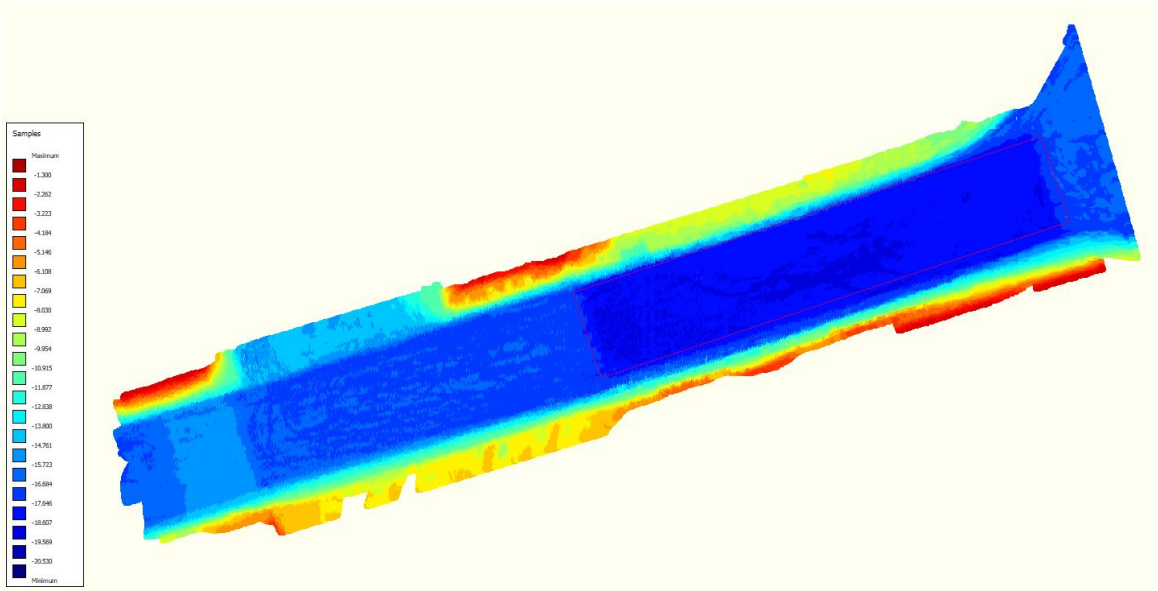

Figure A.2: Example of data files for the survey of October 4 obtained by the echosounder surveys. The right border is connected to the Botlek mouth and river Meuse. With red lines the polygon is given for which the sediment trap data is used.

polygon the depth is averaged over the width, resulting in 1D bottom profiles for each survey measurement. The bathymetry profiles of each of the measurements is given in Figure 4.8. As the echosounder measures the top of the fluid-mud layer, the bathymetry profile maxima are expected to shift between the surveys. The contrary is however visible. A gradual, almost evenly distributed, sedimentation pattern can be observed. Larger sediment accumulation is observed near the start of the sediment trap. Near the edges of the sediment trap less accumulation is observed. This may be due to settling, but it is also hypothesized that increased turbulence may increase erosion near the edges. In that case a scour hole should be present after 6-7 times the depth of the trap should theoretically would be expected with the analogy of a backward facing step as given in Chapter 3 'Sediment trap dynamics'.

Appendix B

Additional formulations hydrodynamics and sediment transport

This chapter contains extra formulations to support the main chapters. The chapter is split in two sections: 'Hydrodynamics' and 'Sediment'.

B.1 Hydrodynamics

B.1.1 Bed shear stress for waves and currents

The North Sea is relatively shallow, the interaction between the water column and the bed therefore plays an important role. Even the sediment concentrations near the surface are highly influenced by waves. The wave-induced motion of the water particle creates a relatively thin, turbulent boundary layer. The orbital wave motion transfers energy and momentum of the water particles to the turbulent motion in the boundary layer (Holthuijsen, 2010). The relation between the orbital wave motion $\hat{u_b}$ and bed shear stress $\hat{\tau}_w$ is given in Equation B.1 (Schiereck, 2003). The bed shear stress is a function of roughness coefficient c_f, density ρ and orbital wave motion $\hat{u_b}$, which in turn depends on the wave number k, amplitude a and water depth h. It must be kept in mind that storm events have high waves, which expresses in high bed shear stresses, in turn resulting in a lot of resuspension of sediment.

$$\hat{\tau}_w = \frac{1}{2}\rho c_f \hat{u_b}^2 \text{ with } \hat{u} = \omega a_b = \frac{\omega a}{\sinh\, kh} \text{ and } u = \hat{u}_b \sin \omega t \tag{B.1}$$

For the estuarine area the depth is very small compared to the width and depth. The water-bed exchange is very relevant for the fine sediment dynamics. Flow induces a bed shear stress just like waves do. For uniform flow, the boundary layer is able to

develop and an equilibrium exists between the bottom shear stress and the pressure-induced component of the fluid. The relation between the bottom shear stress τ_b and the time-averaged, depth-averaged flow velocity $\bar{\bar{u}}$ is then given in Equation B.2 (Schiereck, 2003). It is a function of the roughness coefficient c_f, also expressed in Chézy coefficient C for uniform flow.

$$\tau_b = c_f \rho \bar{\bar{u}}^2 = \frac{g}{C^2} \rho \bar{\bar{u}}^2 \tag{B.2}$$

B.2 Sediment

B.2.1 Stokes settling

Stokes's law describes the settling of suspended sediment in a fluid. The law can be used to describe the settling time needed in a harbour basin for certain sediment sizes. It describes an expression for the drag forces exerted on a spherical object with small Reynolds numbers. For silt this method can however be questionable, since silt particles are generally not spherical. The law can be applied for low SPM concentrations and is given in equation B.3 (Lamb, 1932). Here ρ_p and ρ_w represent the densities of the particles and water respectively, R is the radius of the particle, ν represent the fall velocity, μ is the dynamic viscosity and g is the gravitational acceleration.

$$\nu = \frac{2}{9} R^2 \frac{\rho_p - \rho_w}{\mu} g \tag{B.3}$$

The equation verifies that the velocity scales with the size squared. A twice as large particle settles four times faster. The term $\rho_p - \rho_w$ indicates that if the particle and the water have the same density, the particle does not settle but remain in suspension or the particle may even float for smaller particle densities. These initial verifications help to understand the behaviour of very fine sediment in flows.

B.2.2 Hindered settling

The Mehta approach describes the non-hindered settling velocity w_{s0} is reduced by a reduction factor depending on the volume concentration ϕ, resulting in a hindered settling velocity w_s. The volume concentration ϕ is the ratio between the mass concentration c and the gelling concentration c_{gel}, i.e. the concentration at which the pore volume is reduced greatly due to the effects of flocculation. The hindered settling velocity is then given in Equation B.4.

$$w_s = (1 - \phi)^5 w_{s0} \tag{B.4}$$

The hindered settling formulation results in a strong density difference between the fluid mud layer and the water column. Due to the formation of this so-called lutocline, vertical mixing is greatly damped.

Appendix C

Hydrodynamics by Delft3D-FLOW

This chapter considers the formulations of hydrodynamics transport by the Delft3D online SED model. This chapter provides a mathematical description of the hydrodynamics that are used in the simulation studies.

C.1 Equations of motion

The Reynolds Averaged Navier Stokes (RANS) equations for an incompressible fluid describe the flow and hydrodynamic processes that drive the motion of the fluid. To describe the physics governing the flow, the hydrodynamic processes are explained on the basis of the Navier Stokes equations in a Cartesian coordinate system as can be seen in Equations C.1 and C.2 for respectively x and y directions in Appendix Hydrodynamics governing flow. The RANS are solved under a number of assumptions. The horizontal length scale is much larger than the depth, therefore vertical accelerations are neglected and hydrostatic pressure holds. Vertical velocities are computed from the continuity equation for an incompressible fluid. Small density differences are assumed in the horizontal to use the Boussinesq approximation. Coriolis is assumed to be constant for a given latitude under the F-plane approximation. Finally, turbulence is calculated with the k-ϵ turbulence closure model for the turbulent eddy viscosity. Horizontal viscosities are applied by the user. In this section, first the mathematical description of the RANS are given with their just mentioned assumptions. Afterwards, each of the terms of the RANS equations is eloborated on its applications.

C.1.1 Mathematical description RANS

The momentum equation in x and y direction given in Equations C.1 and C.2 are used to describe hydrodynamic processes that govern flow. Term indicated with [1] indicates the local acceleration. This means the rate of change of flow in x or y direction, u and v respectively. The three terms indicated with [2] describe the advective acceleration of the fluid. [3] gives the pressure driven flow, where baroclinic terms are included and ρ_0 can be distinguished due to the Boussinesq assumption. Pressure gradients within the fluid drive [3], which can be due to density differences due to salinity, temperature or sediment, but also tidal flow and river flow cause pressure gradients. This is more elaborately explained in 'Pressure driven flow' The next term [4] describes the turbulent eddy viscosity and diffusivity, determined by the k-ϵ model as described in 'Turbulence'. Coriolis forces are described with [5] and elaborated in 'Coriolis'. Finally, external sources and sinks such as a.o. hydraulic structures, discharge and withdrawal of water, wind shear stresses, bed shear stresses due to (wave shear stresses only WAQ, not in FLOW) currents as described in Equation B.2 are included in term [6] (Delft Hydraulics, 2006). In the model the influence of waves is only included on the sediment transport, not on the flow.

$$\underbrace{\frac{\delta u}{\delta t}}_{1} + \underbrace{\frac{\delta u^2}{\delta x} + \frac{\delta uv}{\delta y} + \frac{\delta uw}{\delta z}}_{2} + \underbrace{\frac{1}{\rho_0}\frac{\delta p}{\delta x}}_{3} - \underbrace{F_x - \frac{\delta}{\delta z}\left(\nu_V \frac{\delta u}{\delta z}\right)}_{4} - \underbrace{fv}_{5} = \underbrace{M_x}_{6} \tag{C.1}$$

$$\underbrace{\frac{\delta v}{\delta t}}_{1} + \underbrace{\frac{\delta vu}{\delta x} + \frac{\delta v^2}{\delta y} + \frac{\delta vw}{\delta z}}_{2} + \underbrace{\frac{1}{\rho_0}\frac{\delta p}{\delta y}}_{3} - \underbrace{F_y - \frac{\delta}{\delta z}\left(\nu_V \frac{\delta v}{\delta z}\right)}_{4} + \underbrace{fu}_{5} = \underbrace{M_y}_{6} \tag{C.2}$$

Hydrostatic pressure assumption For almost any numerical model, the hydrostatic pressure assumption holds. The assumption does not solve the momentum equation for the depth, but instead uses the hydrostatic balance. The hydrostatic assumption can be made if the horizontal scale is large compared to the vertical scale. The vertical pressure gradient is a function of gravitational acceleration and density as in Equation C.3. For the entire Navier Stokes equations referred is to Appendix Hydrodynamics governing flow.

$$\frac{\delta p}{\delta z} = -\rho g \tag{C.3}$$

Continuity equation Vertical velocities are computed from the continuity equation for an incompressible fluid. Under the assumption that water is an incompressible fluid, water density can be removed from the continuity equation as can be seen in Equation C.4.

$$\frac{\delta u}{\delta x} + \frac{\delta v}{\delta y} + \frac{\delta w}{\delta z} = 0 \tag{C.4}$$

C.1.2 Pressure driven flow

Equation for the free surface The depth integrated continuity equation, also known as the equation for the free surface, is derived by integrating the continuity equation from the bed to the surface. The equation completes the equations of motion. The depth is the water depth in addition with the surface elevation. The equation for the free surface is given in Equation C.5 (Pietrzak, 2017).

$$\frac{\delta \eta}{\delta t} + \frac{\delta \bar{u} H}{\delta x} + \frac{\delta \bar{v} H}{\delta y} = 0 \tag{C.5}$$

C.1.3 Pressure terms

The pressure term [3] under the Boussinesq assumption in Equations C.1 and C.2 is a term that includes rather important processes. The term is expressed in Equation C.6 by an atmospheric pressure, barotropic and baroclinic term respectively. The Boussinesq approximation is an assumption that the effects of density do not affect the horizontal momentum. It is common practise to apply the Boussinesq approximation to the equations of motion (Pietrzak, 2017). It states that density differences are relatively small, $\Delta\rho << \rho$, as can be seen in density differences between fresh and salt water. Pressure gradients due to density differences are included in the baroclinic forcing term. A constant reference density ρ_0, i.e. fresh water, is assumed in other terms of the momentum equations.

$$\frac{1}{\rho_0}\frac{\delta p_h}{\delta x} = \frac{1}{\rho_0}\frac{\delta p_{atm}}{\delta x} + g\frac{\delta \zeta}{\delta x} + \frac{g}{\rho_0}\int_z^\zeta \frac{\delta \rho}{\delta x}\delta z \tag{C.6}$$

Pressure gradients due to density differences are included in the baroclinic forcing term. A constant reference density ρ_0, e.g. fresh water, is assumed in other terms of the momentum equations. The atmospheric pressure term is self explanatory. The barotropic forcing includes effect such as river and tidal flow. The baroclinic forcing implies a density difference (in this case over x-direction), resulting in a horizontal pressure gradient.

C.1.3.1 Barotropic driven flow

Tidal flow A large contribution to the import of sediment in the Rotterdam port area is the import of sediment due to the tide. Because of the mild conditions that are present in the harbour basins with regard to the river Meuse and the North Sea. The in-flowing tide imports sediment in the port area. During high water slack the sediment is able to sink in the water column and even accumulate. The out-flowing tide therefore exports less sediment out of the port area. This effect results in a net import of sediment.

Tidal flow causes a pressure gradient caused by a surface elevation $g\frac{\delta\zeta}{\delta x}$. This pressure gradient drives the acceleration $\frac{\delta u}{\delta t}$ of the flow in the momentum Equations C.1 and C.2. The same mechanism applies for the y-direction.

River flow For most landward areas, the largest contribution of import of sediment is due to the input from the river Meuse. The river transports a wide grading of sediment, from sand particles to very fine mud-like sediment. Larger sediments (sand etc.) accumulate when the shear stress threshold is not met anymore. This can occur through the entire harbour area. However, in the outer basins the flow velocity is almost zero due to the mild conditions. Here the amount of sediment that accumulates is fully dependent on the inflow, which is determined mostly by very fine silt particles.

A pressure gradient due to the gravitational force drives the flow. The water surface has a small gradient, driving the acceleration of the river. For uniform river flow, an equilibrium between bed shear stress and this gravity induced momentum occurs. In the momentum equations, the momentum is included in the barotropic $g\frac{\delta\zeta}{\delta x}$ term.

C.1.3.2 Baroclinic driven flow

The harbour area experiences baroclinic pressure gradients due to salinity differences, density differences and even temperature differences. The density of the water is not equal over the horizontal, resulting in a gradient $\nabla p \cdot \nabla \rho \neq 0$, driving a baroclinic flow.

The port area (Europort, Botlek) acts like an estuary that experiences a strong fresh-water run-off from the river Meuse and tidal inflow from the North Sea. The interaction of these flows cause a stratified flow pattern. The fresh water with a relatively low density flows on top of the salt water with a relatively high density from the sea. This causes an extra flow pattern inside the harbour area near the

bottom and an extra outside flow near the surface. The further we move land inward, the degree of mixing changes. This differs from a stratified, partially stratified to fully homogeneous flow. The degree of stratification determines the driving force of the baroclinic flow. Field measurements carried out by (De Nijs, 2012) show that the salt water stratification is not broken as far as the Botlek down by bed generated turbulence, local turbulence and internal wave instabilities. The stable salt wedge therefore has significant influence in the baroclinic driven flow. The exact densities of the water, influenced by salinity and temperature, are calculated by the full equation of state as can be found in (Gill, 1982).

One of the most obvious reasons that siltation occurs, is due to the decrease of turbulence and flow velocities in harbour basins or navigation channels. The mud suspension becomes supersaturated, implying that the sediment load is larger than the sediment carrying capacity of the water. With silt-like sediment, this results in a very large concentration at the lower part of the water column, which in turn may trigger the development of sediment-induced baroclinic driven flows (J. Winterwerp, 2001). These baroclinic flows contribute significantly to the transport of suspended sediment for high sediment concentrations. The density increase due to present sediment is calculated with the Equations of State.

Just like the sediment is transported with a advection-diffusion equation as in Equation 3.9, so is the salinity and temperature. These relations are given in Equation C.7 and C.8 respectively. Here, rate of change in salinity s and temperature T are described by advection terms, diffusion terms with horizontal background diffusivity parameters D_h, vertical turbulent diffusivity parameters D_t from $k-\epsilon$ model and source terms S. For temperature, an additional heating flux source term Q_h should be included.

$$\frac{\delta S}{\delta t} + \frac{\delta uS}{\delta x} + \frac{\delta vS}{\delta y} + \frac{\delta wS}{\delta z} - 2D_h\left(\frac{\delta^2 S}{\delta x^2} + \frac{\delta^2 S}{\delta y^2}\right) - \frac{\delta}{\delta z}\left(D_t \frac{\delta S}{\delta z}\right) = S_S \tag{C.7}$$

$$\frac{\delta T}{\delta t} + \frac{\delta uT}{\delta x} + \frac{\delta vT}{\delta y} + \frac{\delta wT}{\delta z} - 2D_h\left(\frac{\delta^2 T}{\delta x^2} + \frac{\delta^2 T}{\delta y^2}\right) - \frac{\delta}{\delta z}\left(D_t \frac{\delta T}{\delta z}\right) = \frac{1}{\rho} Q_h + S_T \tag{C.8}$$

C.1.4 Turbulence

Turbulence, indicated with term [4] in the momentum equations C.1 and C.2, can be described as velocity fluctuations around the mean velocity values of flows. It is important to include turbulence as it induces an effective drag on top of the regular

friction and it induces turbulent mixing, which causes suspended matter a.o. to be transported in space. Turbulent shear stress can be expressed by decomposition and averaging over the turbulent time scale of the non-linear terms in the momentum equations.

Turbulence can be described according to many models such as the standard k-ϵ model. This model best resembles the current understanding of relevant processes in turbulent flow. The model focuses on mechanisms that affect turbulent energy. The turbulent viscosity is considered to be isotropic, having a constant ratio between Reynolds stress and rate of deformation in all directions (Versteeg & Malalasekera, 2007). The equation for respectively turbulent kinetic energy k and dissipation ϵ is given in Equations C.9 and C.10. The equations are non-linearly coupled by the eddy diffusivity terms D_k and D_ϵ and their dissipation terms (Delft Hydraulics, 2006).

$$\underbrace{\frac{\delta k}{\delta t}}_{1} + \underbrace{\frac{\delta uk}{\delta x} + \frac{\delta vk}{\delta y} + \frac{\delta wk}{\delta z}}_{2} = \underbrace{\frac{\delta}{\delta z}\left(D_k \frac{\delta k}{\delta z}\right)}_{3} + \underbrace{P_k + P_{kw} + B_k}_{4} - \underbrace{\epsilon}_{5} \tag{C.9}$$

$$\underbrace{\frac{\delta \epsilon}{\delta t}}_{1} + \underbrace{\frac{\delta u\epsilon}{\delta x} + \frac{\delta v\epsilon}{\delta y} + \frac{\delta w\epsilon}{\delta z}}_{2} = \underbrace{\frac{\delta}{\delta z}\left(D_\epsilon \frac{\delta \epsilon}{\delta z}\right)}_{3} + \underbrace{P_\epsilon + P_{\epsilon w} + B_\epsilon}_{4} - \underbrace{c_{2\epsilon}\frac{\epsilon^2}{k}}_{5} \tag{C.10}$$

In the equations, D_k and D_ϵ are given by $D_k = \frac{\nu_{mol}}{\sigma_{mol}} + \frac{\nu_{3D}}{\sigma_k}$ and $D_\epsilon = \frac{\nu_{3D}}{\sigma_\epsilon}$. The term indicated with [1] represents the rate of change of k or ϵ. [2] represents the amount of transport of k or ϵ due to advection. Term [3] is known as the rate of change of k or ϵ due to diffusion. The rate of production and buoyancy terms of k or ϵ is represented by [4]. [5] shows the sink or destruction of k or ϵ.

Within the momentum equations in C.1 and C.2, the terms F_x and F_y represent the imbalance of the horizontal Reynold's stresses within numerical model Delft3D. The equations that describe these terms are given in Equation C.11 and C.12. Unlike turbulence in the vertical matter, horizontal turbulence is not described by an elaborate k-ϵ model. The horizontal grid usually is too coarse and the time step too large to resolve the turbulent motion. Horizontal eddy viscosity coefficents ν_H and eddy diffusivity coefficient D_H are much larger than their vertical counterparts. The values of the horizontal background viscosity coefficient and eddy diffusivity coefficient must be determined manually (Delft Hydraulics, 2006).

$$F_x = 2\nu_H \frac{\delta^2 u}{\delta x^2} \tag{C.11}$$

$$F_y = 2\nu_H \frac{\delta^2 v}{\delta y^2} \tag{C.12}$$

The terms $\frac{\delta}{\delta z}\left(\nu_V \frac{\delta u}{\delta z}\right)$ and $\frac{\delta}{\delta z}\left(\nu_V \frac{\delta v}{\delta z}\right)$ in the momentum equations represent the turbulent eddy diffusivity based on the vertical eddy diffusivity coefficient ν_V as calculated in the k-ϵ model.

C.1.5 Coriolis

The Coriolis term indicated with term [5] in the momentum equations C.1 and C.2 and represents an inertial force that acts on objects that are in motion as in this case the earth within a frame of reference that rotates with respect to an inertial frame. The momentum induced by Coriolis can be expressed as the product of the Coriolis parameter and the flow perpendicular to the momentum balance direction, e.g. v-flow drives the Coriolis force in the x-direction and u-flow drives the force in y-direction. The parameter f depends on the latitude on earth ϕ and is determined by the gravitational acceleration of the earth Ω. The relation is given in Equation C.13 called the f-plane assumption.

$$f = 2\Omega \sin\phi \tag{C.13}$$

Appendix D

Generation SPM time-series

Taking constant sediment profiles at the boundary results in a large overprediction of the sediment inflow in the domain. Therefore, the creation of SPM time-series to correspond with a variable concentrations at the open boundary would yield more reliable results. This important parameter for numerical modelling is however very hard to determine. The modelling is supply-limited, and all sediment in the domain is a delicate combination of available sediment and hydrodynamics at the boundary. To generate a SPM time series, a first look is taken at the measurement profiles of the survey of De Nijs (2012), taken into the New Waterway just in front of the Botlek Harbour. Figure 4.1 in Chapter 4 shows the location of these measurements. The measurements are taken April 14, 2005. The fresh-water discharge was about 1500 $m^3 s^{-1}$ during this period. The survey was carried out during average Rhine discharge conditions and prior to neap tides. De Nijs also did measurements inside the Botlek Harbour, but because of the many events that have taken place, these measurements are considered to be unreliable. Sediment seems to be very much unavailable for the entire tidal period except for the period when the salinity increases in time for a single location. At that moment, an increased SPM concentration is observed for the height of the dense water of the stratification, see Figure D.1. For the fresh-water part, zero to none concentrations are observed. This period occurs around High Water due to the 1-2 hours out of phase coupling between the tidal motion and salinity profile. This local accumulation of sediment in the salt water tip is referred to as the ETM. To generate a new sediment profile for an existing salinity and water level time-series, the following assumptions are made:

1. The concentrations measured by De Nijs on April 14, 2005 can be used as reference concentration values for the period of August 2018.

2. The behaviour of the measurement of April 14, 2005 can be used as a returning profile to represent more tidal periods.

3. The Rouse profile represents the sediment distribution for the salt water part of the water column adequately.

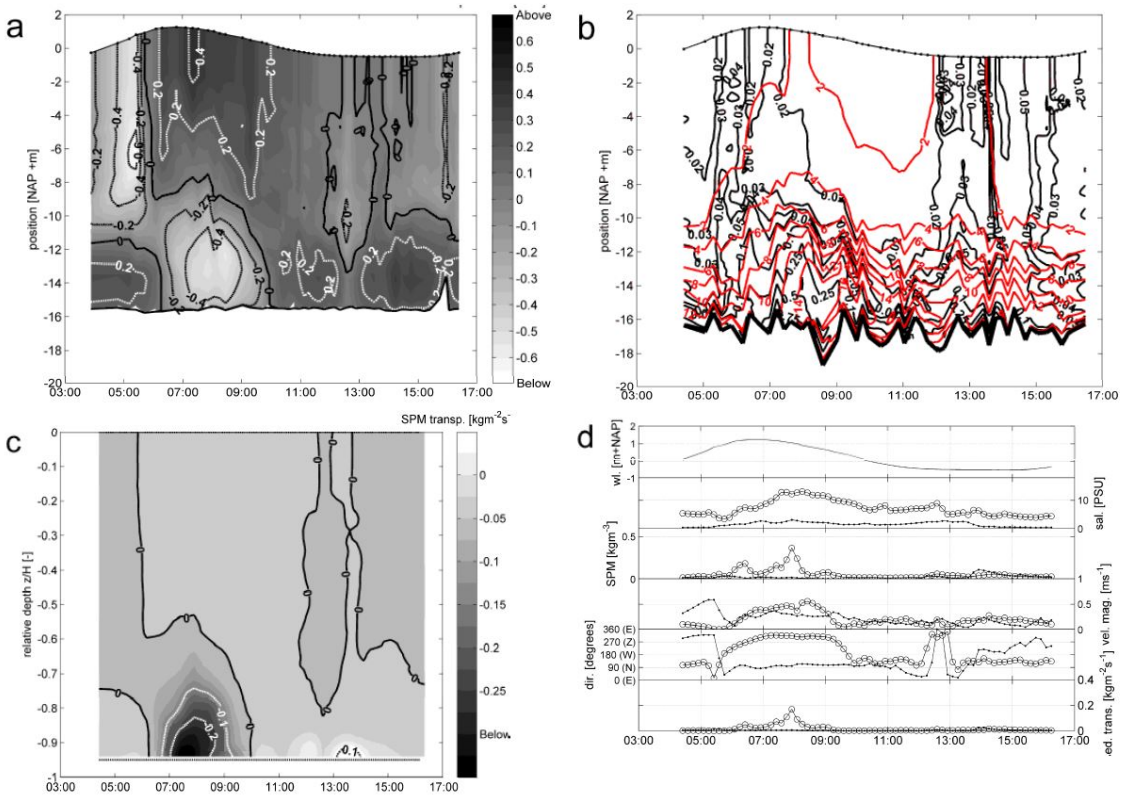

Figure D.1: (De Nijs, 2012) presented results of the survey on April 14, 2005 in four graphs. For each graph, the x-axis represents the time of the survey of one tidal period. The y-axis shows the position within the water column. Graph (a) shows the velocity component, graph (b) the salinity (shaded) and SPM concentration (contour), graph (c) shows the SPM transport and graph (d) the water level, salinity, SPM conc., velocity magnitude, velocity direction, transport of SPM from top to bottom, respectively. Graph (d) shows data near the surface (+) at NAP -3m and near the bed (0) at NAP-12m.

D.1 The Rouse profile

When only a sediment concentration at a location in the water column is known, a concentration distribution must be assumed. The Rouse profile is an excellent assumption for uniform flow. The Rouse profile is based on the balance between the settling flux and turbulence flux. A Rouse profile results in higher concentration near the bed and lower concentrations near the surface. The turbulent mixing tends to homogenize a suspension, while settling disturbs this effect. Based on a.o. the

settling velocity of the sediment, a distribution profile is determined, where a higher settling velocity results in a stronger distribution towards the bed. The Rouse profile describes the concentration distribution over the entire water column h, or in this case the saltwater part of the water column. A concentration c at a vertical location z is calculated in comparison with a reference concentration c_a at a reference vertical location a. This is defined in Equation D.1. The Rouse number defines the shape of the distribution and is given by Equation D.2. It is a function of the Schmidt number for the fluid, the settling velocity, Karman-constant and the shear velocity.

$$\frac{c}{c_a} = \frac{a(h-z)}{z(h-a)}^{\beta} \tag{D.1}$$

$$\beta = \frac{\sigma_T w_s}{\kappa u_*} \tag{D.2}$$

The Rouse profiles goes under the assumptions that there is a steady flow in a uniform channel, a constant and uniform density, the eddy viscosity profile is parabolic distributed, the settling velocity is constant and uniform and the Schmidt number is constant and uniform (van Prooijen et al., 2017). In the case of a rising tide with stratified influence, accelerations due to the tidal signal are sufficiently slow to consider the flow uniform. Therefore, the Rouse profile is considered to give an adequate representation of the saltwater part of the water column. The water column in the Rotterdam Waterway shows a strongly stable stratified character with little mixing, the eddy viscosity profile is parabolic distributed and therefore a logaritmic velocity distribution, the settling velocity input in the computational model is considered constant and the Schmidt number is uniform. The upper boundary condition for the Rouse profile is the location of the pycnocline, in this case this border is taken at a salinity level of 17 ppt. A Karman-contant $\kappa = 0.4$, settling velocity $w_s = 0.6mm/s$, Schmidt number $\sigma_T = 0.7$ and shear velocity $u_* = 0.02m/s$ yields a Rouse number of $\beta = 0.0525$ according to Equation D.2. Applying the Rouse profile to the first timestep in the salinity timeseries yield the generalized as can be seen in Figure D.2. The extent to where the sediment is present depends on the salinity values in the time series. The generated SPM profiles can be found in Chapter 4 Setup of hydrostatic Delft3D-FLOW online SED model.

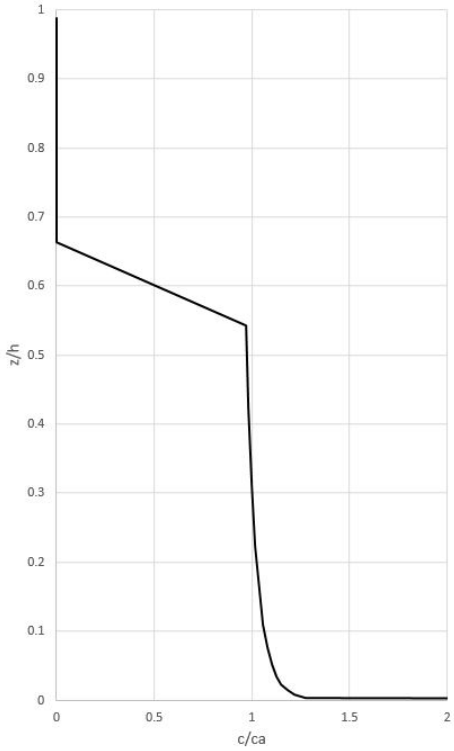

Figure D.2: The generalized Rouse profile for the first timestep. For each timestep the SPM distribution may vary, but the approach is the same. A Rouse number of $\beta = 0.0525$ is applied. The reference concentration c_a is taken at about $z/h = 0.3$

Appendix E

Parameterization of the model

In this Chapter the determination of the parameters in the model are elaborated based on literature research and model applications. It is an extensive expansion on the Chapters 4 'Setup of the hydrostatic numerical model' and 5 'Analyses of trapping mechanisms'.

E.1 Fixed parameters

The first model parameter that needs attention is the **settling velocity**. Various studies for the port of Rotterdam use different values. (De Groot, 2018) has used three fractions to model the sediment in the port of Rotterdam with settling velocities of 1 mm/s, 0.125 mm/s and 0.00116 mm/s, where the last fraction would never settle. (J. C. Winterwerp & van Kessel, 2003) uses a settling velocity of 0.5 mm/s for the port of Rotterdam and (Van Kessel, 2005) distinguished between a fine silt fractions with a settling velocity of 0.3 mm/s and a fine sand fraction of 3 mm/s. Since the area of interest is the Botlek basin, known to attract large silt concentrations, the focus lies on the silt fraction. The silt fraction is the dominant sediment fraction that causes harbour siltation in the Botlek area (De Nijs, 2012). Silt is characterized by a particle size of $< 63\ \mu m$. If we apply Stokes' Law for the perfect spheres as formulated in Appendix B 'Additional formulations hydrodynamics and sediment transport' to typical sizes of silt of < 10 to 30 μm, settling velocities between 0.10 mm/s and 0.80 mm/s would be reasonable for silt. A settling velocity of 0.60 mm/s has been used.

An important value for the sediment trap is the impact of the updating bottom on the hydrodynamics thus sediment transport. For the bottom updates a Patheniades-Krone formulation is used as explained in Chapter 3 'Sediment trap dynamics'. For this formulation, many parameters need to be determined before a reasonable and realistic result can be obtained. In the formulations of Partheniades for erosion, a

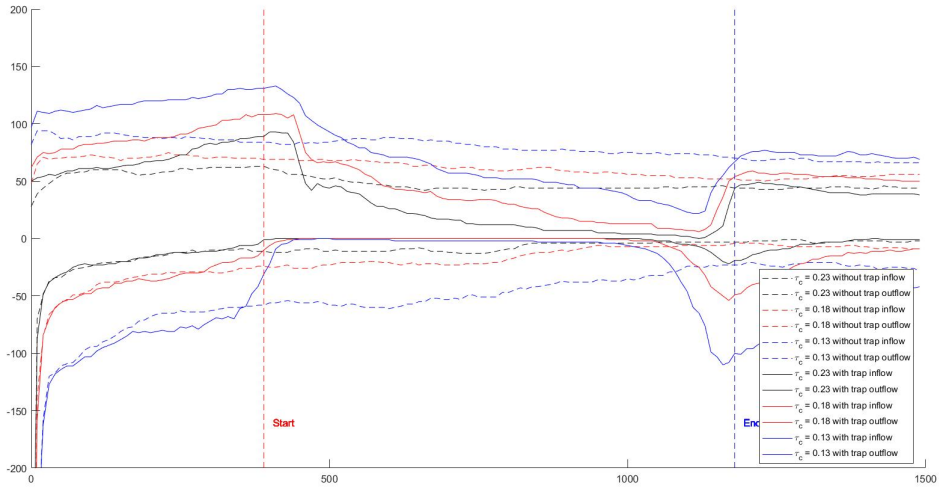

Figure E.1: The amount of times the critical bed shear stresses of 0.13 Pa, 0.18 Pa and 0.23 Pa are exceeded over a total of 1352 timesteps. The y-axis shows the times of exceedence while the x-axis shows cells in the x-direction. Cell 0 is the boundary. The vertical dashed red and blue lines shows the start and end of the trap respectively.The horizontal dashed lines show the simulation without a trap, while the solid lines show the situation with a trap. Positive values are amount of timesteps that are exceeded for the inflow of water in the basin, while negative values are for the outflow of the basins.

critical bed shear stress for erosion $\tau_{c,e}$ and **erosion parameter** M can be observed. For the formulation of Krone for deposition, a **critical bed shear stress for deposition** $\tau_{c,d}$ is needed. It may however be convenient to run the model with a very large bed shear stress for deposition, namely $\tau_{c,d} = 1000$. In this way sediment always settles as it hits the bed. Then only the critical bed shear stress for erosion needs to be calibrated. This approach is used commonly in numerical models and also applied in this model.

For the determination of critical shear stress, a look is taken for values as given in van Rijn (2005). Van Rijn finds critical bed-shear stresses for different dry bed sediment concentrations in various enviroments. He finds for the Delfzijl Harbour values of 0.05-0.15, 0.15-0.20, 0.20-0.25, 0.40-0.60 Pa for concentrations of 100, 150, 200 and 250 $kg/m3$, respectively. For the Breskens Harbour values of 0.15-0.25, 0.25-0.35, 0.35-0.45, 0.60-0.80 Pa for concentrations of 100, 150, 200 and 250 $kg/m3$, respectively, are found. The values gives an indication at what range of bed shear stresses must be looked at. For a very dynamic environment such as a strongly siltating harbour basin, bed concentrations are assumed to be very low. There are differences in critical shear stresses for fresh and saltwater environments. Two estuaries are researched by Van Rijn, with varying critical shear stresses for erosion between 0.05 Pa for very loose grains in the bed in the Delfzijl Harbour to 0.80 Pa for consolidated grains in

the Breskens Harbour. For the application of the silt-like environment as has to be dealt with in the numerical model, a tendency towards the lower limit is experienced. However, the choice for the critical bed shear stress for erosion is substantiated a bit more. The bed shear stress induced by the hydrodynamics as explained in Chapter 3 'Sediment trap dynamics' is assessed for each timestep. For certain threshold values of 0.13 Pa, 0.18 Pa and 0.23 Pa, the amount of times the threshold values for bed shear stress are exceeded are counted as can be seen in Figure E.1. Each threshold value is assessed for the case with a sediment trap and without one. The cases without sediment trap experience more frequent exceeding of the threshold value, except for location close to the boundary. This effect is hypothesized in Chapter 3 'Sediment trap dynamics', and is thought to be due to the increased turbulence levels near the edges. According to the Partheniades formulation each time shear stress threshold value $\tau_{c,e}$ is exceeded, the erosion increases linearly with the erosion parameter M as multiplication factor. Because of this linear relation between the erosion parameter and the amount of erosion present in the model, the choice was made to calibrate the Erosion parameter M and not the critical shear stress for erosion. An erosion parameter has been chosen such that erosion is sufficiently present in the model. The amount of erosion that yields realistic results is then calibrated by the Erosion parameter M. A representative erosion threshold value is set to 0.18 Pa. This value is based on the amount of timesteps that the bed shear stress is exceeded by this value. No consolidation effects are taken into account as the critical shear stress is uniform for the entire domain. Accumulated sediment does not have an increase in the critical shear stress (van Rijn, 2005).

E.2 Parameterization of erosion and fluid mud

This section provides support figures and analyses of the sedimentation patterns for Chapter 5 'Analyses of trapping mechanisms'.

E.2.1 Erosion

When looking at Figure E.2 and Table E.1 the importance of the erosion/deposition mechanism can be assessed. Sediment immediately settles as it hits the bed so the effect of density driven suspension flows is thought to be of minimal importance. The increased local turbulence may play a role in the simulations. It can be seen that even without fluid mud behaviour and without erosion a small decrease of accumulation can be observed at the start of the trap and a small increase at the end of the

trap. This could be expected due to the varying area the settling sediment is able to hit. With an increasing erosion parameter a decreasing amount of accumulation can be observed near the edges of the trap, as was hypothesized. Also an increase of sediment in the sediment trap can be observed. The accumulation pattern resembles the survey data quite well for a moderate or substantial erosion. The run with 'Lots of erosion' is said to be unreliable. During simulation the erosion hits the bottom of the grid, where no initial sediment is present. This effect prevents any further erosion while shear stresses exceeded the critical shear stress values. Adding initial sediment to the domain could solve this problem. These large erosion values are however considered realistic, so an expansion of the model to include initial sediment is not included. When we look at the tabled values that correspond with the figure, some interesting observations can be made. First we look at the total accumulation of sediment for the various runs. The difference between the runs is quite considerable. A net decrease of 7 % for a simulation with trap without erosion and without fluid mud behaviour can be observed. This difference of almost 30000 m3 is significant. For increasing erosion parameters this difference decreases until eventually it even slightly increases for the simulation with substantial erosion. Another interesting observation that can be made is about the location of accumulated sediment. Although the amount of accumulated sediment in the sediment trap relatively increases for an increasing erosion parameter compared to the simulations without trap (1000 m3 for little erosion, 10000 m3 for moderate erosion and 13500 m3 for substantial erosion), what happens with the accumulation in the other parts of the domain is unexpected. Apparently, the presence of the sediment trap increases erosion at the mouth of the domain. The extra sediment is distributed over the sediment trap and basins, causing no significant benefits for the maintenance dredging strategy.

Erosion	**M**	**DepEff**	**Trap**	**Acc. Sed. Mouth [0-390 m]**		**Acc. Sed. Trap [400-1190 m]**		**Acc. Sed Basins [1200-8770 m]**		**Acc. Sed. Total [0-8770 m]**		**Favourable sediment**
	[-]	[-]	[yes / no]	[m3]	[% of total]	[m3]	[% of total]	[m3]	[% of total]	[m3]	Net increase trap/no trap [%]	[%]
No	0	1.0	yes	127382	33	136488	35	124644	32	388514	-7	68
No	0	1.0	no	130100	31	145926	35	141511	34	417537	7	66
Little	0.0002	1.0	yes	108581	29	139884	38	122341	33	370806	-2	67
Little	0.0002	1.0	no	116829	31	138792	37	123536	33	379157	2	67
Moderate	0.0005	1.0	yes	89687	24	139566	38	137156	37	366409	0	63
Moderate	0.0005	1.0	no	104351	28	129822	35	132481	36	366654	0	64
Substantial	0.0008	1.0	yes	78815	21	142642	38	151618	41	373075	1	59
Substantial	0.0008	1.0	no	92850	25	129272	35	148433	40	370555	-1	60
Lots	(0.0020)	(1.0)	(yes)	(12767)	(4)	(138846)	(40)	(193857)	(56)	(345470)	(-3)	(44)
Lots	(0.0020)	(1.0)	(no)	(39125)	(11)	(98906)	(28)	(219619)	(61)	(357649)	(4)	(39)

Table E.1: Five erosion scenarios are assessed with the same hydrodynamics and SPM time series. The values correspond with Figure E.2.

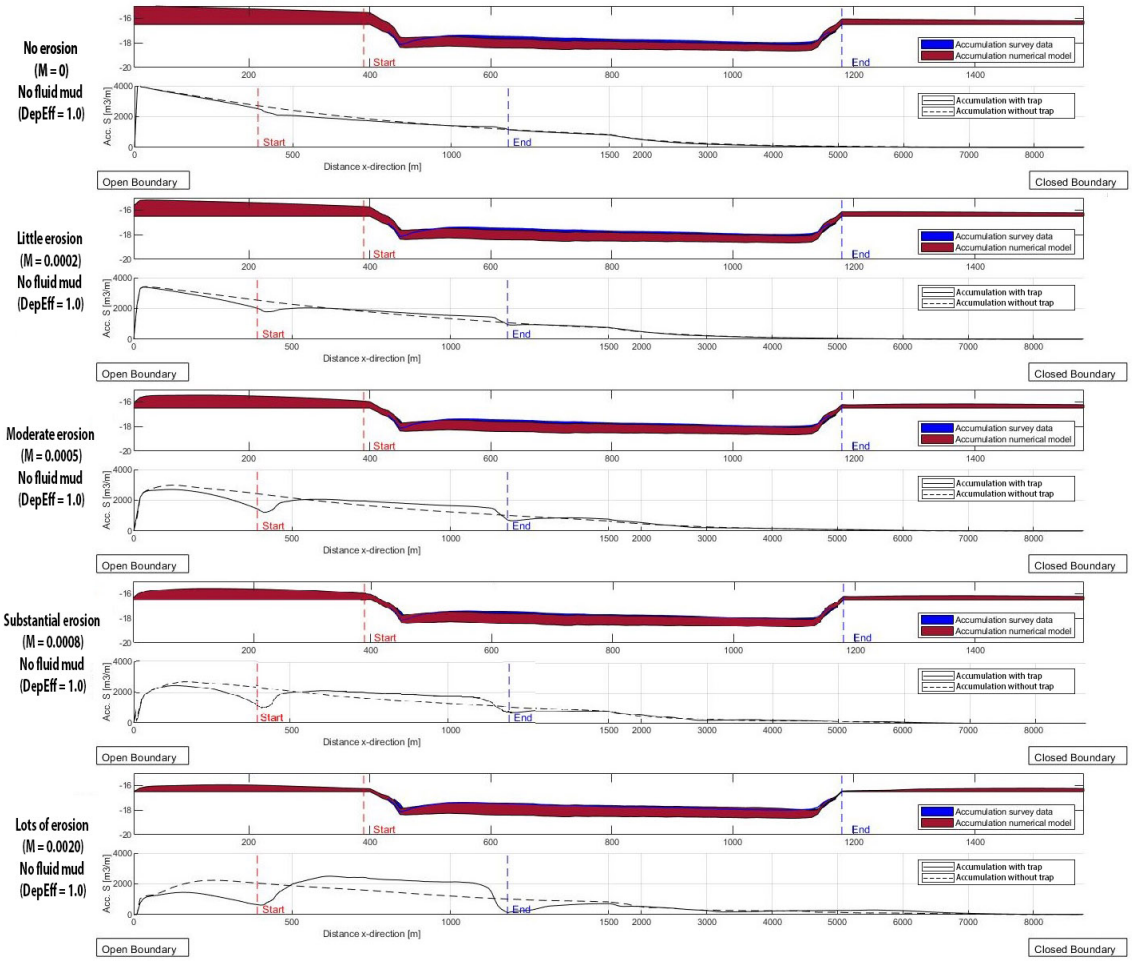

Figure E.2: Five erosion scenarios are assessed for a simulation with (solid line) and without (dashed line) trap for a varying SPM boundary condition (ETM) over time. The top figure of each scenario shows the accumulation pattern of the model (red) and the accumulation pattern of the survey (blue) for the case with sediment trap. The bottom figure of each scenario shows the magnitude of accumulation of sediment over the entire domain. Please note the non-equidistant x-axis. The first 1500 m have a higher resolution as it is the domain of interest.

E.2.2 Fluid mud

After the erosion parameter was determined, the same has been done for the fluid mud parameter. This can be seen in Figure E.3 with its corresponding values in Table E.2.

Fluid mud	**M**	**DepEff**	**Trap**	**Acc. Sed. Mouth [0-390 m]**		**Acc. Sed. Trap [400-1190 m]**		**Acc. Sed Basins [1200-8770 m]**		**Acc. Sed. Total [0-8770 m]**		**Favourable sediment**
	[-]	[-]	[yes / no]	[m3]	[% of total]	[m3]	[% of total]	[m3]	[% of total]	[m3]	Net increase trap/no trap [%]	[%]
No	0.0	1.0	yes	127382	33	136488	35	124644	32	388514	-7	68
No	0.0	1.0	no	130100	31	145926	35	141511	34	417537	7	66
Little	0.0	0.7	yes	115520	30	134425	35	133594	35	383539	-7	65
Little	0.0	0.7	no	120499	29	140951	34	155170	38	412882	7	65
Moderate	0.0	0.5	yes	104713	27	138010	36	143139	37	385862	2	66
Moderate	0.0	0.5	no	110823	29	129828	34	138613	37	379264	-2	63
Substantial	0.0	0.2	yes	79386	22	137038	38	145320	40	361744	-9	60
Substantial	0.0	0.2	no	95980	24	123539	31	179879	45	399398	9	55
Lots	0.0	0.1	yes	61729	18	141740	40	147283	42	350751	-5	58
Lots	0.0	0.1	no	82444	22	116409	31	171473	46	370326	5	54
Extreme	0.0	0.05	yes	46478	13	153990	44	150300	43	350768	1	57
Extreme	0.0	0.05	no	70663	20	105218	29	171173	47	347055	-1	63

Table E.2: Six fluid mud scenarios are assessed with the same hydrodynamics and SPM time series. The values correspond with Figure E.3.

E.3 Constant SPM scenarios

In Table E.3 the three scenarios for settling only, erosion and fluid mud are given for the constant SPM boundary condition.

M	**DepEff**	**Trap**	**Acc. Sed. Mouth [0-390 m]**		**Acc. Sed. Trap [400-1960 m]**		**Acc. Sed Basins [1970-8770 m]**		**Acc. Sed. Total [0-8770 m]**		**Favourable sediment**
[-]	[-]	[-]	[m3]	[% of total]	[m3]	[% of total]	[m3]	[% of total]	[m3]	Net increase vs no trap [%]	[%]
0	1.0	yes	88894	25	117677	33	152316	43	355848	-8	58
0	1.0	no	91485	24	125217	32	172557	45	389259	+8	56
0.0005	1.0	yes	55941	17	116843	35	157808	48	330592	-4	52
0.0005	1.0	no	67923	20	109064	32	168259	49	345247	0	51
0	0.2	yes	52948	15	116158	34	175346	45	344452	-3	49
0	0.2	no	64159	18	100983	28	189751	54	354894	0	47

Table E.3: The three scenarios for settling only, erosion and fluid mud are assessed with the same hydrodynamics and contant SPM time series. The values correspond with Figure 5.11.

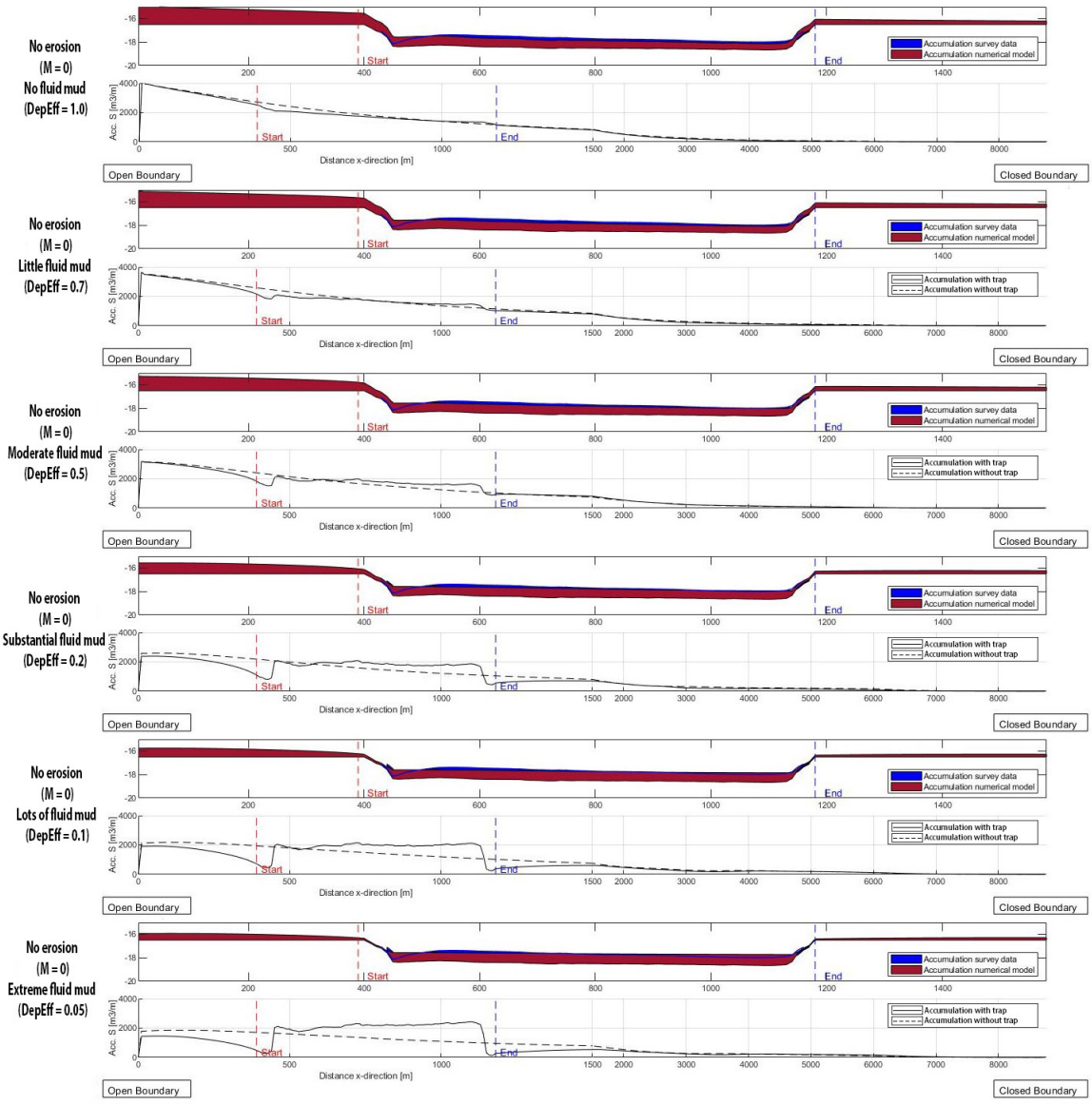

Figure E.3: Six fluid mud scenarios are assessed for a simulation with (solid line) and without (dashed line) trap for a varying SPM boundary condition (ETM) over time. The top figure of each scenario shows the accumulation pattern of the model (red) and the accumulation pattern of the survey (blue) for the case with sediment trap. The bottom figure of each scenario shows the magnitude of accumulation of sediment over the entire domain. Please note the non-equidistant x-axis. The first 1500 m have a higher resolution as it is the domain of interest.

Appendix F

Supporting tables optimization

In this Chapter the supporting tables for Chapter 6 'Optimization of the sediment trap design' are given. In Table F.1 the values for an erosion scenario are given. In Table F.2 the values for a fluid mud scenario is given. In Table F.3 both scenarios are given for a twice as long sediment trap.

M	**DepEff**	**Trap**	**Acc. Sed. Mouth [0-390 m]**		**Acc. Sed. Trap [400-1190 m]**		**Acc. Sed Basins [1200-8770 m]**		**Acc. Sed. Total [0-8770 m]**		**Percentage filled**	**Favourable sediment**
[-]	[-]	[-]	[m3]	[% of total]	[m3]	[% of total]	[m3]	[% of total]	[m3]	Net increase vs no trap [%]	[%]	[%]
0.0005	1.0	no	67923	20	109064	32	168259	49	345247	0	-	51
0.0005	1.0	basic	55941	17	116843	35	157808	48	330592	-4	32	52
0.0005	1.0	2x deep	45611	14	111608	34	168850	52	326068	-6	15	48
0.0005	1.0	2x shallow	63174	18	119181	35	162714	47	345068	0	64	53
0.0005	1.0	2x short	57679	18	109475	34	156686	48	323840	-6	59	52
0.0005	1.0	V-shape	54002	15	113218	32	181279	52	348499	+1	31	48
0.0005	1.0	sill	71467	22	106294	32	152879	46	330640	-4	-	48

Table F.1: Each of the sediment trap designs is simulated on a moderate erosion scenario with a constant SPM boundary condition. The tabled values correspond with Figure 6.1 and Table 6.1.

M	**DepEff**	**Trap**	**Acc. Sed. Mouth [0-390 m]**		**Acc. Sed. Trap [400-1190 m]**		**Acc. Sed Basins [1200-8770 m]**		**Acc. Sed. Total [0-8770 m]**		**Percentage filled**	**Favourable sediment**
[-]	[-]	[-]	[m3]	[% of total]	[m3]	[% of total]	[m3]	[% of total]	[m3]	Net increase vs no trap [%]	[%]	[%]
0	0.2	no	64159	18	100983	28	189751	54	354894	0	-	47
0	0.2	basic	52948	15	116158	34	175346	51	344452	-3	31	49
0	0.2	2x deep	49643	15	117677	34	171156	51	338477	-2	16	48
0	0.2	2x shallow	55412	16	115917	33	176668	51	347999	-2	62	49
0	0.2	2x short	54025	17	101294	31	171747	53	327066	-8	55	47
0	0.2	V-shape	56960	16	116625	33	181155	51	354740	0	32	49
0	0.2	sill	64744	19	99615	30	172150	51	336509	-5	-	49

Table F.2: Each of the sediment trap designs is simulated on a substantial fluid mud scenario with a constant SPM boundary condition. The tabled values correspond with Figure 6.2 and Table 6.2.

M	**DepEff**	**Trap**	**Acc. Sed. Mouth [0-390 m]**		**Acc. Sed. Trap [400-1960 m]**		**Acc. Sed Basins [1970-8770 m]**		**Acc. Sed. Total [0-8770 m]**		**Percentage filled**	**Favourable sediment**
[-]	[-]	[-]	[m3]	[% of total]	[m3]	[% of total]	[m3]	[% of total]	[m3]	Net increase vs no trap [%]	[%]	[%]
0.0005	1.0	no	67923	20	164045	48	112729	33	344698	0		67
0.0005	1.0	basic	55941	17	169100	51	105516	32	330558	-4	46	68
0.0005	1.0	2x long	49853	14	183554	53	110424	32	343831	0	25	68
0	0.2	no	64159	18	161387	46	129008	36	354554	0		64
0	0.2	basic	52948	15	168697	49	122821	36	344466	-3	46	64
0	0.2	2x long	52636	15	178219	50	127569	35	358423	+1	24	64

Table F.3: The twice as long sediment trap is tested on the moderate erosion and substantial fluid mud scenario with a constant SPM boundary condition. The tabled values correspond with Figure 6.8 and Table 6.3

Appendix G

Model challenges

This chapter is dedicated to the many model challenges that were faced during the setup of the numerical Delft3D model. This chapter is included to provide insight in the choices that have to be made in numerical modelling, specifically for the simplification of the Botlek harbour as provided in the research. Most important runs are treated in a chronological order, distinguished by the number in their name, e.g. botlek_001 for the first run. Runs are provided with figures to emphasize on encountered problems. Distinctive changes between runs are elaborated, while other parameters are kept constant compared to previous runs.

G.1 Exploration of domain and boundary conditions

Simulations botlek_001 until botlek_015 were used to get some feeling with the setup of a numerical 2DV model and to explore some of the possibilities for the setup of the 2DV model. The grid was setup and simulation were done with 10, 16 to 20 sigma layers. One of the requirements for the layer thickness was given in Delft Hydraulics (2006), namely that each of the consecutive layers has a ratio of maximum 1.5 to the adjacent layers. To increase resolution towards the bottom, the layer distribution as in Table 4.1 is chosen. New boundary conditions and morphological factors were added. Bathymetries were made for a simulation with and without trap. The model is run with a 4 day tidal signal. A SPM boundary condition has been generated based on the measurements of De Nijs (2012) (Appendix D 'Generation SPM time-series') and is referred to as the 'Variable SPM time series' in the main report. The sediment trap was located at 2000 meter from the boundary to provide sufficient distance from

the boundary. No exchange with the bottom was possible in this first 2000 meters as can be seen in Figure G.1. Later on this has shown to be way too large.

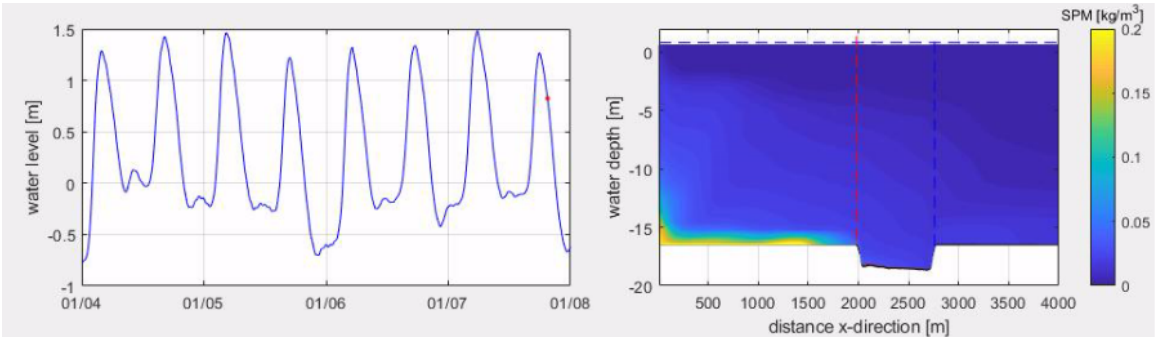

Figure G.1: Simulation botlek_017 is shown in a water elevation (left) and SPM concentration (right). Sediment is not able to deposit in the first 2000m of the grid and large concentrations gather in the bottom layers of the domain. The sediment concentrations at the boundary were quite low such that sedimentation quantities were too low. Very little accumulation has taken place.

G.2 Too much erosion, too little sediment

In simulation botlek_016 erosion was added. Some parameters are based on simulations done by Van Kessel et al. (2011). The same erosion parameters were added in the form of an erosion parameter $M = 0.005$ and a critical shear stress for erosion of $t_{c,e} = 0.11$ Pa. This was however too much erosion and at the end of the simulation, very little sediment was left in the trap. This can be seen in Figure G.2. Erosion was temporarily removed from the simulations.

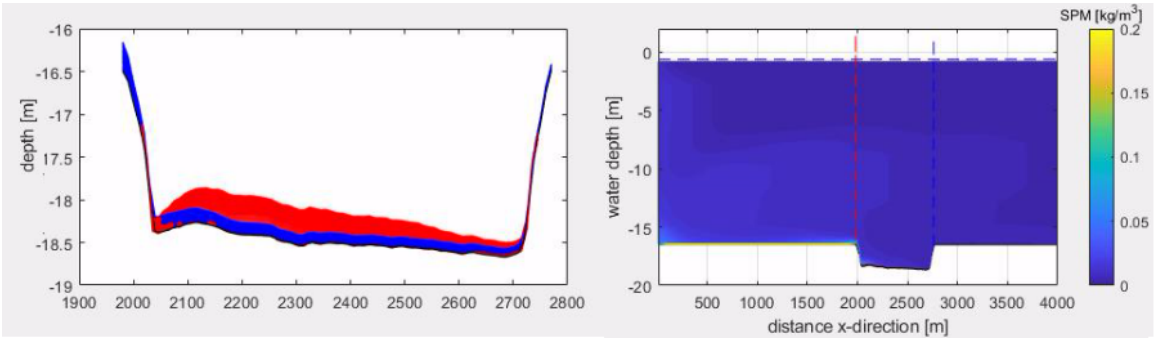

Figure G.2: Simulation botlek_016 is shown in a accumulated sediment (left) by the numerical model (blue) and by the survey data (red) at the end of the simulation. Most of the deposited sediment is eroded due to the wrong erosion parameters. The right graph shows the SPM concentration in the water column at the end of the simulation. Sediment is not able to deposit in the first 2000m of the grid and large concentrations gather in the bottom layers of the domain.

G.3 Too large distance from boundary

The problem sketched above is nicely visualized in simulation botlek_021. This is a simulation where the first 2000 m is used to create distance with the boundary. During this 2000 m no exchange with the bottom is possible. While usually one would want the domain of interest to be sufficiently far from the boundary, in this simulation this is not the case. A sediment distribution of the tumultuous Meuse is applied at the boundary. The mild conditions in the harbour basin allow the sediment to settle. The distance between the boundary and the sediment trap should therefore represent reality as much as possible. In this case, a large distance between the boundary and domain of interest is not desirable. Here, we see a large increase of sediment concentrations in the lowest layer. As soon as the sediment is able to accumulate, the large concentration causes a large peak. This is highly unrealistic and large non-linear effects are imposed on the flow velocity. This is shown in Figure G.3.

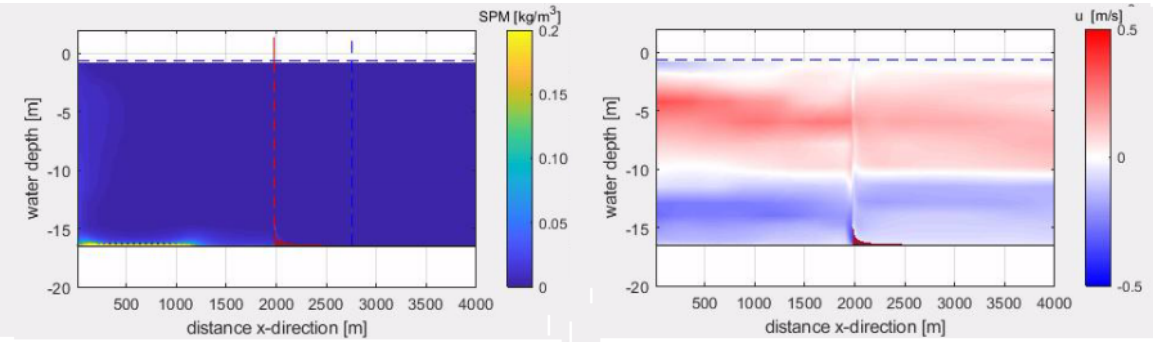

Figure G.3: The left graph shows the SPM concentration in the water column at the end of the simulation without sediment trap. Large concentrations of SPM gather in the lowest layers of the water column in the first 2000 m. The first cell after 2000 m, the large concentrations are able to accumulate and the large concentrations cause a peak in accumulation. The right graph shows the flow velocity and the large influence of the accumulation on the hydrodynamics. In both figures, dark red shows the accumulated sediment.

G.4 Varying SPM boundary conditions and parameters

Simulations until botlek_049 were used to get a feeling with different SPM boundary conditions and sediment-related parameters. Various boundary conditions were created with excel files that result in different quantities of sediment in the domain. This made it easily adjustable to result in a sediment profile that was considered adequate. Also sediment-related parameters were played around with. By varying the erosion parameter M, critical shear stress for erosion $t_{c,e}$, critical shear stress for

depostion $t_{c,d}$, DepEff for fluid mud, initial sediment in the domain and hindered settling, a optimal combination of parameters was looked for. Although other modelling studies such as Van Kessel et al. (2011),Van Kessel (2005), De Groot (2018) and van Prooijen et al. (2017) gave a nice indication about what values should be close to, too many parameters required calibration. Only making use of the survey data by the echosounder multibeam and maintenance dredging data provided by Port of Rotterdam (2019) made it impossible to calibrate so many parameters. After speaking with Deltares' experts THijs van Kessel and Alex Kirichek, some adjustments were made. First of all, the above mentioned 2000 m distance boundary problem was removed. The domain of interest, i.e. the sediment trap was moved to 40 m from the boundary, resembling the same distance in the Botlek Harbour. The second change that was made was by starting with a really basic model. Let's call this the base model. From this base model we slowly add more and more processes so that each of the processes can be adjusted separately. This approach resulted in way better understandable results. The simulations, also called the parameterization of the model in the report, can be found in Appendix E 'Parameterization of the model' and the chosen scenarios in Chapter 4 'Setup of hydrostatic Delft3D-FLOW online SED model'.

G.5 Consideration scope of research

G.5.1 Exclude influence of certain parameters

Of course we want to assess as many parameters as possible in the model. Unfortunately, it is impossible to be able to assess each of the parameters that are sediment related. Sometimes, even entire processes have to be left out of the research. By starting the parameterization of the model, some major assumptions had to be made. First of all, the settling velocity had to be assumed. Although this was one of the main concerns at the start of the modelling, a quite clear range of values was attained by the various modelling studies for the port of Rotterdam. A value of $w_s = 0.6mm/s$ was chosen as a appropriate value. We were more interested in how the various processes and shapes would influence the sedimentation in the basin, rather than exactly mimicking the sediment properties. This would still be highly uncertain anyway. Therefore, also hindered settling, consolidation, flocculation and the two-layer model by Thijs van Kessel were left out of the scope of the research. The model had to be kept simple to get straightforward results. One single sediment fraction with a single

layered bed, no deposition threshold ($\tau_{c,d}$ = 1000 Pa allows sediment to always settle), allowed the dinstinction between two adjustable parameters, namely the critical shear stress for erosion $\tau_{c,e}$ and the deposition parameter for fluid mud DepEff.

G.5.2 Settling only, erosion and fluid mud

To investigate various mechanisms choices have to be made. In this report, the choice was made to investigate various trapping mechanisms. We distinguish between settling only, erosion and fluid mud scenarios. However, it is probably a combination of the scenarios that are actually present in reality. The choice was however made to distinguish between each of the scenarios separately. Some simulations are done with the scenarios combined, but it actually requires a whole new calibration of parameters. using the same parameters as used in the scenarios separately, result in unrealistic results. This is because the parameters influence each other. If fluid mud behaviour and erosion are present, eroded material starts to behave as fluid mud, therefore the amount of accumulated sediment is highly underestimated. The processes greatly exaggerate each other. Some simulations have been ran with the scenarios combined, but there was insufficient time to look for a parameterset that was able to represent both scenarios.

G.6 Hitting bottom grid

Some simulations had such large amounts of erosion, that they would hit the bottom grid. All sediment above the rigid bottom was eroded, and therefore very optimistic results were retrieved. An example is the simulation with a trap for botlek_086 and without trap botlek_086. These runs include lots of erosion, namely $M = 0.005$ for $\tau_{c,e}$ = 0.18 Pa. A proportional distribution between 'Mouth'/'Trap'/'Basins' of sediment was found of 9/43/48 % with a total of 363539 m3 for simulation with trap. A distribution of 16/33/51 was found with a total of 363067 m3 for simulation without trap. This would seem like a great improvement for the installation of a sediment trap. What actually happened, is showed in Figure G.4. The difference in accumulated sediment in half a tidal cycle is enormous. This can be seen when looking at the dark red colour in the flow velocity graphs. The difference between the top right and bottom right graph is only a quarter of a tidal cycle. Yet all sediment on the left part of the sediment trap was eroded and the bottom grid was reached. This can be solved by adding some initial sediment to the domain. However, the

amount of erosion that was encountered is these simulation were considered highly unrealistic and research on this subject is stalled here.

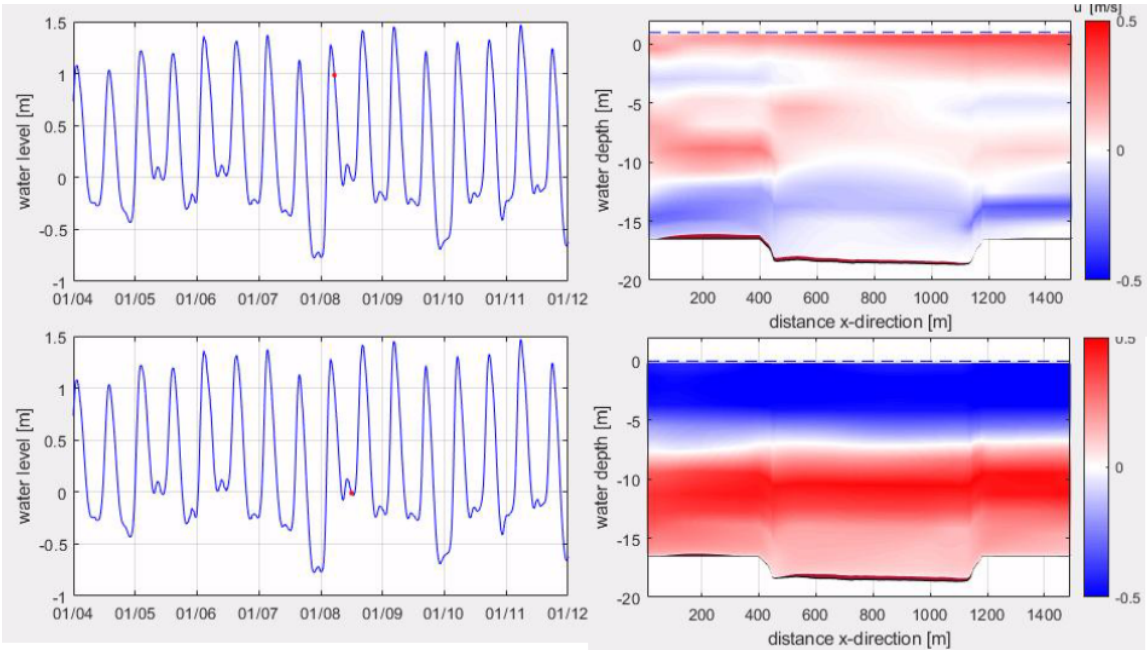

Figure G.4: The left graphs shows the water level (tidal forcing) where the progress of the simulation is indicated with the red marker. The right graph shows the flow velocity and the accumulated sediment in dark red. The time difference between the top two graph and bottom two graphs is only a quarter of a tidal cycle.

G.7 Influence of density driven currents by SPM

One point of interest that is not really a challenge, but rather confirms the application of a two-way coupling between flow and sediment is the parameter 'Include effect of sediment on fluid density'. This parameter was turned on for all simulations. Although theoretically hypothesized that this is the driven factor for capturing fluid mud flow, it is still nice to quantify this with simulations. Therefore, the simulations for substantial fluid mud as shown in Table 5.2 in Chapter 5 'Analyses of trapping mechanisms' are used for reference. The simulations for substantial fluid mud with DepEff = 0.2 are done with trap, i.e. botlek_094, and without trap, i.e. botlek_095. The same simulations are ran without the update between the hydrodynamics and the sediment, i.e. by turning 'Include effect of sediment on fluid density' off. This is done in run botlek_094b for simulation with trap and in run botlek_095b for simulation without sediment trap. The results in Chapter 5 'Analyses of trapping mechanisms' are shortly repeated. We've found a proportional distribution between

'Mouth'/'Trap'/'Basins' for simulation botlek_094 (density currents, trap) a distribution of 22/38/40 % with a total of 361744 m3 accumulated sediment. For simulation botlek_095 (density currents, no trap) a proportional distribution of 24/31/45 % with a total of 399398 m3 accumulated sediment was found. When we exclude density currents. we've found for simulation botlek_094b (no density currents, trap) a proportional distribution of 22/34/46 with a total of 355394 m3 accumulated sediment. For the simulation without trap botlek_095b (no density currents, no trap) the distribution 24/30/46 with a total of 363150 m3 accumulated sediment was found. We see that for the simulation without trap the trapping is less for the simulation without density currents. We do however also see that the even without density currents, the trapping still does increase for the simulation with trap compared to the simulation without trap. This is due to the reduced flow velocities in the sediment carrying water layers above the sediment trap, Of course this is for the fluid mud scenario, where the influence of the density current is the driven factor. For the erosion scenarios, the concentrations in the water column are lower and this difference will be less pronounced.

Appendix H

Two-layer system

The application of a single boundary layer, such as the classical Partheniades-Krone formulation for homogeneous, well-consolidated mud bed, is considered insufficient to describe the buffering of fines and the behaviour of the mud-like sediment in the Rotterdam port area. Therefore a second boundary layer as formulated by Van Kessel et al. (2011) is slightly adjusted and added to describe the exchange between sediment within the water column and the bed. Various transport formulae exist for the transport of sediment in case of an alluvial bed, e.g. when the sediment is not limited. In the harbour area, often is dealt with a starved bed, for which non-equilibrium conditions exist. The water-bed exchange progress needs to be formulated explicitly in form of a pick-up function. Van Kessel formulated a model to deal with this problem. The bottom is schematized as two layers, an upper layer where sediment erodes and accumulates rapidly and a deeper bottom layer, defined as a sand-like layer, where exchange only occurs during energetic conditions. The bottom layer acts as a buffer layer in calm conditions, but sediments are resuspended from this layer during storms or tumultuously situations. In the upper layer the erosion rate is dependent on the sediment mass per unit area, in contrast to the Partheniades-Krone formulation. The exchange between the fines in the water column and the two layers is shown in Figure H.1. Here, both layers are said to exchange sediment with the water column. This should not be seen as the actual physical behaviour, but it is a good representation of the non-linear exchange of the consolidated material in the buffer layer, the fluffy bed layer and the water column. The fluffy fluid mud layer exchanges sediment of the three IM classes with the water column through resuspension E_{1,IM_i} and deposition D_{1,IM_i}. The resuspension depends on the product of the excess shear stress, which is the ratio between the shear stress τ and the critical shear stress per fraction τ_{cr,S_1IM_i}, and first-order rate V_{Res,IM_i}, which depends on the grain size of the sediment. After

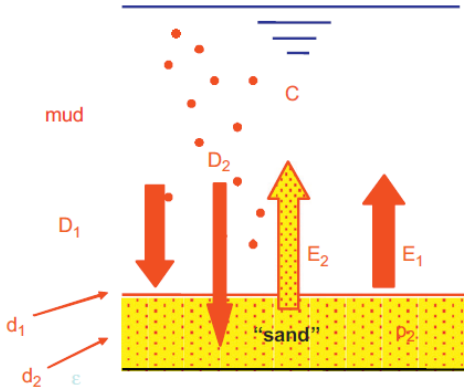

Figure H.1: Schematic representation of the two bottom layer model of Van Kessel et al. (2011).

a certain saturation concentration is reached, a uniform zero-order rate Z_{Res,IM_i} applies. The resuspension of the upper layer E_1 is given in Equation H.1. The subscript i denotes each IM fraction. The deposition of the fluffy fluid mud layer D_1 is defined by the product of the settling velocity V_{Sed,IM_i}, concentration of IM C_{IM_i} and a factor α_{IM_i} that depends on the IM class as can be seen in Equation H.2.

$$E_{1,IM_i} = \min\left(Z_{Res,IM_i}, V_{Res,IM_i} M_{i,1}\right) \left(\frac{\tau}{\tau_{cr,S_1 IM_i}} - 1\right) \tag{H.1}$$

$$D_{1,IM_i} = \left(1 - \alpha_{IM_i}\right) V_{Sed,IM_i} C_{IM_i} \tag{H.2}$$

The resuspension flux from the buffer layer S_2 is based on a Van Rijn type of formulation, where the excess shear stress is influenced by an empirical power 1.5 (van Rijn, 2005). The formulation uses the critical shear stress τ_{Sh} for sand. The resuspension flux is a function of fraction of fines $f_{IM_i S_2}$, Van Rijn pickup factor F_{ResPUp}, density of sediment ρ_s, solid density over water density ratio s, gravitational acceleration g, nominal diameter D_{50} and shear stress τ. The exact empirical formulation is given in H.3. The deposition flux D_2 is rather similar as D_1 and the fluxes are correlated, see Equation H.5. If the fraction of fines $f_{IM_i S_2}$ reaches a user set saturation rate, the storage to the buffer layer is stopped and all fines are stored in the upper layer ($\alpha_{IM_i} = 0$).

$$E_{2,IM_i} = f_{IM_i S_2} F_{ResPUp} \rho_s \left(\left(s-1\right) g D_{50}\right)^{0.5} D_*^{0.3} \left(\frac{\tau}{\tau_{Sh}} - 1\right)^{1.5} \tag{H.3}$$

$$\text{with } D_* = D_{50} \left(\left(s-1\right) \frac{g}{\upsilon^2}\right)^{1/3} \tag{H.4}$$

$$D_{2,IM_i} = \alpha_{IM_i} V_{Sed,IM_i} C_{IM_i} \tag{H.5}$$

References

Armi, L. (1986). The hydraulics of two flowing layers with different densities. *Journal of Fluid Mechanics*, *163*, 27–58.

Blom, P., & Booij, R. (1995). Turbulent free-surface flow over sills. *Journal of Hydraulic Research*, *33*(5), 663–682.

Bosboom, J., & Stive, M. J. (2015). *Coastal Dynamics I.* Delft Academic Press.

de Boer, G. J., Pietrzak, J. D., & Winterwerp, J. C. (2009). SST observations of upwelling induced by tidal straining in the Rhine ROFI. *Continental Shelf Research*, *29*(1), 263–277.

De Bruijn, L. (2018). Maintenance dredging in the Port of Rotterdam: A research to the increase in maintenance dredging volume at Port of Rotterdam.

De Groot, S. (2018). Suspended Sediment Modelling in the Port of Rotterdam.

Delft Hydraulics. (2006). Delft3D-FLOW user manual. *Delft, the Netherlands*.

de Nijs, M. A., Pietrzak, J. D., & Winterwerp, J. C. (2011). Advection of the salt wedge and evolution of the internal flow structure in the Rotterdam Waterway. *Journal of Physical Oceanography*, *41*(1), 3–27.

De Nijs, M. A. J. (2012). On sedimentation processes in a stratified estuarine system.

El Hamdi, A. (2012). Sedimentation in the Botlek Harbour-A research into driving water exchange mechanisms.

Eysink, W. (1989). Sedimentation in harbour basins. Small density differences may cause serious effects. In *International harbour congress, 9th.*

Geyer, W. R. (1993). The importance of suppression of turbulence by stratification on the estuarine turbidity maximum. *Estuaries*, *16*(1), 113–125.

Gill, A. E. (1982). *Atmosphere-Ocean dynamics (International Geophysics Series).* Academic press.

Grabemann, I., Uncles, R., Krause, G., & Stephens, J. (1997). Behaviour of turbidity maxima in the Tamar (UK) and Weser (FRG) estuaries. *Estuarine, Coastal and Shelf Science*, *45*(2), 235–246.

Holthuijsen, L. H. (2010). *Waves in oceanic and coastal waters*. Cambridge university press.

Jay, D. A., & Smith, J. D. (1990). Circulation, density distribution and neap-spring transitions in the Columbia River Estuary. *Progress in Oceanography*, *25*(1-4), 81–112.

Kessel, T. v., & Kranenburg, C. (1996). Gravity current of fluid mud on sloping bed. *Journal of Hydraulic Engineering*, *122*(12), 710–717.

Kranenburg, C. (1998). Dichtheidsstromen. *Collegedictaat CT5302*.

Krone, R. B. (1962). Flume studies of transport of sediment in estuarial shoaling processes. *Final Report, Hydr. Engr. and Samitary Engr. Res. Lab., Univ. of California*.

Lamb, H. (1932). *Hydrodynamics Sixth edition*. Cambridge University Press.

Langendoen, E. J. (1994). Flow patterns and transport of dissolved matter in tidal harbours.

Li, Y., & Mehta, A. J. (1998). Assessment of hindered settling of fluid mudlike suspensions. *Journal of Hydraulic Engineering*, *124*(2), 176–178.

Long, R. R. (1954). Some aspects of the flow of stratified fluids: II. Experiments with a two-fluid system. *Tellus*, *6*(2), 97–115.

Mayer, F., & Fringer, O. (2017). An unambiguous definition of the Froude number for lee waves in the deep ocean. *Journal of Fluid Mechanics*, *831*.

Miles, J. W. (1961). On the stability of heterogeneous shear flows. *Journal of Fluid Mechanics*, *10*(4), 496–508.

Nakagawa, H., & Nezu, I. (1987). Experimental investigation on turbulent structure of backward-facing step flow in an open channel. *Journal of Hydraulic Research*, *25*(1), 67–88.

Otto, L., Zimmerman, J., Furnes, G., Mork, M., Saetre, R., & Becker, G. (1990). Review of the physical oceanography of the North Sea. *Netherlands journal of sea research*, *26*(2-4), 161–238.

Partheniades, E. (1962). *A study of erosion and deposition of cohesive soils in salt water*. University of California, Berkeley.

Pietrzak, J. (2017). Stratified Flows-CIE5302 lecture notes. *Delft University of Technology*.

Pritchard, D. W. (1967). What is an estuary: physical viewpoint..

Schiereck, G. J. (2003). *Introduction to bed, bank and shore protection*. CRC Press.

Simpson, J. H., Bos, W. G., Schirmer, F., Souza, A. J., Rippeth, T. P., Jones, S. E., & Hydes, D. (1993). Periodic stratification in the Rhine ROFI in the North Sea. *Oceanologica Acta*, *16*(1), 23–32.

Suijlen, J., & Duin, R. (2002). Atlas of near-surface total suspended matter concentrations in the Dutch coastal zone of the North Sea. *Rapportnr.: 2002.059*.

Port of Rotterdam. (2019). Retrieved from `https://www.portofrotterdam.com/nl`

Van der Giessen, A., De Ruijter, W., & Borst, J. (1990). Three-dimensional current structure in the Dutch coastal zone. *Netherlands Journal of Sea Research*, *25*(1-2), 45–55.

Van Kessel, T. (2005). Gevoeligheidsonderzoek effectiviteit bufferput Caland-Beerkanaal. *WL— Delft*.

Van Kessel, T., Winterwerp, H., Van Prooijen, B., Van Ledden, M., & Borst, W. (2011). Modelling the seasonal dynamics of SPM with a simple algorithm for the buffering of fines in a sandy seabed. *Continental Shelf Research*, *31*(10), S124–S134.

Vanlede, J., & Dujardin, A. (2014). A geometric method to study water and sediment exchange in tidal harbors. *Ocean Dynamics*, *64*(11), 1631–1641.

van Prooijen, B., van Maren, B., Chassange, C., & Winterwerp, H. (2017, April). *Lecture notes Sediment Dynamics.* Faculty of Civil Engineering and Geosciences at Delft University of Technology.

van Rijn, L. C. (2005). *Principles of sedimentation and erosion engineering in rivers, estuaries and coastal seas*.

Van Vechgel, R., Veltman, M., Dollée, A., & De Haan, H. (1987). *MKO Minimalisering Kosten Onderhoudsbaggerwerk.* Rijkswaterstaat.

Verlaan, P., & Spanhoff, R. (2000). Massive sedimentation events at the mouth of the Rotterdam Waterway. *Journal of Coastal Research*, 458–469.

Versteeg, H. K., & Malalasekera, W. (2007). *An introduction to computational fluid dynamics: the finite volume method*. Pearson Education.

Vijverberg, T. (2008). Mud dynamics in the Markermeer. *Technische Universiteit Delft, Delft*.

Winters, K. B., & Armi, L. (2012). Hydraulic control of continuously stratified flow over an obstacle. *Journal of Fluid Mechanics*, *700*, 502–513.

Winterwerp, J. (2001). Stratification effects by cohesive and noncohesive sediment. *Journal of Geophysical Research: Oceans*, *106*(C10), 22559–22574.

Winterwerp, J. C. (2002). On the flocculation and settling velocity of estuarine mud. *Continental shelf research*, *22*(9), 1339–1360.

Winterwerp, J. C., & van Kessel, T. (2003). Siltation by sediment-induced density currents. *Ocean Dynamics*, *53*(3), 186–196.

Winterwerp, J. C., & Van Kesteren, W. G. (2004). *Introduction to the physics of cohesive sediment dynamics in the marine environment* (Vol. 56). Elsevier.

Witteveen en Bos. (2005). Quick scan slibproblematiek Markermeer en Eem-en Gooimeer. *Rapport IJG-werkdocument 2006*, *15*.

World Shipping Council. (2013). Top 50 world container ports.